


The Neandertal nature of the Atapuerca Sima de los Huesos mandibles

Rolf Quam^{1,2,3,4}  | Ignacio Martínez⁴ | Yoel Rak⁵ | Bill Hylander⁶ | Ana Pantoja² | Carlos Lorenzo^{7,8} | Mercedes Conde-Valverde^{4,1} | Brian Keeling¹ | María Cruz Ortega Martínez² | Juan Luis Arsuaga^{2,9}

¹Department of Anthropology, Binghamton University (SUNY), Binghamton, New York, USA

²Centro de Investigación UCM-ISCIH sobre la Evolución y Comportamiento Humanos, Madrid, Spain

³Division of Anthropology, American Museum of Natural History, New York, New York, USA

⁴Universidad de Alcalá. Cátedra de Otoacústica Evolutiva y Paleoantropología (HM Hospitales-Universidad de Alcalá), Área de Antropología Física, Departamento de Ciencias de la Vida, Universidad de Alcalá, Madrid, Spain

⁵Department of Anatomy and Anthropology, Sackler Faculty of Medicine, Tel Aviv University, Tel Aviv, Israel

⁶Department of Evolutionary Anthropology, Duke University, Biological Sciences Building, Durham, North Carolina, USA

⁷Àrea de Prehistòria, Departament d'Història i Història de l'Art, Universitat Rovira i Virgili (URV), Tarragona, Spain

⁸Institut Català de Paleocologia Humana i Evolució Social, Tarragona, Spain

⁹Universidad Complutense de Madrid, Departamento de Paleontología, Facultad de Ciencias Geológicas, Ciudad Universitaria s/n, Madrid, Spain

Correspondence

Rolf Quam, Department of Anthropology, Binghamton University (SUNY), Binghamton, NY 13902-6000, USA.
Email: rquam@binghamton.edu

Funding information

Ministerio de Ciencia e Innovación of the Government of Spain, Grant/Award Number: PID2021-122355NB-C31MCIN/AEI/10.13039/501100011033/FEDER,UE,

Abstract

The recovery of additional mandibular fossils from the Atapuerca Sima de los Huesos (SH) site provides new insights into the evolutionary significance of this sample. In particular, morphological descriptions of the new adult specimens are provided, along with standardized metric data and phylogenetically relevant morphological features for the expanded adult sample. The new and more complete specimens extend the known range of variation in the Atapuerca (SH) mandibles in some metric and morphological details. In other aspects, the addition of new specimens has made it possible to confirm previous observations based on more limited evidence. Pairwise comparisons of individual metric variables revealed the only significant difference between the Atapuerca (SH) hominins and Neandertals was a more vertical symphysis in the latter. Similarly, principal components analysis of size-adjusted variables showed a strong similarity between the Atapuerca (SH) hominins and Neandertals. Morphologically, the Atapuerca (SH) mandibles show nearly the full complement of Neandertal-derived features. Nevertheless, the Neandertals differ from the Atapuerca (SH) mandibles in showing a high frequency of the H/O mandibular foramen, a truncated, thinned and inverted gonial margin, a high placement of the mylohyoid line at the level of the M3, a more vertical

This is an open access article under the terms of the [Creative Commons Attribution-NonCommercial-NoDerivs](https://creativecommons.org/licenses/by-nc-nd/4.0/) License, which permits use and distribution in any medium, provided the original work is properly cited, the use is non-commercial and no modifications or adaptations are made.

© 2023 The Authors. The Anatomical Record published by Wiley Periodicals LLC on behalf of American Association for Anatomy.

symphysis and somewhat more pronounced expression of the chin structures. Size-related morphological variation in the SH hominins includes larger retro-molar spaces, more posterior placement of the lateral corpus structures, and stronger markings associated with the muscles of mastication in larger specimens. However, phylogenetically relevant features in the SH sample are fairly stable and do not vary with the overall size of the mandible. Direct comparison of the enlarged mandibular sample from Atapuerca (SH) with the Mauer mandible, the type specimen of *H. heidelbergensis*, reveals important differences from the SH hominins, and there is no morphological counterpart of Mauer within the SH sample, suggesting the SH fossils should not be assigned to this taxon. The Atapuerca (SH) mandibles show a greater number of derived Neandertal features, particularly those related to midfacial prognathism and in the configuration of the superior ramus, than other European middle Pleistocene specimens. This suggests that more than one evolutionary lineage co-existed in the middle Pleistocene, and, broadly speaking, it appears possible to separate the European middle Pleistocene mandibular remains into two distinct groupings. One group shows a suite of derived Neandertal features and includes specimens from the sites of Atapuerca (SH), Payre, l'Aubesier and Ehringsdorf. The other group includes specimens that generally lack derived Neandertal features and includes the mandibles from the sites of Mauer, Mala Balanica, Montmaurin and (probably) Visogliano. The two published Arago mandibles differ strongly from one another, with Arago 2 probably belonging to this former group, and Neandertal affinities being more difficult to identify in Arago 13. Outside of the SH sample, derived Neandertal features in the mandible only become more common during the second half of the middle Pleistocene. Acceptance of a cladogenetic pattern of evolution during the European middle Pleistocene has the potential to reconcile the predictions of the accretion model and the two phases model for the appearance of Neandertal morphology. The precise taxonomic classification of the SH hominins must contemplate features from the dentition, cranium, mandible and postcranial skeleton, all of which are preserved at the SH site. Nevertheless, the origin of the Neandertal clade may be tied to a speciation event reflected in the appearance of a suite of derived Neandertal features in the face, dentition and mandible, all of which are present in the Atapuerca (SH) hominins. This same suite of features also provides a useful anatomical basis to include other European middle Pleistocene mandibles and crania within the Neandertal clade.

KEYWORDS

Europe, mandible, Neandertal, Pleistocene, Spain

1 | INTRODUCTION

The middle Pleistocene site of the Sima de los Huesos (SH) in the Sierra de Atapuerca has yielded a rich collection of carnivore and human fossil remains. The first specimens were discovered at the site in the 1970s

(Aguirre & de Lumley, 1977) and systematic excavations have been ongoing since 1984 (Arsuaga, Martínez, García, Carretero, et al., 1997). The current sample of human fossils surpasses 6,900 specimens, making the Sima de los Huesos the richest human-fossil-bearing deposits in the world. A minimum of 29 dental individuals have been

recognized within the sample (Bermúdez de Castro et al., 2020), corresponding to both sexes and diverse ages. The Atapuerca SH human fossils have been dated to c.430 kya (Arsuaga et al., 2014), and the maximum age of the fossil-bearing deposits has recently been suggested to be c.450 kya (Demuro et al., 2019). The SH hominins are argued to be phylogenetically close to the Neandertals, based on the presence of numerous derived Neandertal features (Arsuaga et al., 1993, 2014; Arsuaga, Martínez, Gracia, & Lorenzo, 1997). DNA has also been extracted from several of the SH fossils, with the mtDNA results revealing the closest affinities were with the enigmatic Denisovans (Meyer et al., 2014), while the nuclear DNA results suggest that they form a sister group to the Neandertals (Meyer et al., 2016).

The sample of human fossils from the Sima de los Huesos includes a large number of mandibular remains (Table 1; Figure 1). Numerous studies have been carried out over the years on the Atapuerca SH mandibles, in part since the first fossils recovered and numbered from the Sima de los Huesos (AT-1, AT-2, and AT-3) were mandibles. Give their association with the middle Pleistocene bear species *U. deningeri*, an early age for the assemblage was recognized for the SH human fossils, and they were initially argued to be more primitive than the Neandertals (Aguirre & de Lumley, 1977). Subsequent studies based on an enlarged sample have highlighted numerous similarities between the Atapuerca (SH) mandibles and the later in time Neandertals (Rosas, 1987, 1992, 1995, 1997, 2001). In particular, numerous derived Neandertal features in both the corpus and ramus are already present in the Atapuerca (SH) mandibles, including a posterior placement of the mental foramen, the presence of a retromolar space and a high frequency of the medial pterygoid tubercle, among others (Bermúdez de Castro et al., 2015; Rosas, 1995, 2001).

Most of the SH specimens represent adolescent and young adult individuals, with only two (Individuals 5 and 21) being considered older adults (35+ years of age at death) (Bermúdez de Castro et al., 2004), and both the growth and aging processes have been studied (Rosas, 2000; Rosas et al., 1999; Rosas & Martínez-Maza, 2010). In addition, the Atapuerca (SH) mandibles have been argued to show an elevated level of sexual dimorphism (Rosas et al., 2002), and the sex has been estimated for a number of the more complete specimens. This resembles the pattern of elevated dimorphism found in the dentition (Bermúdez de Castro et al., 2001) but is distinct from that documented in the postcranial remains at the site, which show a more modest level of dimorphism similar to that found in living human populations (Arsuaga, Carretero, Lorenzo, Gracia, et al., 1997; Lorenzo et al., 1998). The influence of these size differences on the expression of a number of anatomical features in the Atapuerca (SH) mandibles has also been

analyzed (Rosas, 1997; Rosas & Bastir, 2004), and a morphological gradient was proposed to explain the relationship between size and morphology within the sample, with larger individuals argued to show more pronounced expression of certain features of the symphysis and mandibular corpus (Rosas et al., 2019).

The present study provides an update on the adult mandibular sample from the Sima de los Huesos. A number of mandibles are now more complete following recent discoveries and newly recognized associations between specimens. In addition, a few specimens have been included in previous studies (Rosas et al., 2002; Rosas & Bastir, 2004) but have not been described to date. The more complete mandibles make it possible to confirm many of the details of previous studies made on more fragmentary remain. In addition, the enlarged sample has extended the known range of variation in some features and allows for a reassessment of the variation and stability proposed previously for a number of features. While some limited metric dimensions have been published previously, the present study provides standardized metric parameters and the expression of the main morphological features of all the adult mandibles to facilitate comparative studies and to provide an overall assessment of the evolutionary significance of the Atapuerca (SH) mandibles.

Middle Pleistocene systematics is currently an area of active debate among scholars, with different hypotheses about the number of taxa represented in the fossil record (Tattersall, 2011). In particular, the role of *Homo heidelbergensis*, and its presence in Europe and Africa, has figured prominently in these debates (Stringer, 2012). This specific designation was originally proposed based on the discovery of the Mauer mandible in Germany in the early 20th Century (Schoetensack, 1908) at a time when taxonomic categories were understood more as descriptive labels than as biologically meaningful evolutionary units. The Mauer mandible shows a clearly archaic morphology, including a thick corpus and lack of chin structures, combined with some peculiar features, including a very wide ramus and relatively small dentition. At the time of its discovery, the scant fossil record did not allow for much comparison with other taxa. While its generally archaic nature was often recognized, its taxonomic designation did not figure significantly in debates about human evolution until the latter part of the 20th century.

Howell (1960) was an early proponent of using this taxonomic label to refer to most European middle Pleistocene specimens that predated the Neandertals. More recently, some researchers view this taxon as the last common ancestor of Neandertals and modern humans and frequently link middle Pleistocene fossils from Europe, such as Petralona, with their counterparts in Africa, including Kabwe and Bodo (Harvati et al., 2010; Rightmire, 2008;

TABLE 1 Inventory of the mandibular remains assigned to dental individuals from the Atapuerca (SH) site.

| Dental individual | Age at death (years) | Developmental age | Previous specimen Nos. | Recent associations | Preservation | Previous description/inventory |
|-------------------|----------------------|-------------------|-----------------------------|---|--|--|
| I | 16–18 | Young adult | AT-1 | | Mandibular corpus | Aguirre and de Lumley (1977), Rosas (1995, 1997, 2001), Rosas et al. (2002) |
| II | 12.5–14.5 | Subadult | AT-2 | | Fragment of right corpus | Aguirre and de Lumley (1977), Rosas (1995, 1997, 2001) |
| III | 15–17 | Subadult | AT-3 | | Fragment of left corpus | Aguirre and de Lumley (1977), Rosas (1995, 1997, 2001), Rosas et al. (2002) |
| IV | 26–32 | Adult | AT-250 + 793 | AT-2553 | Nearly complete mandible | Rosas (1995, 1997, 2001), Rosas et al. (2002, 2019) |
| V (Cr. 15) | 35+ | Old Adult | | AT-6726 + 6802 + 6901 | Complete mandible | Undescribed |
| VI | 16–18 | Young adult | AT-75 | | Fragment of left corpus | Rosas (1987, 1995, 1997, 2001), Rosas et al. (2002) |
| VII | 24–30 | Adult | AT-1957 + 303a + 303b + 720 | AT-509 + 776 + 1845 + 4791 | Fragment of right corpus, symphysis and partial right and left rami | Rosas (1995, 1997, 2001), Rosas et al. (2002) |
| X | 15–17 | Subadult | AT-172 + 508 | AT-301 + 506 + 6700 | Partial right and left corpus and symphysis | Rosas (1995, 1997, 2001), Rosas et al. (2002) |
| XII | 17–19 | Young adult | AT-300 | AT-4147 | Nearly complete mandible | Rosas (1995, 2001), Rosas and Bastir (2004), Rosas et al. (2002, 2019) |
| XV (Cr. 17) | 17–19 | Young adult | AT-2193 + 2439 | | Right hemimandible and symphysis | Rosas (2001), Rosas and Bastir (2004), Rosas et al. (2002, 2019) |
| XVI (Cr. 9) | 12.5–14.5 | Subadult | AT-1157 | AT-1186 + 2621 + 2902 + 2910+ AT-3880 + 3962 + 4790 + 6468 | Partial right ramus, right corpus symphysis and partial left corpus | Rosas (1997, 2001) |
| XIX | 16–18 | Young adult | AT-505 + 604 + 952 | | Complete mandible | Rosas (1995, 1997, 2001), Rosas and Bastir (2004), Rosas et al. (2002, 2019) |
| XXI (Cr. 5) | 35+ | Old adult | AT-721 + 888 | AT-3876 + 3877 + 3878 | Complete mandible | Rosas (1997, 2001), Rosas and Bastir (2004), Rosas et al. (2002) |
| XXII | 20–26 | Adult | AT-605 | AT-3958 + 4794 | Nearly complete mandible | Rosas (1995, 1997, 2001), Rosas and Bastir (2004), Rosas et al. (2002, 2019) |

TABLE 1 (Continued)

| Dental individual | Age at death (years) | Developmental age | Previous specimen Nos. | Recent associations | Preservation | Previous description/inventory |
|---------------------|----------------------|-------------------|------------------------|------------------------------|----------------------------------|--|
| XXIII (Cr. 16) | 14–16 | Subadult | AT-607 + 771 | | Complete mandible | Rosas (1995, 1997, 2001), Rosas and Bastir (2004), Rosas et al. (2002) |
| XXIV | 12.5–14.5 | Subadult | AT-2438 | AT-2144 + 2430 + 5126 + 5257 | Mandibular corpus and left ramus | Undescribed |
| XXV | 11–13 | Subadult | AT-3888 | AT-6180 | Nearly complete mandible | Rosas and Bastir (2004) |
| XXVI (Cr. 10) | 16–18 | Young adult | AT-1775 | | Fragment of left corpus | Rosas (2001), Rosas et al. (2002) |
| XXVII | 20–26 | Adult | AT-792 | AT-4495 | Corpus and partial left ramus | Rosas (1997, 2001), Rosas et al. (2002, 2019) |
| XXVIII ^a | 24–30 | Adult | AT-950 | AT-3924 | Complete mandible | Rosas (1997, 2001), Rosas and Bastir (2004), Rosas et al. (2002, 2019) |

Note: Assignment of mandibular remains to dental individuals and their age at death follows Bermúdez de Castro et al. (2004, and pers. comm.). Adult developmental age established as fully erupted M3.

^aFormerly Individual XXXI.

Stringer, 2012). In contrast, other researchers have preferred to restrict the term to exclusively European fossils, with most (but not all) specimens showing some derived Neandertal features (Arsuaga et al., 2014; Hublin, 2009).

The dating of the Ceprano cranium to the middle Pleistocene (Muttoni et al., 2009) has led to a growing recognition that more than one hominin group/species was likely present in middle Pleistocene Europe (Roksandic et al., 2018; Tattersall, 2011). European middle Pleistocene cranial remains can be broadly separated into two groups based on the presence or absence of derived Neandertal features. Fossils from the sites of Atapuerca (SH), Petralona, Swanscombe, Aroeira, Steinheim, Reilingen and Ehringsdorf all show clearly derived Neandertal features, while the cranial remains from Ceprano and Arago generally lack them.

While the taxonomic classifications of these middle Pleistocene European fossils is a matter of longstanding debate among scholars, there is a broad consensus that the Atapuerca (SH) sample is closely allied with the Neandertals. The Atapuerca (SH) hominins have previously been attributed to *H. heidelbergensis*, as a chronospecies with *H. neanderthalensis*. However, the notion of chronospecies is fuzzy at best and the division between earlier and later chronospecies is recognized to be subjective and arbitrary.

Given the more central role *H. heidelbergensis* has taken in evolutionary scenarios, several studies have

focused more specifically on the Mauer mandible itself. Its early chronological age, around 600 kya (Wagner et al., 2010), means this specimen predates most other European middle Pleistocene fossils, and Mounier et al. (2009) have argued its morphology is consistent with being a stem species for Neandertals and modern humans. While similarities with Neandertals have been noted by Rosas (Rosas et al., 2019; Rosas & Bermudez de Castro, 1998), most researchers agree that this specimen lacks most, if not all, derived Neandertal features found in other European middle Pleistocene fossils (Arsuaga et al., 2014; Bailey, 2002; Hublin, 2009; Rak et al., 2002).

The central question to resolving some of these differing opinions centers on the presence of derived Neandertal features in the mandible and teeth of Mauer. The absence of derived Neandertal features in Mauer would suggest that the taxonomic label *H. heidelbergensis* should include only those European middle Pleistocene specimens that lack Neandertal features. Alternatively, if derived Neandertal features can be demonstrated to be present in Mauer, then this term could also include specimens that show some derived Neandertal features but still lack others. The expanded sample of mandibular remains from the Atapuerca SH site provides an opportunity for direct comparison with the Mauer mandible, the holotype of *H. heidelbergensis*, and to address the possible presence of derived Neandertal features in this individual. If the SH hominins are members of this species, then

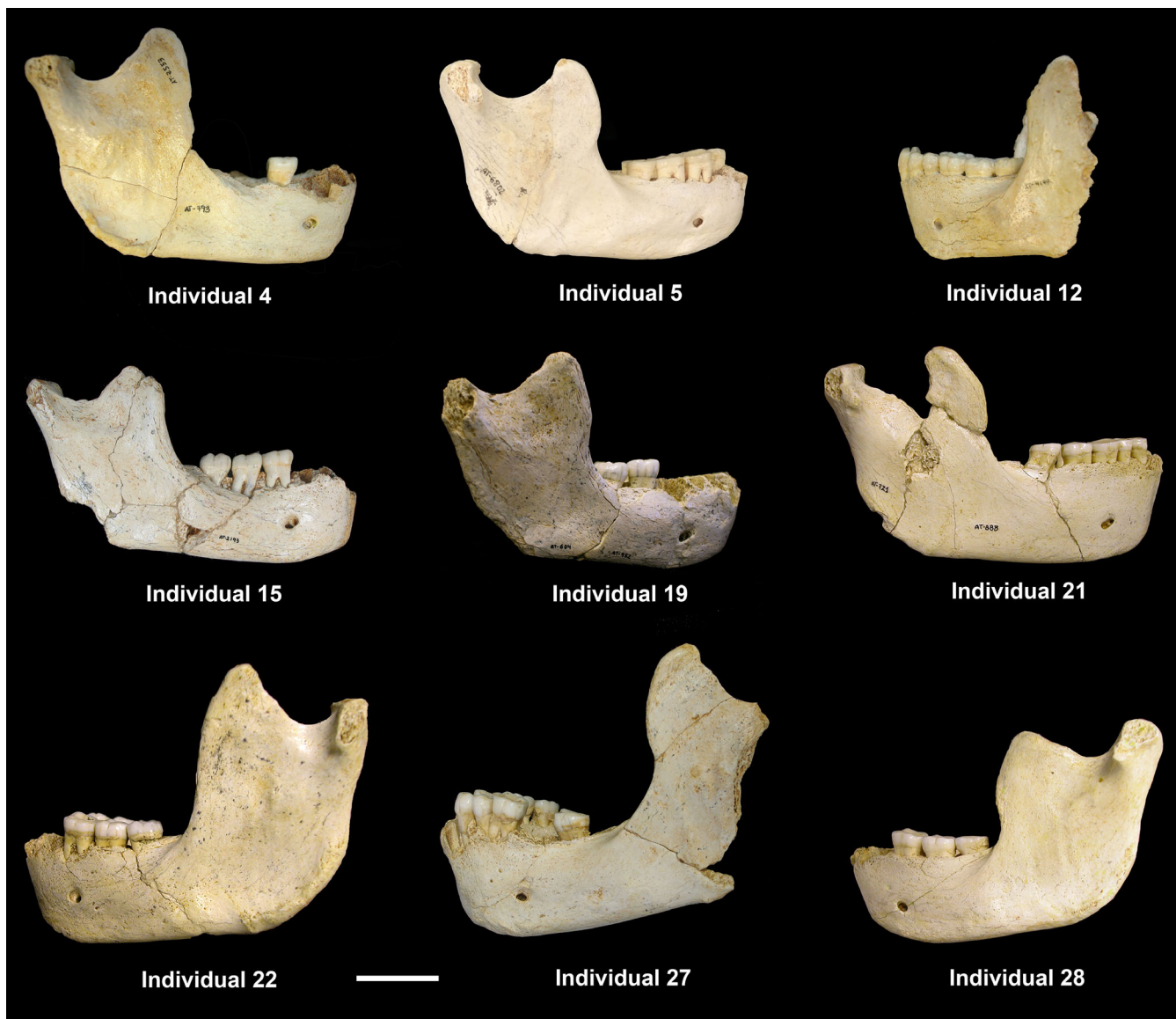


FIGURE 1 The more complete adult SH mandibles in lateral view. Scale bar = 3 cm. *Source:* Image Credit: Javier Trueba, Madrid Scientific Films.

it should be possible to identify a morphological counterpart to Mauer in the SH assemblage. Alternatively, if the anatomical features in Mauer do not fall within the range of variation seen in the SH hominins, this would suggest they do not represent the same species.

2 | MATERIALS AND METHODS

2.1 | The Atapuerca (SH) mandibular sample

The inventory of mandibular remains from the Sima de los Huesos, including recently recognized associations and new individuals, is provided in Table 1. The inventory and labeling of the Atapuerca specimens follow two separate

conventions. Each identifiable fragment is given its own specimen number (e.g., AT-1). Thus, many of the more complete mandibles are comprised of a number of fragments and have more than one specimen number (e.g., AT-300 + AT-4147). In a few cases, it has been possible to associate a particular mandible with one of the crania (e.g., AT-888 with Cranium 5) recovered from the site. In addition, in most cases, it is also possible to assign these more complete specimens to one of the 29 currently recognized dental individuals.

Based on the most recent inventory of the teeth (Bermúdez de Castro et al., 2020) as well as newly reconstructed specimens, a total of 20 mandibles can be assigned to known dental individuals, and this represents the minimum number of individuals (MNI) currently recognizable within the SH mandibular sample. Of these,

13 mandibles represent adult individuals, defined as showing a fully erupted M_3 (Table 1). Among the adult individuals, six individuals are considered young adults with ages ranging from 16 to 19 years, five individuals are considered adult with ages ranging from 20 to 32 years and two individuals are considered old adults whose age can only be estimated as 35+ years. There are a number of additional isolated fragments, some of which are associated with each other, that cannot currently be assigned to any of the dental individuals, but this may be possible in the future when additional fragments are found during the ongoing excavations. The present study focuses on the adult remains, while the juvenile specimens as well as the isolated fragments are not considered in the present study.

2.2 | Comparative samples

For comparative purposes, a number of adult Pleistocene fossil human specimens from Europe and southwest Asia have also been studied (Table 2). Measurements and morphological observations have been taken on the original specimens when possible and complemented with data taken from the literature and on high-quality casts.

Data for European early Pleistocene mandibles are limited to the fragmentary specimen from the site of the Sima del Elefante (1.1–1.2 Ma) (Carbonell et al., 2008) and three incomplete specimens from the site of Gran Dolina (c.900 Ka) (Berger et al., 2008), both also located in the Sierra de Atapuerca. The European middle Pleistocene sample includes some chronologically early specimens including Mauer (c.600 Ka) (Wagner et al., 2010), Arago 2 and 13 (c.450 Ka) (Falguères et al., 2015), BH-1 from Mala Balanica (c.400–500 Ka) (Rink et al., 2013), and Visogliano 2 (c.400–500 Ka) (Falguères et al., 2008), as well as the chronologically younger specimens Payre 15 (c.250 Ka) (Verna et al., 2020) Ehringsdorf 8 (c.230 Ka) (Blackwell & Schwarcz, 1986), l'Aubesier 11 (c.170–190 Ka) (Lebel et al., 2001), and Montmaurin (c.190–240 Ka) (Crégut-Bonnoure et al., 2010). The recently discovered late middle Pleistocene Xiahe mandible (c.160 ka) from Tibet is also included in the comparative sample, and this specimen has been argued to represent the Denisovan population (Chen et al., 2019).

The Neandertal sample includes adult specimens from both Europe and southwest Asia (Table 2). Most of the specimens date to the Late Pleistocene, with the exception of the late middle Pleistocene La Chaise Bourgeois-Delauney 1 specimen. The fossil *H. sapiens* sample includes some earlier specimens from the sites of Skhul and Qafzeh and later specimens from Ohalo 2 in southwest Asia and European Upper Paleolithic individuals.

Finally, a large sample of adult recent humans ($n = 77$) was also included to provide an estimate of the degree of anatomical variation, which can be expected to characterize a biological population. The recent human sample comprises archeological specimens from the site of Kish, Iraq ($n = 41$) (Quam, 1996) and specimens in the osteological teaching collection ($n = 36$) housed at Binghamton University. While some aspects of modern human mandibular diversity may not be reflected in this particular comparative sample, the current sample, comprised of individuals from different chronologies and likely different geographic origins, does represent a reasonable measure of modern human variation to draw inferences on the evolutionary differences from Neandertals and the SH hominins.

The Kish sample was chosen with an emphasis on selecting individuals that were nearly complete and where all the metric and morphological data could be observed and recorded accurately. Sex estimation in the Kish individuals was based on the expression of traits that are known to be sexually dimorphic in the modern human skeleton. Some individuals preserved cranial and postcranial remains in addition to the mandible, making a more reliable sex estimation possible. Of the Kish individuals where a sex estimation was possible, 10 individuals were sexed as male and 11 were sexed as female. The remaining 20 individuals are considered of unknown sex, with most of these deriving from a comingled burial context, where it is not possible to associate mandibles with crania or postcranial bones. The osteological teaching collection from Binghamton University also consists of well-preserved nearly intact mandibles but lacks a known provenience. Sex estimation is again based on the expression of sexually dimorphic features in the modern human skeleton. Here, 22 individuals were sexed as males, 6 individuals as females and the remaining 8 individuals are considered of unknown sex.

2.3 | Measurements

Measurement definitions generally follow Martin and Saller (1956). Linear measurements were taken with sliding calipers and a mandibulometer on the original fossil and recent specimens or high-quality casts and are reported to 0.1 mm. Several indices were also calculated based on the linear measurements. The angle of the ramus was taken using a mandibulometer and the angle of the chin to the alveolar plane was measured in scaled lateral photographs. The geometric mean was calculated based on the metric variables (excluding the angle of the ramus and the angle of the chin) to assess the overall size of the mandible and to standardize the variables for

TABLE 2 Comparative samples of Pleistocene and recent humans used in the present study.

| Specimen/sample | Source |
|------------------------------------|--|
| <i>Lower Pleistocene</i> | |
| ATE9-1 | Bermúdez de Castro et al. (2011) |
| ATD6-5 | Rosas and Bermúdez de Castro (1999) |
| ATD6-96 | Carbonell et al. (2005); Cast |
| ATD6-113 | Bermúdez de Castro et al. (2008) |
| <i>Middle Pleistocene</i> | |
| Mauer | deLumley and Fournier (1982); Cast |
| Arago 2, 13 | Aguirre and de Lumley (1977), de Lumley and Fournier (1982); Casts |
| Ehringsdorf F | Vlcek (1993) |
| Visogliano 2 | Cattani et al. (1991) |
| Montmaurin | Original specimen |
| Aubesier 11 | Lebel and Trinkaus (2002) |
| Mala Balanica (BH 1) | Roksandic et al. (2011) |
| Payre 15 | Verna et al. (2020) |
| Xiahe | Chen et al. (2019) |
| <i>Neandertals</i> | |
| La Chaise (Bourgeois-Delaunay 1) | Condemi (2001) |
| Amud 1 | Original specimen |
| Kebara 2 | Original specimen |
| Shanidar 1 | Trinkaus (1983); Cast |
| Tabun 1 | McCown and Keith (1939); Cast |
| Spy 1 | Cast |
| La Ferrassie 1 | Original specimen |
| La Quina H5, H9 | Original specimen; Martin (1926), Stefan and Trinkaus (1998) |
| Regourdou | Piveteau (1963–1965) |
| Monte Circeo 2, 3 | Sergi (1954, 1955) |
| Cova del Gegant | Original specimen |
| Vindija 206, 207, 226, 231 | Wolpoff et al. (1981); Casts |
| Krapina 57, 58, 59, 63, 66, 68, 69 | Wolpoff et al. (1981), Radovicic et al. (1988); Casts |
| Zafarraya 2 | Barroso et al. (2006) |
| Sima de las Palomas 1, 6, 23, 59 | Trinkaus and Walker (2017) |
| <i>H. sapiens</i> | |
| Qafzeh 7, 9 | Original specimens |

TABLE 2 (Continued)

| Specimen/sample | Source |
|---|--|
| Skhul 2, 5 | McCown and Keith (1939); Original specimen |
| Pestera cu Oase 1 | Trinkaus et al. (2013) |
| Pestera Muerii | Dobos (2010) |
| Dolni Vestonice 3, 13, 14, 15, 16 | Franciscus et al. (2006), Sládek et al. (2000) |
| Pavlov 1 | Franciscus et al. (2006), Sládek et al. (2000) |
| Sunguir 1 | Trinkaus et al. (2014) |
| Ohalo 2 H1, H2 | Original specimens |
| El Mirón | Original specimen |
| Abri Pataud 1 | Original specimen |
| La Madeleine adult | Original specimen |
| Contemporary <i>H. sapiens</i> ($n = 77$) | Original specimens, Quam (1996) |

principal components analysis (PCA). The geometric mean was calculated as the product of n raw variables raised to the power of $1/n$.

To maximize the data available for the fossil samples, we have also estimated some breadth and length dimensions using virtual methods. Measurements were only estimated when at least half of the mandible was preserved and the symphyseal midline could be easily identified. The SH mandibles were scanned using a YXLON MU 2000 high-resolution industrial CT scanner, housed at the Universidad de Burgos in Spain. The scanning parameters are 160 kV, 4 mA, 0.2–0.3 mm interslice distance, and a field of view ranging from 149 to 188 mm. Between 387 and 915 slices per mandible were obtained as a $1,024 \times 1,024$ matrix of 32-bit Float format with a final pixel size that ranged between 0.14 and 0.18 mm (Table S1). Virtual reconstruction of the mandibles, relying on mirror-imaging across the sagittal plane, was carried out using the Mimics v.18 (Materialize, N.V.) software program. The virtual reconstruction initially aligned the two mandibles (the original and its mirror image) relying on the recognition of homologous landmarks. Posteriorly, a “best fit” of the overlapping mesh surfaces was carried out relying on 100 automated iterations (Benazzi et al., 2014). Mirror-imaged measurements are provided for the SH sample in Table S2.

2.4 | Statistical analysis

Statistical analysis of the metric data was carried out using the Statistica v.10™ software program, and a

significance level of $p < 0.05$ was used in all analyses. An analysis of variance (ANOVA) was carried out on the metric variables to test for statistical differences between groups. ANOVA is preferred over multiple t -tests when several groups are compared, since it reduces the chances of a Type I error (Levin et al., 2014). Significant differences between individuals samples were then assessed using the post hoc Tukey's honestly significant difference (HSD) test for unequal samples.

PCA was carried out on the correlation matrix of the size-adjusted metric data (i.e., dividing by the geometric mean) to examine the taxonomic affinities of the SH specimens in multivariate shape space. The PCA included 16 linear measurements, and no indices or angles were included. Only those fossil and recent specimens preserving all the measurements were included in the PCA. By default, PCA generates a similar number of components as variables included in the analysis, however only those components with an eigenvalue >1.0 explain more variation than a single variable in isolation (Kachigan, 1991).

To assess the degree of metric variation in the SH sample, we compared the values for the CV in the metric variables with those for Neandertals and the Kish recent *H. sapiens* samples. The SH sample likely represents a single Pleistocene population (Arsuaga, Martínez, Gracia, Carretero, et al., 1997; Manzi et al., 2000), and variation in this sample is not influenced by the confounding factors of time and geography. For this reason, we restricted the recent *H. sapiens* comparative sample to represent one population for this analysis. The Neandertal sample necessarily includes specimens distributed across a wide geographic region, from Western Europe to southwest Asia, and that represent a considerable time span, mainly during the Late Pleistocene. The sample size for the analysis varied according to the variable under consideration.

In addition, given the differences in sample size, we performed a bootstrapping analysis of the metric variables using the SH and recent *H. sapiens* samples. These both represent single population and the analysis avoids the confounding effects of time and geography. In particular, we generated 5,000 random samples from the Kish *H. sapiens* sample that matched the sample size in the SH hominins. This results in a large number of similarly sized recent *H. sapiens* samples, with a distribution of CV values for comparison with the SH hominin sample.

Finally, to explore potentially size-related variation in the SH sample, we compared correlations between the individual metric variables and the geometric mean. Those variables that are significantly correlated with the geometric mean represent largely size-related variation, while those variables not significantly correlated with the

geometric mean do not vary according to the overall size of the mandible.

3 | ANATOMICAL DESCRIPTIONS OF NEW ADULT ATAPUERCA (SH) INDIVIDUALS AND ASSOCIATIONS BETWEEN SPECIMENS

One new individual and a number of previously recognized individuals which have not been the subject of anatomical descriptions are described here. In addition, a number of new associations have been recognized within the collection. The mandibles described below represent adult specimens, with the M_3 fully erupted, and are all assigned to one of the known dental individuals from the site. Individuals 5, 15, and 27 represent complete or largely complete mandibles that are previously undescribed. Because some of the other mandibles from the SH site have been previously described (detailed below), the morphological descriptions presented here mainly focus on the new additions to these previously known mandibles. Those mandibles not described below were described in previous publications, and no additional elements have been subsequently added. The morphological descriptions of the adult SH specimens presented below generally focus on taxonomically relevant features.

3.1 | Individual IV (AT-250 + 793 + 2553)

The left (AT-250) and right (AT-793) mandibular bodies join near the symphysis, forming a nearly complete mandibular corpus of an adult female individual (Rosas, 1995, 1997; Rosas et al., 2002) (Figure 2). A virtually complete right ascending ramus (AT-2553) was subsequently recovered that joins to the AT-793 right corpus (Figure 2).

The AT-2553 condyle shows pathological alterations. The articular surface is flattened, with exposure of the underlying trabecular bone in a number of spots on the medial portion of the condyle. Taphonomic alterations have led to the loss of a small portion of the right condyle laterally, in the region of the subcondylar tubercle.

The addition of the ascending ramus AT-2553 has confirmed the presence of a retromolar space in Individual IV (Rosas, 2001). An angular notch is absent on the anterior border of the coronoid process, which rises smoothly to the tip, and the AT-2553 ramus shows an asymmetrical configuration, with the coronoid process being much taller than the condyle. The deepest point of the sigmoid notch is located posteriorly, just in front of the condyle, where it intersects it medially. This more medial insertion of the



FIGURE 2 Atapuerca SH Individual 4 consisting of a nearly complete mandibular corpus and complete right ramus. Newly associated elements include the complete right ramus (AT-2553). Clockwise from upper left: superior, inferior, right lateral, left lateral views. *Source:* Image Credit: Javier Trueba, Madrid Scientific Films.

sigmoid notch at the condyle is associated with a large subcondylar tubercle laterally and a well-developed fossa on the medial neck for the insertion of the lateral pterygoid muscle. Moving inferiorly, on the internal surface of the ramus, the muscular insertions for the medial pterygoid are also well developed. Although there is some damage in this region, it is clear that this specimen had a medial pterygoid tubercle marking the superior most point of insertion of this muscle. The mandibular foramen shows a bridge of bone covering the mylohyoid groove, which is enclosed in bone along most of its entire length, being exposed only for a very short distance inferiorly, near its beginning. This corresponds to the horizontal/oval (H/O) condition for the mandibular foramen described previously in some Neandertal specimens (Smith, 1978).

Rosas (2001), based on the more limited evidence previously available, described the masseteric fossa relief as deep in AT-250. This was based on the excavation of the posteriormost aspect of the left lateral corpus. The presence of the right ramus AT-2553 now makes it possible to confirm a deep masseteric fossa as well as a gonial eversion in this specimen. The gonion profile in AT-2553 follows a regular contour and is not truncated. In addition, the basal margin is smooth at the junction between the corpus and ramus and no preangular sulcus is present.



FIGURE 3 Atapuerca SH Individual 5 consisting of a nearly complete mandible. This specimen is associated with Cranium 15 from the SH site. Clockwise from upper left: superior, inferior, right lateral, left lateral views. *Source:* Image Credit: Javier Trueba, Madrid Scientific Films.

3.2 | Individual V (AT-6726 + 6802 + 6901) (Cranium 15)

This is a previously undescribed complete mandible associated with Cranium 15 (Figure 3). The advanced tooth wear indicates this is one of the older individuals within the SH collection. AT-6726 is represented by a nearly complete left hemimandible, preserving the P₃-M₃ in situ in the alveolar sockets. Only slight damage is present in the sigmoid notch. AT-6802 is a right posterior ramus preserving the mandibular condyle and gonial region. Slight damage is present on the medial and lateral aspects of the right mandibular condyle. AT-6901 is most of a right mandibular corpus and anterior ramus that articulates directly with AT-6802. AT-6901 preserves the symphysis, the mandibular corpus and the coronoid process, and the M₁-M₃ are present in the alveolar sockets. There is only slight damage to the anterior alveolar margin.

The symphysis is retreating and largely featureless on its external surface. None of the chin structures are present, nor is there a palpable symphyseal tubercle. A pronounced incisura submandibularis is present along the lower margin of the symphyseal region. Internally, the superior transverse torus is well expressed, with a genioglossal fossa located just inferior to it. The inferior transverse torus is less pronounced, and the digastric fossae are not well defined but oriented posteroinferiorly.

The mandibular corpus shows a fairly even height throughout, with largely parallel alveolar and basal

margins. The corpus shows anterior marginal tubercles, more pronounced on the left side, which accentuate the incisura submandibularis. The single mental foramen is located under the M_1 and is situated in the lower half of the corpus. Moving posteriorly, the lateral prominence is present at around the level of the M_3 . There is a very large retromolar space between the posterior margin of the M_3 and the anterior ramus margin. Internally, the mylohyoid line is well marked and descends diagonally towards the symphyseal region, being more steeply inclined on the right side, and disappearing around the level of the distal M_1 . A pronounced tubercle is present along the internal alveolar margin posterior to the M_3 , representing an alveolar torus. A similar expression of this feature is seen in the maxilla of Cranium 15, which is associated with the mandible.

The anterior margin of the coronoid process shows a clear incisura, and the superior border of the ramus shows a symmetrical configuration, with even heights of the coronoid process and condyle. The sigmoid notch is completely preserved on the right side, and its deepest point is located centrally. The sigmoid notch crest inserts in a central position at the condyle. Both condyles show some evidence of pathological alteration of the articular surface. A well-developed lateral pterygoid fossa is present on the medial neck of the condyle, and a pronounced tuberculum subcondyloideum is present on the lateral aspect of the condylar neck. This is one of the few mandibles in the SH collection where this latter structure is not damaged. On the external surface of the ramus, a masseteric fossa is present and a few markings for the insertion of this muscle can also be discerned. Internally, the markings for the medial pterygoid muscle are well expressed, including the presence of a medial pterygoid tubercle superiorly. The mandibular foramen shows the normal configuration, without bony bridging, and the mylohyoid groove extends inferiorly from the lingula. The gonial region shows a slight truncation, seen better on the left side, but the gonial margin is thickened by the presence of the medial pterygoid muscle markings.

3.3 | Individual VII (AT-303a + 303b + 509 + 776 + 1957 + 4791)

AT-303a and AT-303b were described previously as two fragments coming from the left retromolar area and were associated with the right mandibular corpus fragment of a large male individual AT-1957 (Rosas, 1995, 2001; Rosas et al., 2002) (Figure 4). Recently, AT-303b was recognized as representing a fragment of the right retromolar area and joins with AT-509, a small fragment of the internal corpus from the right side, which was described previously (Rosas, 1995). Together these two fragments join to AT-

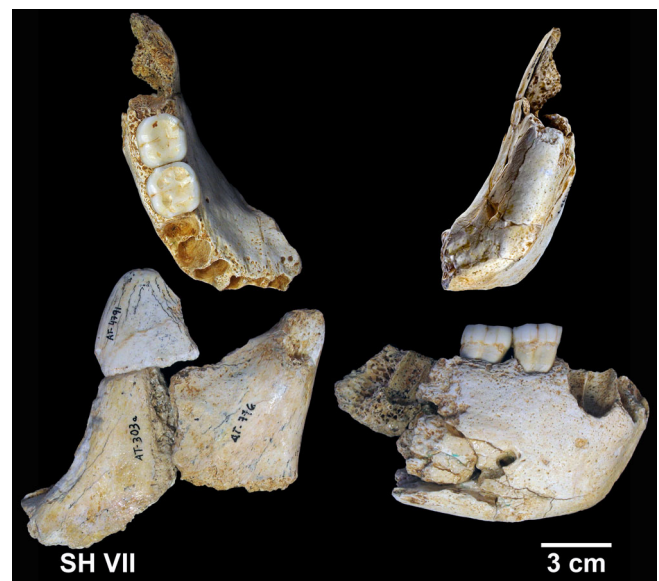


FIGURE 4 Atapuerca SH Individual 7 consisting of a partial right corpus and ramus. Newly associated elements include the left condylar region (AT-776) and the left (AT-4791) and right (AT-1845) coronoid process tips. Clockwise from upper left: superior, inferior, right lateral views of the corpus and lateral view of the left ascending ramus. *Source:* Image Credit: Javier Trueba, Madrid Scientific Films.

1957 to form the posterior margin of the right M_3 alveolus. At the same time, a newly discovered left coronoid process tip (AT-4791) was joined to AT-303a. In addition, AT-776 was previously provisionally ascribed to Individual XXI (Rosas, 1997) but was recently recognized to articulate with AT-303a + 4791. AT-776 is represented by the condylar region of a left mandibular ramus preserving the condyle, a portion of the sigmoid notch and the condylar neck and has been included in previous studies (Rosas, 1997, 2001), but has not been described. AT-720 is a fragment of right mandibular ramus that was described previously (Rosas, 1995, 2001). Recently, the tip of the coronoid process (AT-1845) was joined to the specimen. Although neither the right nor the left rami articulate directly with the right mandibular corpus, based on their robusticity, they can be assigned to Individual VII.

This is the most robust specimen in the collection and shows the strongest superior transverse torus and alveolar planum within the Atapuerca (SH) sample. The symphysis lacks a lateral tubercle on the right side where this region is preserved, and no curvature of the symphysis is visible. The left ramus shows a very large retromolar space. Although the anterior margin of the coronoid process is abraded, there is no angular notch. In addition, the tip of the coronoid process is taller than the condyle, giving the sigmoid notch an asymmetrical appearance. Despite some damage to the condyle, it is clear that the sigmoid notch inserted in a relatively medial position at



FIGURE 5 Atapuerca SH Individual 12 consisting of a complete corpus and partial right and left rami. Newly associated elements include the left corpus and partial ramus (AT-4147). Clockwise from upper left: superior, inferior, left lateral, right lateral views. *Source:* Image Credit: Javier Trueba, Madrid Scientific Films.

the condyle and a large subcondylar tubercle was present. The condyle is large (AP = 10.2 mm, ML = 28.0 mm est.) and has a robust appearance. However, the lateral pterygoid fossa is not particularly developed.

3.4 | Individual XII (AT-300 + 4147)

AT-300 is a right hemimandible of a young adult male individual which has been described previously and included in a number of studies (Rosas, 1995, 1997, 2001; Rosas et al., 2002; Rosas & Bastir, 2004) (Figure 5). A left hemimandible (AT-4147) was subsequently discovered and joins to AT-300 at the symphysis, forming a nearly complete mandible. The new left side preserves the mandibular corpus from the I₁-M₃ (with I₂-M₃ in situ in the alveolar sockets) and the coronoid process of the ramus, which is eroded at its tip.

AT-300 was previously suggested to show a retromolar space (Rosas, 1995, 2001). However, when the M₃s are aligned in lateral view in the complete specimen, the anterior margin of the coronoid process overlaps the posterior margin of the M₃ on both sides. Thus, this specimen lacks a retromolar space. The anterior margin of the coronoid process is better preserved on the left side and runs smoothly superiorly, lacking an angular notch.

The structures of the lateral corpus in AT-4147 show a posterior placement relative to the tooth row and resemble those described previously in AT-300 (Rosas, 1995). The

mental foramen on the left side is single and is located below the P4/M1 septum in a relatively low position on the corpus. The anterior marginal tubercle in AT-300 was said to show the maximum expression within the Atapuerca (SH) sample, and the new left hemimandible AT-4147 also shows an extreme development of this feature. Internally, the mylohyoid line in AT-4147 follows a less diagonal course than in AT-300, suggesting some degree of variation in this feature. Both sides do, however, show a clear submandibular fossa.

The presence of a complete symphysis also makes it possible to address the development of the mental trigone and anterior symphyseal curvature in this specimen. Both these structures were argued to be present in AT-300 (Rosas, 1995, 1997). However, the more complete specimen does not show any significant development of either a symphyseal tubercle or anterior curvature. Their reported presence in AT-300 may be a product of the misalignment of the C₁ and I₂ on the right side, which gives the impression of a more pronounced curvature (Rosas, 1995). The complete symphysis does not show any sign of lateral tubercles, a mental trigone or mental fossae.

The internal aspect of the complete symphysis shows a deep genioglossal fossa bounded by well-developed superior and inferior transverse tori. Separation of the two halves along the midline of the symphysis makes it possible to study aspects of the symphyseal cross-section, which is better preserved in the new left hemimandible. In cross-section, the cortical bone shows a marked thickening at each of the tori and in the base of the symphysis. In basal view, the symphyseal region shows a square contour, exaggerated by the extreme development of the anterior marginal tubercles of the lateral corpus. In addition, the large anterior marginal tubercles contribute to the formation of a well-developed incusura submentalis in the basal region of the symphysis. However, the impressions for the digastric fossae are barely discernible.

3.5 | Individual XV (AT-2193 + 2439) (Cranium 17)

These two specimens were previously recognized as belonging to the same individual (Rosas et al., 2002) and have been included in previous studies of the mandibular remains from the site (Rosas, 2001; Rosas & Bastir, 2004) (Figure 6). This mandible corresponds to a young adult individual and was considered to represent a female (Rosas et al., 2002), but it has not been described previously.

AT-2193 is a right hemimandible, which includes the ascending ramus and mandibular corpus up to the level of the distal alveolar socket of the right I₂. The gonial region is missing, as is a small area of bone on the external



FIGURE 6 Atapuerca SH Individual 15 consisting of a complete right hemimandible and symphyseal region. This specimen is associated with Cranium 17 from the SH site. Clockwise from upper left: superior, inferior, right internal, right lateral views. *Source:* Image Credit: Javier Trueba, Madrid Scientific Films.

posterior corpus, and the tip of the coronoid process is slightly eroded. The symphyseal region (AT-2439), preserving the symphysis from the mesial portion of the alveolar socket for the right I₂ to the mesial portion of the alveolar socket for the left C₁ articulates with AT-2193.

A clear retromolar space is present, and the anterior margin of the ascending ramus lacks an angular notch, rising smoothly to the coronoid process tip. The original height of the coronoid process is difficult to determine due to the erosion of its tip, but it would have been somewhat taller than presently preserved. Thus, this specimen would most likely have shown an asymmetrical configuration of the coronoid process and condyle, although perhaps less pronounced than in other Atapuerca (SH) mandibles. The deepest point of the mandibular incisure is located centrally and the incisure crest inserts lateral of the condyle articular surface. A well-developed subcondylar tubercle was present lateral of the condyle.

On the medial surface of the ramus, the lateral pterygoid insertion is not pronounced. The mandibular foramen shows the horizontal/oval (H/O) morphology, being crossed by a bridge of bone at its opening, and the mylohyoid groove is visible further inferiorly. Despite damage to the gonial region, a clear medial pterygoid tubercle is present.

On the external aspect of the ramus, a masseteric fossa is present. Anterior to this, the basal margin continues smoothly from the corpus to the ramus and there is no preangular sulcus. The lateral prominence is located

at the level of the M₃, and the mental foramen is placed under the mesial root of the M₁ in the lower half of the corpus. The anterior marginal tubercle lies just below this along the basal margin. On the internal aspect of the corpus, the mylohyoid line runs diagonally and is in a low position at the level of the M₃. A clear submandibular fossa is present below the mylohyoid line, which disappears at around the mesial root of the M₁. Anterior to this, there is no sublingual fossa.

The external symphysis is receding and shows no signs of any of the structures associated with the modern human chin. In particular, the symphyseal tubercle, lateral tubercles, mental trigone, mental fossa, and incurvatio mandibulae anterior are all absent, and the external surface is largely featureless. Internally, a genioglossal fossa is bounded by superior and inferior transverse tori. At the base of the symphysis, the digastric fossae are difficult to discern, but there is a well-developed incisura submandibulae.

3.6 | Individual XXI (AT-888 + AT-721 + AT-3876 + AT-3877 + AT-3878) (Cranium 5)

The mandibular corpus (AT-888) and right ramus (AT-721) of this mandible have been previously described (Rosas, 1997) (Figure 7). This specimen articulates well with Cranium 5 shows a similar degree of tooth wear and is considered to represent an adult male individual (Rosas et al., 2002). It was previously suggested that the left ramus fragment AT-776 might also belong to this same individual (Rosas, 1997). However, this specimen directly articulates with AT-303a and belongs to Individual VII. Subsequently, the left condylar region (AT-3876), gonion (AT-3877) and coronoid process (AT-3878) were recovered and join the previously described mandibular corpus (AT-888). The addition of these fragments results in a largely complete mandible.

The morphological details of the left ramus largely mirror those described previously for the right side. It is notable that this specimen does not show an asymmetrical configuration of the coronoid process and condyle, which appear to be approximately equal in height.

3.7 | Individual XXII (AT-605 + AT-3958 + AT-4794)

The specimen AT-605 was described previously (Rosas, 1995) and has been assigned to a young adult male individual (Rosas et al., 2002) (Figure 8). The retromolar area and base (AT-4794) as well as the tip (AT-



FIGURE 7 Atapuerca SH Individual 21 consisting of a nearly complete mandible. Newly associated elements include the left condylar region (AT-3876), gonion (AT-3877) and coronoid process (AT-3878). This specimen is associated with Cranium 5 from the SH site. Clockwise from upper left: superior, inferior, left lateral, right lateral views. *Source:* Image Credit: Javier Trueba, Madrid Scientific Films.

3958) of the right coronoid process were subsequently recovered and join to the right mandibular corpus. The anatomical details mirror those of the left side. This specimen shows a very large retromolar space, and the anterior margin of the tall coronoid process rises smoothly superiorly, with no trace of an angular notch.

3.8 | Individual XXVII (AT-792 + AT-4495)

AT-792 consists of a largely complete mandibular corpus of an adult male individual (Rosas, 1997, 2001; Rosas et al., 2002) (Figure 9). It has been included in previous studies but never described. In addition, a portion of the left ascending ramus (AT-4495) conserving the complete coronoid process, part of the sigmoid notch, the mylohyoid groove and mandibular foramen was subsequently recovered and joins to AT-792.

The external symphysis presents a symphyseal tubercle along the midline, but lacks lateral tubercles, a mental trigone or mental fossae. The anterior curvature of the symphysis is more pronounced than in other specimens in the collection, but this appears to be largely due to the premortem loss of the right I_1 and subsequent alveolar resorption. The degree of expression (or absence) of most of the other chin structures in this specimen is similar to that seen in most of the other SH mandibles.



FIGURE 8 Atapuerca SH Individual 22 consisting of a complete corpus and left ramus and a partial right ramus. Newly associated elements include the retromolar area and base (AT-4794) as well as the tip (AT-3958) of the right coronoid process. Clockwise from upper left: superior, inferior, left lateral, right lateral views. *Source:* Image Credit: Javier Trueba, Madrid Scientific Films.

The internal face of the symphysis descends steeply below the alveolar margin to a clear superior transverse torus about midway down the symphysis. Moving inferiorly, a genioglossal fossa is present along the midline and sublingual fossae are present on either side. This is the only specimen in the collection that shows a sublingual fossa. A blunt crest emanates from the genioglossal fossa and courses over the inferior transverse torus. The modest degree of expression of both the superior and inferior transverse tori is less pronounced than in other mandibles within the Atapuerca (SH) collection. The digastric fossae are well marked and face inferiorly and a clear *incisura submentalis* is present along the basal margin of the symphysis.

On the lateral corpus, a single mental foramen is located below the M_1/M_2 alveolar socket and is placed in the lower half of the mandibular corpus. The anterior marginal tubercle is located along the basal margin below the mental foramen, but no posterior marginal tubercle is present. The lateral prominence is located near the posterior border of the M_3 , and no preangular sulcus is present along the posterior basal margin. Internally, the mylohyoid line is placed relatively far from the alveolar margin at the level of the M_3 and descends in a diagonal course anteriorly, delimiting a deep submandibular fossa.

This specimen shows the largest retromolar space within the collection. Some remodeling of the posterior



FIGURE 9 SH Individual 27 consisting of a nearly complete mandibular corpus and newly associated portion of the left ascending ramus (AT-4495). Clockwise from upper left: superior, inferior, left lateral, right lateral views. *Source:* Image Credit: Javier Trueba, Madrid Scientific Films.

alveolar margin and anterior border of the coronoid process seems to be present and may be contributing to the large size of the retromolar space. The alveolar socket for the M_3 is enlarged, and the alveolar margin extends posteriorly for approximately 11.0 mm behind the M_3 . In addition, the tall coronoid process shows a clear angular notch along its anterior border. Although the condyle is not present, the preserved course of the sigmoid notch descends rapidly from the tip of the coronoid and is clearly asymmetrical, with the deepest point located posteriorly, near the (missing) condyle. Internally, the mylohyoid groove is visible along its entire length and reaches the mandibular foramen, which shows a normal morphology. Externally, a masseteric fossa is present and several bony ridges extend more or less vertically marking insertion points of the masseter muscle.

3.9 | Individual XXVIII (AT-950 + 3924)

AT-950 consists of a nearly complete mandible of an adult female individual described previously (Rosas, 1997, 2001; Rosas et al., 2002). A fragment of the internal aspect of the right corpus comprising the medial margin of the M_1 alveolus (AT-3924) was subsequently recovered.

4 | SEX ESTIMATION AND SEX RATIO IN THE SH MANDIBULAR SAMPLE

Sex assignments for the SH mandibular sample (Table 3) have been approached previously based on metric and morphological criteria in the mandibles and associated teeth (Bermúdez de Castro et al., 2001, 2004; García-Campos et al., 2020; Rosas et al., 2002). The discovery of some new specimens and the addition of elements to previously analyzed specimens make it possible to re-examine some of these sex assignments. In particular, some of the most sexually dimorphic dimensions identified by Rosas et al. (2002) are also included in the present study and can now be examined in a few additional individuals to provide further insights into their sex assignment.

Individual 4 was previously classified as female based on the preserved mandibular corpus, but Rosas et al. (2002) noted that some morphological features might indicate a male classification. No canine is currently associated with the mandible from Individual 4, but the canine socket is large, consistent with a male classification. The discovery of a complete right ramus makes it possible to consider a more complete set of measurements. In particular, the bicondylar and bigonial breadths in this specimen are the largest in the adult SH sample, while the bicoronoid breadth is only surpassed by one other individual. The geometric mean for this specimen is also among the largest in the SH sample, indicating an overall large mandible. These considerations indicate that the mandible representing Individual 4 should be reclassified as a male.

The mandible associated with Individual 5 was only discovered recently and was not studied by Rosas et al. (2002). Analysis of the canine was inconclusive regarding the sex assignment (García-Campos et al., 2020) in this individual. Regarding the sexually dimorphic dimensions identified by Rosas et al. (2002), the bicoronoid and bigonial breadths as well as the corpus heights at the symphysis and mental foramen are all below the adult SH mean values, while the total mandibular length and gonial length are just above the adult SH means and the geometric mean is nearly identical to the SH sample mean. The mandible is associated with Cranium 15, one of the older individuals from the SH site, and the cranial capacity is only slightly above the adult SH mean. We tentatively assign a female sex to this individual, based on the modest dimensions in the mandible, but the pronounced masseter and medial pterygoid muscle markings, could perhaps be considered to be more consistent with a male assignment.

Individual 7 was previously classified as male based both on the mandible and canine (García-Campos

TABLE 3 Sex estimation of the SH mandibles.

| Dental individual | Developmental age | Mandible sex ^a | Mandible + teeth sex ^b | Canine sex ^c | This study | Final sex estimation |
|-------------------|-------------------|---------------------------|-----------------------------------|-------------------------|------------|----------------------|
| I | Young adult | F | F | F | | F |
| II | Subadult | | | ? | | ? |
| III | Subadult | F | F | F | | F |
| IV | Adult | F | F | | M | M |
| V (Cr. 15) | Old adult | | | ? | F | F |
| VI | Young adult | F | F | | | F |
| VII | Adult | M | M | M | M | M |
| X | Subadult | F | F | F | | F |
| XII | Young adult | M | M | M | M | M |
| XV (Cr. 17) | Young adult | F | F | F | | F |
| XVI (Cr. 9) | Subadult | | | F | | F |
| XIX | Young adult | F | F | | | F |
| XXI (Cr. 5) | Old adult | M | M | | M | M |
| XXII | Adult | M | M | | | M |
| XXIII (Cr. 16) | Subadult | F | F | F | | F |
| XXIV | Subadult | | | F | | F |
| XXV | Subadult | | F | F | | F |
| XXVI (Cr. 10) | Young adult | F | F | | | F |
| XXVII | Adult | M | M | M | | M |
| XXVIII | Adult | F | F | F | | F |

^aRosas et al. (2002).

^bBermúdez de Castro et al. (2004).

^cGarcía-Campos et al. (2020).

et al., 2020; Rosas et al., 2002). The new association of additional elements supports this diagnosis. The mandibular corpus is the thickest and most robust within the SH sample, and the associated coronoid process and condyle show a similarly robust appearance. Thus, all indications are that this is a male individual.

Individual 12 was previously classified as a male by Rosas et al. (2002) and García-Campos et al. (2020). The discovery of the left corpus and partial ramus make it possible to consider a more complete set of measurements. The bicoronoid and bicondylar breadths are close to the adult SH mean and are not suggestive of a particular sex assignment. However, this specimen shows the most pronounced expression of the anterior marginal tubercles in the entire adult SH sample, resulting in a very wide and flaring basal margin for the anterior mandibular corpus. This exaggerated expression, based on the more complete mandible, seems to clearly suggest a male classification, consistent with the previous suggestions.

The mandible representing Individual 21 is associated with the most complete cranium from the site (Cranium

5) and a complete set of cervical vertebrae. This mandible was previously classified as a male, although Rosas et al. (2002) noted that some morphological features might indicate a female classification. The cranium combines some clearly male features, including a well-developed supraorbital torus and large, projecting mastoid processes with an absolutely small brain size (Arsuaga, Martínez, Gracia, & Lorenzo, 1997), and the atlas and axis have been sexed as male (Gómez-Olivencia et al., 2007). The addition of the left ramus now makes it possible to measure the bicondylar, bicoronoid and bigonial breadths, but the modest values for these measures do not provide any clear insights into the sex assignment, and this individual is still best regarded as male.

Rosas et al. (2002) previously reported a bias in the sex ratio within the mandibular sample, with an overabundance (66.7%) of females (10 of 15 sexed individuals). Nevertheless, most females were represented by adolescent and young adult (<20 years of age at death) individuals, while most male individuals were represented by older adult individuals (>20 years of age at death). The few exceptions were a female assignment for SH

Individuals 4 (26–32 years of age) and 28 (24–30 years of age) and a male assignment for Individual 12 (17–19 years of age).

The expanded mandibular sample in the present study includes one new adult specimen sexed as female (Individual 5) and one adult individual being reclassified from female to male (Individual 4). The combined evidence continues to suggest a bias towards females in the SH mandibular sample, with 13 individuals representing females (65%), 6 individuals representing males (30%), and 1 individual, whose sex could not be estimated (5%). If the analysis is restricted to only adult individuals, then the sample represents a nearly balanced-sex composition of seven females (53.8%) and six males (46.2%).

Based on the individuals with an associated mandible, there appears to be an age bias in the sex assignments, with all the subadult individuals being sexed as females (Table 3). However, the MNI for the site based on the dentition does include some subadult male individuals that currently lack associated mandibles (Individuals 18 and 20) (Bermúdez de Castro et al., 2004). When the entire sample is considered, male and female individuals can be found in all age categories and the SH sample is considered sex balanced (Bermúdez de Castro et al., 2004).

5 | METRIC ANALYSIS

5.1 | Geometric mean

The geometric mean shows some variation in the SH sample, with Individuals 5, 15, 19, and 28 falling on the smaller side and Individuals 4, 21, and 22 representing larger individuals (Table 4). Among the European MP specimens, Arago 13 and Mauer fall above the SH range of variation, and these are the largest mandibles in any of the samples. Nevertheless, only the recent *H. sapiens* sample shows a statistically smaller geometric mean, indicating considerably smaller mandibles overall. While the fossil groups are fairly similar in overall size, 83% (20/24) of the recent *H. sapiens* individuals fall below the lower limit of the range of variation in the fossil groups. The coefficient of variation (CV) in the geometric mean in the fossil groups, except for the European MP sample, falls within the CV of recent *H. sapiens*, indicating a broadly similar range of size variation across the samples.

5.2 | Mandibular lengths and breadths

The total mandibular lengths and gonial lengths in the adult SH individuals show a nearly bimodal distribution,

with Individuals 12, 15, 19, and 28 showing small dimensions and Individuals 4, 5, 21, and 22 showing considerably larger dimensions. The adult SH individuals show no significant differences in either the total mandibular length or gonial length when compared to the European MP specimens and Neandertals (Table 4). Among the European MP specimens, Mauer (121.0 mm) shows the longest mandible, while l'Aubesier (102.0 mm) is the shortest, falling just below the smallest SH mandible. Similarly, La Ferrassie 1 (127.0 mm), Shanidar 1 (120.0 mm), Amud 1 (118.0 mm) and Krapina 59 (117.0 mm) are among the longest Neandertal specimens, while Zafarraya 2 (103.0 mm) and Tabun 1 (c.95.0 mm) fall toward the lower end of the Neandertal range of variation and at or below the lower limit of the SH range. The SH sample is statistically longer than the recent *H. sapiens* sample in both the total mandibular length and the gonial length but does not differ from the fossil *H. sapiens* in either measurement.

Among the SH specimens, Individual 4 shows the widest bicondylar (148.8 mm) and bigonial (110.7 mm) breadths, and the bicoronoid breadth (120.2 mm) is only exceeded by that in Individual 27 (121.5 mm). Individual 19 uniformly shows the smallest breadth values. The remaining SH individuals are fairly similar in their bicondylar breadths, but vary more in the bicoronoid and bigonial breadths. There are no significant differences in the bicondylar, bicoronoid or bigonial breadths between the SH sample and European MP specimens or Neandertals. In contrast, the bicondylar and bicoronoid breadths in the SH sample are significantly larger than both the fossil and recent *H. sapiens* samples. Three fossil *H. sapiens* (Skhul 5, Oase 1 and Sunghir 1) and one recent *H. sapiens* individual fall within the adult SH range for the bicondylar breadth, while the bigonial breadth measure shows more overlap. Indeed, the bigonial breadth did not differ between any of the samples under comparison.

A scatterplot comparing the total mandibular length with the bicondylar breadth reveals a significant correlation ($r = 0.61$) and generally separates the Neandertal clade samples from fossil and recent *H. sapiens* (Figure 10). Nearly all the Neandertal clade specimens fall above the pooled regression line, indicating wide bicondylar breadths for their mandibular length. Only SH Individual 19 and the La Chaise B-D 1 Neandertal fall within the recent human 95% confidence ellipse. The longest fossil specimen is represented by Arago 13, while the widest specimens include SH Individual 4, Kebara 2 and La Quina H9. However, the resulting mandibular index shows significant differences only between Neandertals and the fossil and recent *H. sapiens* (Table 4).

TABLE 4 Length and breadth measurements (mm) of the mandible in the Atapuerca (SH) sample and Pleistocene and recent humans.

| Specimen/sample | Total mandibular length M 68(1) | Gonial length M 68 | Bicondylar breadth M 65 | Biconoid breadth M 65(1) | Bigonial breadth M 66 | Dental arcade length M 80(a) | Dental arcade breadth (M3) M 80(1) | Mandibular index | Dental arcade index | Geometric mean |
|---------------------------------|------------------------------------|-------------------------|----------------------------|-----------------------------|---------------------------|---------------------------------|---------------------------------------|-------------------------|-------------------------|-------------------------|
| <i>Atapuerca (SH)</i> | | | | | | | | | | |
| Individual I | | | | | | 54.7 | 74.4 | | 73.5 | |
| Individual IV | 117.7 ^a | 94.7 ^a | 148.8 ^a | 120.2 ^b | 110.7 ^a | 49.3 | 75.2 | 79.1 | 65.6 | 51.4 |
| Individual V (Cr. 15) | 115.0 | 93.0 | 135.0 | 106.0 | 96.4 | 50.8 | 67.4 | 85.2 | 75.4 | 48.5 |
| Individual XII | 102.9 ^a | | 133.1 ^a | 113.4 ^a | | 53.4 | 73.4 | 77.3 | 72.8 | |
| Individual XV (Cr. 17) | 103.5 ^a | 83.0 ^a | 135.8 ^a | 112.6 ^a | 93.1 ^a | 49.6 ^a | 73.0 ^a | 76.2 | 67.9 | 46.7 |
| Individual XVI | | | | | | 56.7 ^a | 70.5 ^a | | 80.4 | |
| Individual XIX | 104.0 | 79.0 | 126.9 ^a | 103.4 | 91.1 ^a | 50.7 | 67.8 | 82.0 | 74.8 | 44.6 |
| Individual XXI (Cr. 5) | 121.5 | 96.0 | 130.2 ^a | 105.0 | 102.0 | 54.8 | 70.7 | 86.8 | 77.5 | 51.0 |
| Individual XXII | 121.9 ^a | 96.0 ^a | 133.0 ^a | 118.1 | 109.2 ^a | 54.3 | 72.2 | 93.3 | 75.2 | 52.2 |
| Individual XXVII | | | | 121.5 | | 54.1 | 74.2 ^a | | 72.9 | |
| Individual XXVIII | 108.0 | 85.0 | 133.7 | 104.1 | 102.7 | 55.2 | 69.7 | 80.8 | 79.2 | 46.8 |
| Atapuerca (SH) | 111.8 ± 8.1 (7.3) | 89.5 ± 7.0 (7.9) | 134.6 ± 6.4 (4.8) | 111.6 ± 7.2 (6.5) | 100.7 ± 7.6 (7.5) | 53.1 ± 2.5 (4.7) | 71.7 ± 2.7 (3.7) | 82.6 ± 5.7 (6.8) | 74.1 ± 4.4 (6.0) | 48.7 ± 2.9 (5.9) |
| Mean ± s.d. (CV) | | | | | | | | | | |
| Atapuerca (SH) | 102.9–121.9 (8) | 79.0–96.0 (7) | 126.9–148.8 (8) | 103.4–121.5 (9) | 91.1–110.7 (7) | 49.3–56.7 (11) | 67.4–75.2 (11) | 76.2–93.3 (8) | 65.6–80.4 (11) | 44.6–52.2 (7) |
| Range (n) | | | | | | | | | | |
| Xiahe | | | | | 96.8 | | | | | |
| Euro. Mid. Pleist. | 114.9 ± 10.0 (8.7) | 96.1 ± 6.2 (6.5) | 135.6 ± 4.9 (3.6) | 113.5 ± 9.5 (8.3) | 98.5 ± 11.5 (11.7) | 59.2 ± 7.2 (12.1) | 72.0 ± 5.5 (7.6) | 87.2 ± 6.1 (7.0) | 82.3 ± 7.4 (9.0) | 51.2 ± 4.0 (7.7) |
| mean ± s.d. (CV) | | | | | | | | | | |
| Euro. Mid. Pleist. | 102.0–129.0 (5) | 87.3–100.9 (4) | 131.0–140.9 (4) | 100.0–122.0 (4) | 83.2–107.4 (4) | 52.0–72.5 (6) | 64.0–79.0 (6) | 80.5–92.4 (4) | 74.3–94.9 (6) | 46.6–55.1 (4) |
| Range (n) | | | | | | | | | | |
| Neandertal | 112.2 ± 8.4 (7.5) | 90.5 ± 5.4 (6.0) | 136.3 ± 10.9 (8.0) | 108.3 ± 8.3 (7.7) | 97.2 ± 9.0 (9.2) | 53.6 ± 2.8 (5.2) | 73.8 ± 3.2 (4.3) | 80.9 ± 7.0 (8.6) | 72.9 ± 4.9 (6.7) | 49.4 ± 2.3 (4.6) |
| mean ± s.d. (CV) | | | | | | | | | | |
| Neandertal range | 98.5–127.0 (10) | 79.0–100.0 (10) | 110.0–150.0 (11) | 94.0–117.1 (8) | 82.0–108.0 (11) | 50.0–58.0 (15) | 67.1–80.1 (16) | 70.7–93.4 (10) | 66.1–81.8 (15) | 45.2–51.6 (7) |
| (n) | | | | | | | | | | |
| Fossil <i>H. sapiens</i> | 110.0 ± 6.7 (6.1) | 87.0 ± 4.8 (5.5) | 119.6 ± 10.5 (8.8) | 93.6 ± 8.7 (9.3) | 96.2 ± 8.3 (8.7) | 54.7 ± 5.3 (9.8) | 66.3 ± 3.9 (5.8) | 93.6 ± 6.0 (6.4) | 80.9 ± 6.8 (8.4) | 48.1 ± 1.6 (3.3) |
| mean ± s.d. (CV) | | | | | | | | | | |
| Fossil <i>H. sapiens</i> | 101.0–122.0 (10) | 80.0–95.0 (11) | 103.0–133.0 (9) | 81.0–112.0 (11) | 83.0–107.0 (10) | 46.2–63.5 (8) | 62.5–72.6 (13) | 86.1–100.9 (8) | 68.9–88.2 (8) | 45.9–49.7 (4) |
| range (n) | | | | | | | | | | |
| Recent <i>H. sapiens</i> | 100.8 ± 6.5 (6.5) | 73.3 ± 4.9 (6.6) | 111.1 ± 8.1 (7.3) | 92.0 ± 6.5 (7.0) | 93.4 ± 7.1 (8.3) | 48.5 ± 3.2 (6.6) | 59.6 ± 4.4 (7.4) | 90.6 ± 7.7 (8.5) | 82.1 ± 7.7 (9.4) | 41.8 ± 2.5 (6.0) |
| mean ± s.d. (CV) | | | | | | | | | | |
| Recent <i>H. sapiens</i> | 85.0–114.0 (74) | 64.0–87.0 (76) | 93.0–131.0 (54) | 77.0–116.0 (67) | 81.0–114.0 (69) | 41.0–54.0 (56) | 51.0–71.0 (57) | 75.2–111.2 (54) | 67.2–100.0 (49) | 38.6–48.9 (24) |
| range (n) | | | | | | | | | | |

TABLE 4 (Continued)

| Specimen/sample | Total mandibular length M 68(1) | Gonial length M 68 | Bicondylar breadth M 65 | Bicoronoid breadth M 65(1) | Bigonial breadth M 66 | Dental arcade length M 80(a) | Dental arcade breadth (M3) M 80(1) | Mandibular index | Dental arcade index | Geometric mean |
|--|------------------------------------|-----------------------|----------------------------|-------------------------------|--------------------------|---------------------------------|---------------------------------------|------------------|---------------------|---------------------|
| ANOVA (p value) | p < 0.001 | p < 0.001 | p < 0.001 | p < 0.001 | <i>p</i> = 0.07 | p < 0.001 | p < 0.001 | p = 0.001 | p < 0.001 | p < 0.001 |
| SH versus MP Europe | 0.999 | 0.577 | 0.999 | 0.999 | 0.835 | 0.347 | 0.999 | 0.996 | 0.586 | 0.650 |
| SH versus Neandertals | 0.999 | 0.941 | 0.994 | 0.886 | 0.706 | 0.970 | 0.824 | 0.972 | 0.999 | 0.989 |
| SH versus fossil <i>H. sapiens</i> | 0.985 | 0.976 | 0.007 | <0.001 | 0.541 | 0.734 | 0.027 | 0.067 | 0.190 | 0.997 |
| SH versus recent <i>H. sapiens</i> | 0.016 | <0.001 | <0.001 | <0.001 | 0.228 | 0.040 | <0.001 | 0.275 | 0.042 | <0.001 |
| MP Europe versus Neandertals | 0.999 | 0.848 | 0.999 | 0.994 | 0.999 | 0.619 | 0.837 | 0.943 | 0.481 | 0.849 |
| MP Europe versus fossil <i>H. sapiens</i> | 0.998 | 0.353 | 0.220 | 0.029 | 0.999 | 0.901 | 0.354 | 0.713 | 0.999 | 0.437 |
| MP Europe versus recent <i>H. sapiens</i> | 0.185 | <0.001 | 0.011 | 0.014 | 0.999 | 0.002 | <0.001 | 0.913 | 0.981 | <0.001 |
| Neandertals versus fossil <i>H. sapiens</i> | 0.954 | 0.554 | 0.001 | 0.001 | 0.998 | 0.963 | <0.001 | 0.013 | 0.123 | 0.955 |
| Neandertals versus recent <i>H. sapiens</i> | 0.003 | <0.001 | <0.001 | <0.001 | 0.869 | 0.001 | <0.001 | 0.035 | 0.003 | <0.001 |
| Fossil <i>H. sapiens</i> versus recent <i>H. sapiens</i> | 0.030 | <0.001 | 0.234 | 0.985 | 0.970 | 0.003 | <0.001 | 0.961 | 0.996 | 0.011 |

Note: Mandibular index = (total mandibular length/bicondylar breadth) × 100. Dental arcade index = (dental arcade length/dental arcade breadth) × 100. See main text for calculation of geometric mean.

*Estimated using mirroring (see Section 2).

Values in bold indicate a significant difference (p < 0.05).

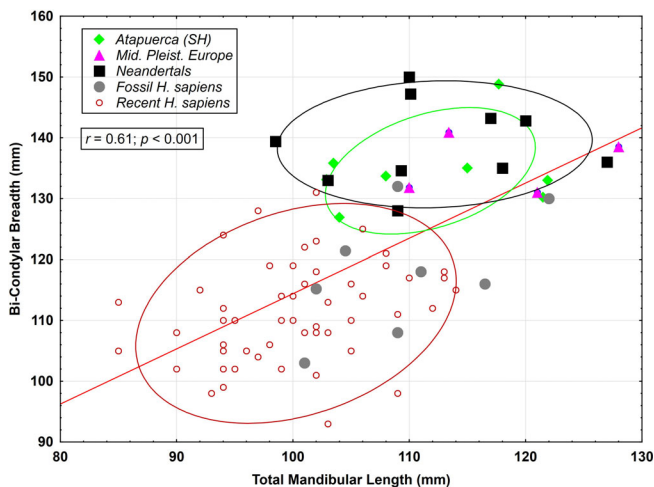


FIGURE 10 Scatterplot of total mandibular length versus bicondylar breadth (mandibular index) in the fossil and recent specimens. The pooled sample regression line is shown.

5.3 | Dental arcade

The dental arcade length and breadth in the SH sample show some of the lowest CV values of any of the linear measurements, suggesting a degree of stability in the dimensions of the dental arcade. The dental arcade length in the SH sample shows no significant differences from either the European MP sample or Neandertals (Table 4). Nevertheless, 67% of the European MP sample shows dental arcades that are longer than in SH, falling above the range of variation. All the fossil samples show significantly longer dental arcades than do recent *H. sapiens*. In terms of the dental arcade breadth, no significant differences were found between the SH sample, European MP specimens or Neandertals, while the fossil and recent *H. sapiens* samples showed a narrower dental arcade compared with the fossil groups. The dental arcade index in the SH sample does not differ significantly from either the European MP specimens or Neandertals. However, the majority of the European MP sample again falls above the adult SH range of variation, mainly related to their longer dental arcades.

5.4 | Symphysis

The symphysis is clearly retreating in the SH hominins. Within the SH sample, the highest value for the chin angle is seen in individual 12 (75°), while similarly high values are also found in individuals 5, 15 and 21 (72°) (Table 5). The lowest angle is seen in individual 27 (65°), followed by individuals 7 (66°) and 1 (67°). The mean angle in the adult SH sample is nearly identical to the

small sample of European MP fossils. Both samples show a very similar range of variation and are not significantly different from one another. In contrast, the mean angles in both samples are significantly lower than in the Neandertals, who show more vertical symphyses. Fourteen of 19 Neandertal specimens (74%) fall above the adult SH range of variation. Thus, there is a clear metric trend for more vertical symphyses within the Neandertal clade (Figure 11). The recent *H. sapiens* sample has a significantly higher chin angle than any of the Neandertal clade samples, and a similar mean to the fossil *H. sapiens* sample, reflecting a largely vertical symphysis.

Within the adult SH sample, Individual 27 shows the tallest symphysis (40.3 mm), followed by individuals 4 (36.2 mm) and 21 (36.0 mm), while individual 19 shows the shortest (27.0 mm) symphysis (Table 5). Regarding the thickness of the symphysis, Individual 1 (17.8 mm) shows the thickest symphysis, followed by individual 4 (16.8 mm), while individual 19 (13.3 mm) has the thinnest symphysis in the SH sample. The resulting robusticity index is highest in SH Individual 1 (56.7) and lowest in Individual 27 (40.0). Both the early Pleistocene mandible ATE 9-1 from the Sima del Elefante site and the late middle Pleistocene Xiahe 1 specimen show values for the symphysis which are very similar to the mean values in the SH sample. Pairwise comparison of the fossil and recent samples for the height, thickness and robusticity at the symphysis revealed no statistically significant differences between any of the groups.

5.5 | Mental foramen

The bimental foramen breadth provides a measure of the width of the anterior mandibular corpus. Within the SH sample, Individual 27 (61.1 mm) shows the widest bimental foramen breadth, followed by Individual 4 (57.0 mm), while Individual 15 (49.9 mm) and Individual 19 (50.9 mm) show the narrowest breadths (Table 6). The bimental foramen breadth shows no significant differences between the SH hominins, European MP specimens or Neandertals. In contrast, the fossil and recent *H. sapiens* sample shows significantly narrower breadths than the other three groups. Thus, there is a clear separation between the Neandertal clade groups and the *H. sapiens* groups in the bimental foramen breadth.

The vertical position of the mental foramen within the mandibular corpus can be assessed by an index comparing its height above the basal margin to the corpus height at the level of the mental foramen (Figure 12). A value of 50 indicates a mental foramen that is located exactly at mid-corpus, and a value of <45 would indicate

TABLE 5 Symphysis measurements (mm) of the mandible in the Atapuerca (SH) sample and Pleistocene and recent humans.

| | Angle of chin to alveolar plane (deg.) | Corpus height at symphysis | Corpus thickness at symphysis | Robusticity index at symphysis |
|--|--|----------------------------|-------------------------------|--------------------------------|
| Specimen/sample | M 79(1b) | M 69 | | |
| <i>Atapuerca (SH)</i> | | | | |
| Individual I | 67.0 | 31.4 | 17.8 | 56.7 |
| Individual IV | 69.0 | 36.2 | 16.8 | 46.4 |
| Individual V (Cr. 15) | 72.0 | 29.3 | 14.3 | 48.8 |
| Individual VII | 66.0 (est.) | | 17.8 | |
| Individual XII | 75.0 | 33.8 | 14.6 | 43.2 |
| Individual XV (Cr. 17) | 72.0 | 32.3 | 13.6 | 42.1 |
| Individual XIX | 69.0 | 27.0 | 13.3 | 49.3 |
| Individual XXI (Cr. 5) | 72.0 | 36.0 | 15.7 | 43.6 |
| Individual XXII | 71.0 | 34.7 | 16.0 | 46.1 |
| Individual XXVII | 65.0 | 40.3 | 16.1 | 40.0 |
| Individual XXVIII | 69.0 | 29.4 | 13.8 | 46.9 |
| Atapuerca (SH) mean ± s.d. (CV) | 69.7 ± 3.0 (4.3) | 33.0 ± 4.0 (12.0) | 15.4 ± 1.6 (10.5) | 46.3 ± 4.7 (10.1) |
| Atapuerca (SH) range (n) | 65–75 (11) | 27.0–40.3 (10) | 13.3–17.8 (11) | 40.0–56.7 (10) |
| ATE9-1 | | 33.5 | 15.3 | 45.7 |
| Xiahe | | 32.6 | 15.4 | 47.2 |
| Euro. Mid. Pleist. mean ± s.d. (CV) | 69.5 ± 3.7 (5.3) | 33.3 ± 4.6 (13.7) | 17.0 ± 2.3 (13.4) | 49.5 ± 6.9 (13.9) |
| Euro. Mid. Pleist. range (n) | 66–74 (4) | 26.0–39.0 (7) | 13.4–20.2 (6) | 38.3–58.4 (6) |
| Neandertal mean ± s.d. (CV) | 79.4 ± 6.0 (7.6) | 34.6 ± 4.7 (13.6) | 15.8 ± 2.4 (15.1) | 46.4 ± 6.0 (13.0) |
| Neandertal range (n) | 70.0–90.0 (19) | 25.4–42.2 (19) | 12.8–23.7 (17) | 34.4–58.1 (18) |
| Fossil <i>H. sapiens</i> mean ± s.d. (CV) | 93.7 ± 7.7 (8.2) | 32.3 ± 4.0 (12.4) | 15.2 ± 1.8 (12.1) | 45.6 ± 6.6 (14.5) |
| Fossil <i>H. sapiens</i> range (n) | 81.0–105.0 (13) | 26.0–39.0 (16) | 11.9–18.3 (9) | 40.3–57.5 (9) |
| Recent <i>H. sapiens</i> mean ± s.d. (CV) | 94.8 ± 6.8 (7.2) | 31.1 ± 3.3 (10.7) | 14.8 ± 1.7 (11.6) | 48.1 ± 6.5 (13.5) |
| Recent <i>H. sapiens</i> range (n) | 79.0–111.0 (78) | 24.0–38.0 (76) | 11.0–18.0 (78) | 34.3–66.7 (76) |
| ANOVA (<i>p</i> value) | <i>p</i> < 0.001 | <i>p</i> = 0.009 | <i>p</i> = 0.046 | <i>p</i> = 0.549 |
| SH versus MP Europe | 0.999 | 0.983 | 0.455 | 0.863 |
| SH versus Neandertals | 0.004 | 0.920 | 0.938 | 0.999 |
| SH versus fossil <i>H. sapiens</i> | <0.001 | 0.999 | 0.999 | 0.999 |
| SH versus recent <i>H. sapiens</i> | <0.001 | 0.781 | 0.994 | 0.969 |
| MP Europe versus Neandertals | 0.194 | 0.999 | 0.793 | 0.879 |
| MP Europe versus fossil <i>H. sapiens</i> | <0.001 | 0.998 | 0.443 | 0.775 |
| MP Europe versus recent <i>H. sapiens</i> | <0.001 | 0.661 | 0.293 | 0.984 |
| Neandertals versus fossil <i>H. sapiens</i> | <0.001 | 0.987 | 0.941 | 0.999 |
| Neandertals versus recent <i>H. sapiens</i> | <0.001 | 0.081 | 0.541 | 0.940 |
| Fossil <i>H. sapiens</i> versus recent <i>H. sapiens</i> | 0.999 | 0.648 | 0.997 | 0.916 |

Values in bold indicate a significant difference ($p < 0.05$).

a clear placement in the lower half of the corpus. All of the SH individuals show an index <50 , as do all of the other fossil specimens, and the mean values in all of the fossil groups are <45 (Table 6). The highest value (49.5)

among the fossils is seen in Montmaurin and Tabun 1, both of which have a mental foramen placed approximately at mid-corpus. Although no significant differences were found between any of the groups under study, 65%

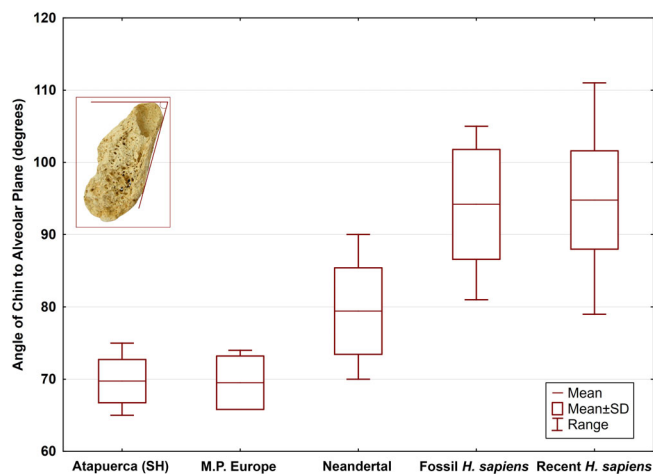


FIGURE 11 Box and whisker plot of symphyseal angles in the fossil and recent samples. The symphyseal cross-section of SH Individual 12 is shown.

(50/77) of the recent *H. sapiens* individuals show a mental foramen placed at mid-corpus or higher.

5.6 | Mandibular corpus

Within the SH sample, Individual 7 shows the largest dimensions of the mandibular corpus, particularly in the corpus thickness dimensions. The mandibular corpus in the SH sample shows an approximately uniform height from the symphysis to the M_2 and a steady increase in thickness moving posteriorly (Tables 5 and 7). A similar pattern in these measurements characterizes the European MP specimens and the Neandertals. In contrast, fossil and recent *H. sapiens* mandibles tend to show a slight decrease in corpus height posteriorly and are thinnest in the region of the mental foramen. The resulting robusticity indices show no difference between the fossil groups, but the fossil and recent *H. sapiens* samples show the lowest robusticity indices at the mental foramen (Tables 5 and 7). Robusticity increases posteriorly in the SH sample, but the SH specimens show slightly lower values than the European MP mandibles and resemble more closely the mean values in the Neandertal sample. Among the fossil specimens, Arago 13 stands out for showing the thickest mandibular corpus and highest robusticity indices. The robusticity index at the M_2 in two *H. antecessor* mandibles (62.5, 67.3) is high, falling toward or above the upper limit of the SH range of variation, but close to the European MP mean value (65.9). Similarly, the late MP Xiahe 1 mandible shows high robusticity values, at the upper limit or outside the SH range of variation and falling close to the mean or at the upper limit of variation in the European MP sample.

The height of the symphysis can be compared with the corpus height at the M_2 to reveal whether corpus height changes moving posteriorly. Values >100 for this index indicate a symphysis which is taller than the corpus. The lowest value for this index in the SH sample (94.2) is found in Individual 5 (Table 7), indicating a relatively short symphysis for the corpus height, while the highest value (121.1) is found in Individual 4, indicating a symphysis which is approximately 20% taller than the corpus. On average, the symphysis is only about 6% taller than the posterior corpus in the SH sample, indicating nearly parallel alveolar and basal margins. The mean values in the European MP sample, Neandertals and fossil *H. sapiens* indicate that the symphysis is approximately 12%–14% taller than the posterior corpus, respectively. Within the recent human sample, only four individuals (5.6%) showed values below 100, and on average, the symphysis was approximately 20% taller than the posterior corpus. Nevertheless, no significant differences were identified in the pairwise comparisons.

5.7 | Ramus

The angle of the posterior border of the ascending ramus shows the lowest values in SH Individual 22 (107°) and Individual 5 (109°), indicating a more vertical ramus, while the highest value is seen in Individual 19 (121°) (Table 8), indicating a more obliquely angled ramus. There are no significant differences among the fossil samples in the ramus angle, but the recent *H. sapiens* sample differed significantly from all other groups. The ramus height seems to show a bimodal distribution in the SH mandibles, with larger values seen in Individuals 4, 5, 21, and 22 and smaller values seen in Individuals 15, 19, and 28. The values in the European MP specimens are more uniform. However, the Neandertals also seem to show a bimodal distribution, with larger values seen in Zafarraya 2, Amud 1, La Quina H5 and La Ferrassie 1 and smaller values seen in Vindija 207, Tabun 1 and Regourdou 1 (Table 7). Nevertheless, no significant differences were observed in any pairwise comparisons between groups.

Among the SH hominins, the width of the ramus is largest in SH Individual 7 (48.2 mm) and smallest in Individual 19 (37.6 mm) (Table 8). Within the European MP sample, Mauer (52.5 mm) falls above the SH range of variation and has the widest ramus of any fossil specimen in this study, while Arago 2 (48.0 mm) is similar to the widest SH specimen. In contrast, Arago 13 (40.0 mm), Montmaurin (38.4 mm) and l'Aubsier (40.4 mm) are similar to the smaller SH Individuals 19 and 28 (41.9), as is the early Pleistocene *H. antecessor* mandible ATD6-96

TABLE 6 Mental foramen measurements (mm) of the mandible in the Atapuerca (SH) sample and Pleistocene and recent humans.

| Specimen/sample | Bimental foramen breadth | |
|--|----------------------------|--|
| | M 67 | Mental foramen height index ^a |
| <i>Atapuerca (SH)</i> | | |
| Individual I | 55.6 | 42.5 |
| Individual IV | 57.0 | 42.9 |
| Individual V (Cr. 15) | 55.1 | 43.7 |
| Individual VII | | 39.2 |
| Individual XII | 55.5 | 37.4 |
| Individual XV (Cr. 17) | 49.9 | 43.2 |
| Individual XIX | 50.9 | 35.3 |
| Individual XXI (Cr. 5) | 55.2 | 36.3 |
| Individual XXII | 54.9 | 45.5 |
| Individual XXVI (Cr. 10) | | 45.7 |
| Individual XXVII | 61.1 | 41.1 |
| Individual XXVIII | 53.5 | 37.5 |
| Atapuerca (SH) mean ± s.d. (CV) | 54.9 ± 3.1 (5.7) | 40.9 ± 3.6 (8.8) |
| Atapuerca (SH) range (n) | 49.9–61.1 (10) | 35.3–45.7 (12) |
| Euro. Mid. Pleist. mean ± s.d. (CV) | 55.7 ± 4.0 (7.1) | 44.8 ± 4.2 (9.4) |
| Euro. Mid. Pleist. range (n) | 50.1–61.0 (5) | 39.8–49.5 (6) |
| Neandertal mean ± s.d. (CV) | 58.2 ± 3.4 (5.9) | 43.2 ± 4.0 (9.2) |
| Neandertal range (n) | 53.0–63.8 (15) | 35.8–49.5 (12) |
| Fossil <i>H. sapiens</i> mean ± s.d. (CV) | 46.5 ± 2.9 (6.2) | 43.7 ± 2.2 (5.1) |
| Fossil <i>H. sapiens</i> range (n) | 41.0–50.8 (14) | 40.8–47.1 (8) |
| Recent <i>H. sapiens</i> Mean ± s.d. (CV) | 44.8 ± 3.1 (6.9) | 46.1 ± 5.5 (11.9) |
| Recent <i>H. sapiens</i> Range (n) | 39.0–52.0 (77) | 33.3–66.7 (77) |
| ANOVA (<i>p</i> value) | <i>p</i> < 0.001 | <i>p</i> = 0.007 |
| SH versus MP Europe | 0.993 | 0.839 |
| SH versus Neandertals | 0.132 | 0.845 |
| SH versus fossil <i>H. sapiens</i> | <0.001 | 0.785 |
| SH versus recent <i>H. sapiens</i> | <0.001 | 0.081 |
| MP Europe versus Neandertals | 0.419 | 0.996 |
| MP Europe versus fossil <i>H. sapiens</i> | 0.040 | 0.999 |
| MP Europe versus recent <i>H. sapiens</i> | 0.005 | 0.970 |
| Neandertals versus fossil <i>H. sapiens</i> | <0.001 | 0.998 |
| Neandertals versus recent <i>H. sapiens</i> | <0.001 | 0.525 |
| Fossil <i>H. sapiens</i> versus recent <i>H. sapiens</i> | 0.581 | 0.869 |

^a(Height from basal margin/corpus height at mental foramen) × 100.

Values in bold indicate a significant difference (*p* < 0.05).

(40.6 mm). Among the Neandertals, all the Krapina specimens fall below the SH and European MP ranges of variation, indicating narrow rami in the Krapina sample. Nevertheless, no significant differences were found between any of the fossil samples, with only the recent *H. sapiens* sample showing significantly narrower rami.

When the ramus width is compared with the total length of the mandible (Table 8; Figure 13), the recent *H. sapiens* consistently show narrower rami for a given mandibular length than the fossil specimens. All seven SH individuals fall above the pooled sample regression line, indicating a relatively wider ramus for a given

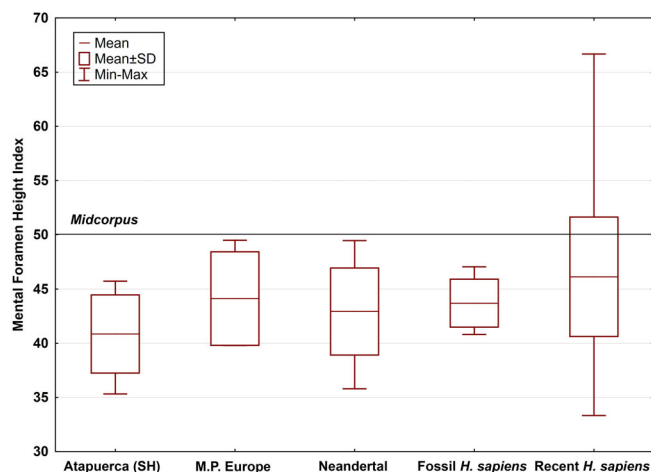


FIGURE 12 Box and whisker plot of the vertical position of the mental foramen. A value of 50 indicates a placement at midcorpus between the alveolar and basal margins.

mandibular length, but within the 95% prediction interval. Among the European MP specimens, only Arago 2 and Mauer fall outside the upper limit of the prediction interval, indicating very wide rami in these individuals. All the Neandertals, except Zafarraya 2, fall within the prediction interval.

5.8 | Principal components analysis

PCA was carried out on the size-transformed variables to assess patterns of variation among the samples. The eigenvalues for the first five principal components were >1.0 (Table 9), indicating they explain more variation than any single variable in isolation. Nevertheless, only the first two PCs consistently separate the groups in the analysis (Figure 14).

PC1 explains 23.5% of the variance, and strong positive correlations were with the bimental foramen, bicoronoid and dental arcade breadths, as well as the gonial length, while strong negative correlations were seen with the heights of the corpus at the symphysis and mental foramen, as well as the ramus height (Table 9). Thus, individuals that show high positive values along PC1 generally show wider distances between the coronoid processes, the mental foramina and across the posterior dental arcade, an AP longer mandibular corpus, a shorter mandibular corpus height at the symphysis and mental foramen and a shorter ramus. The distribution of the recent *H. sapiens* largely overlaps that of the fossil samples, although the SH hominins, Neandertals and European MP specimens tend to fall on the positive side of PC1.

PC2 explains 18.2% of the variance, and strong positive correlations were found with the width of the ramus,

the bicondylar breadth and corpus height at M_2 , while strong negative correlations were found with the dental arcade length and the thickness of the corpus at the symphysis and M_2 (Table 9). Thus, individuals with high positive values along PC2 are characterized by wider rami and bicondylar breadths, taller mandibular bodies at the symphysis and M_2 . A clearer separation between samples is evident along PC2, with most of the fossil and recent *H. sapiens* falling toward negative values, while the SH hominins and Neandertals all fall on the positive side of PC2. The European MP specimens are widely distributed along PC2.

The 95% confidence ellipse of the SH hominins falls essentially within that of the Neandertals, indicating a similar placement of these two groups in shape space. It is interesting to note the location of some individual specimens in PCA space. Although SH Individuals 21 and 22 fall somewhat apart from the other SH individuals, mainly along PC1, there is no clear division within the sample based on sex or age of the specimen. Regarding the European MP specimens, Arago 2 is closest to the SH confidence ellipse, falling within shape space occupied by the SH hominins and Neandertals, and the two nearest individuals are SH Individual 15 and Tabun 1. The remaining European MP specimens fall closer to (Montmaurin) or within (Mauer, Arago 13) the recent *H. sapiens* confidence ellipse, with Arago 13 falling the furthest from the SH hominins, mainly along PC2. Within the Neandertals Tabun 1 is somewhat of an outlier, showing the highest value of any individual along PC1. The fossil *H. sapiens* individual Skhul 5 falls just outside the recent *H. sapiens* confidence ellipse and close to that of Neandertals.

5.9 | Metric variation in the SH hominins

Within the SH sample, the measures associated with height and thickness of the symphysis and corpus showed the highest CVs among the metric variables (Figure 15). In contrast, the angle of the chin and ramus, the bicondylar breadth and the length and breadth of the dental arcade showed the lowest CVs. These latter measures represent the more stable aspects of the SH mandible, and they seem to reflect a functional module, likely related to the need to maintain functional occlusion with the maxillary dental arcade. This same pattern seems to characterize the Neandertal and the Kish recent *H. sapiens* samples as well (Figure 15), strengthening the argument that these represent a functional module.

TABLE 7 Measurements of the mandibular corpus in the Atapuerca (SH) sample and Pleistocene and recent humans.

| Specimen/sample | Corpus height at mental foramen at M2 | | Corpus thickness at mental foramen at M2 | | Robusticity index | | Symphysis/M2 height index |
|--|---------------------------------------|--------------------------|--|--|--------------------------|---------------------------|----------------------------|
| | M 69(1) | M 69(2) | M 69(3) | Corpus thickness at mental foramen at M2 | Corpus at mental foramen | Robusticity index at M2 | |
| <i>Atapuerca (SH)</i> | | | | | | | |
| Individual I | 29.9 | 29.0 | 17.6 | 18.3 | 58.9 | 63.1 | 108.3 |
| Individual IV | 31.0 | 29.9 | 17.4 | 17.5 | 56.1 | 58.5 | 121.1 |
| Individual V (Cr. 15) | 31.1 | 31.1 | 16.6 | 16.6 | 53.4 | 53.4 | 94.2 |
| Individual VI | | 28.0 | | 16.7 | | 59.6 | |
| Individual VII | 37.8 | 37.0 | 21.8 | 20.8 | 57.7 | 56.2 | |
| Individual XII | 33.7 | 30.1 | 18.2 | 19.7 | 54.0 | 65.4 | 112.3 |
| Individual XV (Cr. 17) | 31.5 | 28.6 | 15.2 | 15.9 | 48.3 | 55.6 | 112.9 |
| Individual XIX | 28.6 | 27.2 | 14.6 | 16.7 | 51.0 | 61.4 | 99.3 |
| Individual XXI (Cr. 5) | 35.5 | 36.1 | 16.7 | 16.9 | 47.0 | 46.8 | 99.7 |
| Individual XXII | 36.5 | 34.1 | 17.0 | 18.2 | 46.6 | 53.4 | 101.8 |
| Individual XXVI (Cr. 10) | 29.3 | | 16.7 | 17.2 | 57.0 | | |
| Individual XXVII | 38.0 | 35.3 | 17.8 | 18.1 | 46.8 | 51.3 | 114.2 |
| Individual XXVIII | 28.8 | 29.6 | 14.8 | 15.6 | 51.4 | 52.7 | 99.3 |
| Atapuerca (SH) mean ± s.d. (CV) | 32.6 ± 3.5 (10.8) | 31.3 ± 3.4 (10.8) | 17.0 ± 1.9 (11.2) | 17.6 ± 1.5 (8.4) | 52.3 ± 4.5 (8.6) | 56.5 ± 5.4 (9.5) | 106.3 ± 8.6 (8.1) |
| Atapuerca (SH) range (n) | 28.6–38.0 (12) | 27.2–37.0 (12) | 14.6–21.8 (12) | 15.6–20.8 (13) | 46.6–58.9 (12) | 46.8–65.4 (12) | 94.2–121.1 (10) |
| ATE9-1 | 30.0 | | | | | | |
| ATD6-5 | | 26.6 | | 17.9 | | 67.3 | |
| ATD6-113 | | 32.0 | | 20.0 | | 62.5 | |
| Xiahe | 30.7 | 25.9 | 17.9 | 21.5 | 58.3 | 83.0 | 125.9 |
| Euro. Mid. Pleist. Mean ± s.d. (CV) | 32.9 ± 3.9 (11.8) | 30.9 ± 3.8 (12.2) | 17.6 ± 2.2 (12.5) | 18.5 ± 2.7 (14.8) | 55.5 ± 8.7 (15.7) | 62.6 ± 12.8 (20.5) | 112.5 ± 15.6 (13.9) |
| Euro. Mid. Pleist. range (n) | 28.5–37.7 (6) | 27.0–35.6 (5) | 15.0–22.0 (8) | 15.9–23.6 (8) | 45.4–71.0 (6) | 49.2–82.8 (5) | 100.3–136.8 (5) |
| Neandertal Mean ± s.d. (CV) | 32.3 ± 3.3 (10.2) | 31.2 ± 2.9 (9.2) | 15.6 ± 1.6 (10.1) | 16.1 ± 1.4 (8.8) | 48.4 ± 4.6 (9.6) | 52.3 ± 4.3 (8.2) | 111.7 ± 8.7 (7.8) |
| Neandertal range (n) | 26.4–37.3 (22) | 26.2–35.1 (19) | 12.8–20.3 (22) | 14.0–20.2 (18) | 37.8–58.1 (22) | 44.7–60.7 (17) | 91.7–127.5 (16) |
| Fossil <i>H. sapiens</i> mean ± s.d. (CV) | 31.0 ± 3.6 (11.6) | 28.2 ± 3.7 (13.1) | 13.2 ± 2.8 (20.8) | 15.5 ± 2.9 (18.9) | 42.8 ± 7.3 (17.0) | 56.4 ± 12.5 (22.1) | 113.6 ± 14.2 (12.5) |
| Fossil <i>H. sapiens</i> range (n) | 25.0–36.7 (18) | 21.0–33.0 (15) | 10.0–21.2 (17) | 12.0–21.5 (14) | 33.2–58.4 (17) | 37.5–76.2 (14) | 87.5–133.6 (14) |
| Recent <i>H. sapiens</i> mean ± s.d. (CV) | 30.2 ± 3.1 (10.4) | 26.1 ± 3.1 (11.8) | 12.1 ± 1.7 (14.4) | 15.3 ± 1.6 (10.3) | 40.4 ± 6.4 (15.8) | 59.4 ± 9.1 (15.4) | 120.3 ± 11.5 (9.6) |
| Recent <i>H. sapiens</i> range (n) | 21.0–37.0 (77) | 19.0–33.5 (73) | 8.0–18.0 (77) | 11.5–18.0 (74) | 27.3–55.6 (77) | 37.7–85.4 (73) | 92.9–145.5 (71) |
| ANOVA (p value) | p = 0.111 | p < 0.001 | p < 0.001 | p < 0.001 | p < 0.001 | p = 0.032 | p = 0.016 |

(Continues)

TABLE 7 (Continued)

| | Corpus height a t mental foramen | Corpus height at M2 | Corpus thickness at mental foramen | Corpus thickness at M2 | Corpus thickness at M2 | Robusticity index at mental foramen | Robusticity index at M2 | Symphysis/M2 height index |
|--|-------------------------------------|------------------------|---------------------------------------|---------------------------|---------------------------|---|----------------------------|------------------------------|
| SH versus MP Europe | 0.997 | 0.976 | 0.611 | 0.447 | 0.451 | 0.565 | 0.846 | |
| SH versus Neandertals | 0.999 | 0.999 | 0.944 | 0.573 | 0.975 | 0.843 | 0.894 | |
| SH versus Fossil <i>H. sapiens</i> | 0.950 | 0.207 | 0.006 | 0.218 | 0.046 | 0.999 | 0.667 | |
| SH versus recent <i>H. sapiens</i> | 0.563 | 0.006 | <0.001 | 0.109 | 0.003 | 0.931 | 0.153 | |
| MP Europe versus Neandertals | 0.999 | 0.974 | 0.323 | 0.073 | 0.246 | 0.208 | 0.992 | |
| MP Europe versus fossil <i>H. sapiens</i> | 0.999 | 0.939 | 0.004 | 0.025 | 0.007 | 0.604 | 1.000 | |
| MP Europe versus recent <i>H. sapiens</i> | 0.973 | 0.475 | <0.001 | 0.014 | 0.001 | 0.857 | 0.992 | |
| Neandertals versus fossil <i>H. sapiens</i> | 0.964 | 0.104 | 0.019 | 0.950 | 0.094 | 0.705 | 0.988 | |
| Neandertals versus recent <i>H. sapiens</i> | 0.536 | 0.001 | <0.001 | 0.804 | 0.006 | 0.238 | 0.508 | |
| Fossil <i>H. sapiens</i> versus recent <i>H. sapiens</i> | 0.903 | 0.517 | 0.403 | 0.996 | 0.850 | 0.931 | 0.809 | |

Note: Robusticity index = (Corpus thickness/Corpus height) \times 100. Symphysis/height index = (symphysis height/corpus height at M2) \times 100. Values in bold indicate a significant difference ($p < 0.05$).

TABLE 8 Measurements (mm) of the mandibular ramus in the Atapuerca (SH) sample and Pleistocene and recent humans.

| | Angle of ramus (deg.) | Height of ramus (post. border) | Minimum ramus width | Ramus/length index |
|--|----------------------------|--------------------------------|----------------------------|----------------------------|
| Specimen/sample | M (79) | M (70) | M 71(a) | |
| <i>Atapuerca (SH)</i> | | | | |
| Individual IV | 114.5 | 64.2 | 46.3 | 39.3 |
| Individual V (Cr. 15) | 109.0 | 65.5 | 45.7 | 39.7 |
| Individual VII | | | 48.2 | |
| Individual XV (Cr. 17) | 116.5 | 57.5 | 42.8 | 41.4 |
| Individual XIX | 121.0 | 55.2 | 37.6 | 36.2 |
| Individual XXI (Cr. 5) | 112.0 | 64.9 | 45.2 | 37.2 |
| Individual XXII | 107.0 | 69.9 | 47.2 | 38.7 |
| Individual XXVIII | 115.0 | 57.8 | 41.9 | 38.8 |
| Atapuerca (SH) mean ± s.d. (CV) | 113.7 ± 4.8 (4.2) | 62.1 ± 5.4 (8.6) | 44.4 ± 3.4 (7.8) | 38.8 ± 1.7 (4.4) |
| Atapuerca (SH) range (n) | 107.0–121.0 (7) | 55.2–69.9 (7) | 37.6–48.2 (8) | 36.2–41.4 (7) |
| ATD6-96 | 118.0 | 60.0 | 40.6 | |
| Euro. Mid. Pleist. mean ± s.d. (CV) | 110.1 ± 2.5 (2.3) | 63.2 ± 1.7 (2.6) | 43.9 ± 6.1 (13.9) | 38.3 ± 5.1 (13.4) |
| Euro. Mid. Pleist. range (n) | 108.0–113.0 (4) | 61.2–65.0 (4) | 38.4–52.5 (5) | 31.3–43.4 (5) |
| Neandertal mean ± s.d. (CV) | 110.3 ± 6.9 (6.2) | 62.4 ± 6.1 (9.7) | 39.6 ± 3.4 (8.5) | 36.1 ± 3.5 (9.7) |
| Neandertal range (n) | 99.0–120.0 (13) | 52.0–70.0 (13) | 34.8–44.0 (18) | 32.1–42.7 (10) |
| Fossil <i>H. sapiens</i> mean ± s.d. (CV) | 111.3 ± 6.4 (5.8) | 65.8 ± 4.3 (6.6) | 38.0 ± 3.9 (10.4) | 35.1 ± 3.8 (10.8) |
| Fossil <i>H. sapiens</i> range (n) | 96.0–120.0 (13) | 63.0–74.5 (6) | 31.9–46.2 (15) | 27.4–41.8 (10) |
| Recent <i>H. sapiens</i> mean ± s.d. (CV) | 124.4 ± 7.2 (5.8) | 57.4 ± 6.9 (12.1) | 32.1 ± 3.5 (11.1) | 31.9 ± 3.5 (10.9) |
| Recent <i>H. sapiens</i> range (n) | 101.0–141.0 (75) | 44.0–77.0 (73) | 25.0–41.0 (72) | 23.8–38.8 (69) |
| ANOVA (<i>p</i> value) | <i>p</i> < 0.001 | <i>p</i> = 0.005 | <i>p</i> < 0.001 | <i>p</i> < 0.001 |
| SH versus MP Europe | 0.952 | 0.999 | 0.997 | 0.982 |
| SH versus Neandertals | 0.978 | 0.999 | 0.280 | 0.523 |
| SH versus Fossil <i>H. sapiens</i> | 0.911 | 0.873 | 0.045 | 0.277 |
| SH versus Recent <i>H. sapiens</i> | 0.033 | 0.653 | <0.001 | 0.003 |
| MP Europe versus Neandertals | 0.999 | 0.999 | 0.348 | 0.420 |
| MP Europe versus Fossil <i>H. sapiens</i> | 0.999 | 0.980 | 0.068 | 0.248 |
| MP Europe versus Recent <i>H. sapiens</i> | 0.033 | 0.723 | <0.001 | 0.010 |
| Neandertals versus fossil <i>H. sapiens</i> | 0.998 | 0.874 | 0.861 | 0.991 |
| Neandertals versus recent <i>H. sapiens</i> | 0.001 | 0.482 | <0.001 | 0.161 |
| Fossil <i>H. sapiens</i> versus recent <i>H. sapiens</i> | 0.005 | 0.182 | 0.051 | 0.258 |

Note: Ramus/length index = (Minimum ramus width/total mandibular length) × 100.

Values in bold indicate a significant difference (*p* < 0.05).

For most of the metric variables, the SH sample showed a lower CV, indicating less variation, than either the Kish recent *H. sapiens* or Neandertals. The Neandertal sample comprises individuals separated geographically and chronologically, and, thus, should be more variable than the SH sample. Indeed, the Neandertal sample shows the highest CV in over half of the variables. Only the gonial length, the height and thickness of

the mandibular corpus at the mental foramen and the corpus height at M₂ were more variable in the SH sample than in the Neandertals.

Bootstrap analysis comparing the SH sample with 5,000 randomly generated similarly-sized samples from the Kish recent *H. sapiens* reveals that the SH sample is not more variable than recent *H. sapiens* in most measures (Table 10). The few exceptions include the gonial

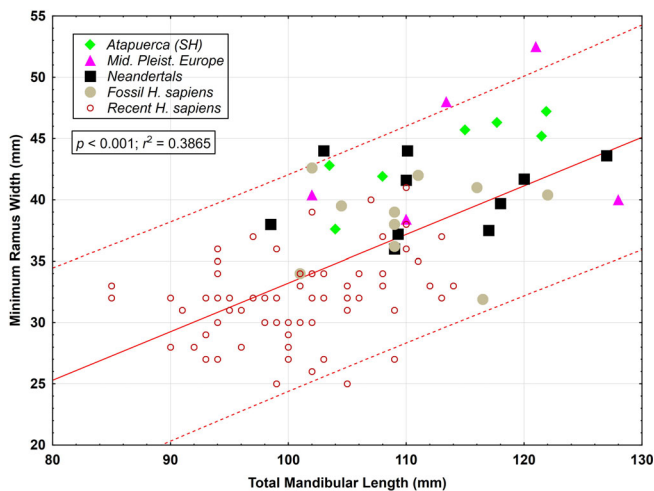


FIGURE 13 Scatterplot of total mandibular length versus minimum ramus width in the fossil and recent specimens. The pooled sample regression line and 95% prediction interval are shown.

and total mandibular lengths, and the corpus height at the symphysis and mental foramen. A previous study (Lorenzo et al., 1998) based on a smaller sample of SH fossils found them to be less variable than *H. sapiens* in the region of the mental foramen. Interestingly, the few measures found to be more variable than *H. sapiens* in the present study are some of the variables that Rosas et al. (2002) identified as being among the most sexually dimorphic dimensions of the mandible. Additionally, both the Neandertals and the SH hominins were more variable than the *H. sapiens* sample in the total mandibular length (Figure 15), a variable that is related to the degree of facial prognathism. Thus, there appears to be more variation in facial prognathism in the fossil samples than in the recent *H. sapiens* sample.

Size-related metric variation can be assessed by correlation of the individual measurements with the geometric mean (Table 11). When the fossil and recent samples are pooled together, all the metric variables are significantly correlated with the geometric mean. When the analysis is restricted to Neandertal clade specimens (i.e., SH, European MP, and Neandertals), most of the variables remain significantly correlated. However, the angles of the chin and ramus, the dental arcade length and breadth and the bicondylar breadth are not correlated with the geometric mean. A similar pattern was seen when the analysis is restricted to the SH fossils only, and these were the variables that showed the lowest CVs in the SH sample as well. These results for the dental arcade agree with those of Stelzer et al. (2019) who found the distinctive shape of the Neandertal dental arcade is not size related but represents a stable feature.

6 | COMPARATIVE MORPHOLOGY

6.1 | Symphysis

The symphysis shows a fairly constant morphological pattern within the SH adult sample (Table S3; Figure 16). The symphyseal tubercle is present in 7 out of 10 specimens (70%) with the symphysis preserved, being absent only in Individuals 1, 5, and 15. The symphyseal tubercle reaches its maximum expression in Individual 4, but even here is not pronounced. All the SH mandibles generally lack any trace of lateral tubercles, mental trigones, mental fossae or anterior curvature. Only Individual 22 shows a slight curvature on the anterior symphysis below the incisors. The more pronounced anterior curvature seen in Individual 27 is most likely related to remodeling of the anterior alveolar margin due to the premortem loss of the right incisors and subsequent alveolar resorption. Although these are two of the larger individuals within the sample, the degree of expression (or absence) of the other chin structures is similar to that seen in the other mandibles within the collection.

Based on the criteria for mentum osseum development outlined by Dobson and Trinkaus (2002), 7 out of 10 (70%) of the SH mandibles are ranked as category 2, showing the “clear presence of a tuber symphyseos, but minimally altering the profile of an otherwise rounded anterior symphysis” (Dobson & Trinkaus, 2002, p. 73). The remaining three specimens (Individuals 1, 5 and 15) are ranked as category 1, based mainly on the absence of a tuber symphyseos. Interestingly, a tuber symphyseos and slight anterior curvature of the external symphysis are present on the early Pleistocene ATE9-1 mandible from the Sima del Elefante site, also in the Sierra de Atapuerca (Carbonell et al., 2008). Among the European MP specimens, Mauer, Arago 2 and 13 and Payre 15 are all scored a rank of 1, while l’Aubesier and Montmaurin are scored a rank of 2. All the middle Pleistocene specimens included in the study by Dobson and Trinkaus (2002) were ranked in category 1 or 2, while the Neandertal sample was fairly evenly distributed across ranks 1–3, indicating a more frequent presence of a symphyseal tubercle and a somewhat greater anterior projection of the inferior symphysis.

Well-developed superior and inferior transverse tori and alveolar planum on the internal aspect of the symphysis seem to be constant features in the SH sample (Table S3; Figure 17). Some variation in the development of these structures can be found within the collection, but they are present in all individuals. The expression is not strictly related to overall size of the mandible, since some large specimens (Individual 27) have modest tori, but the development of the internal tori in the SH

TABLE 9 Eigenvalues and factor loadings of the mandibular variables in the principal components analysis (PCA).

| Analysis/variables | Factor 1 | Factor 2 | Factor 3 | Factor 4 | Factor 5 |
|--|------------------|------------------|------------------|-----------------|------------------|
| Eigenvalue | 3.8 | 2.9 | 2.2 | 1.6 | 1.2 |
| % Variance explained | 23.5 | 18.2 | 14.0 | 9.9 | 7.7 |
| Factor loadings of transformed variables | | | | | |
| Bimental foramen breadth | 0.582108 | 0.180497 | 0.274854 | 0.448420 | 0.005473 |
| Ramus height | -0.592412 | 0.178226 | -0.057927 | -0.396262 | -0.3525757 |
| Minimum ramus width | 0.262145 | 0.593972 | -0.366261 | 0.218896 | -0.317669 |
| Bicondylar breadth | 0.400372 | 0.637556 | 0.251609 | -0.207776 | 0.250513 |
| Bicoronoid breadth | 0.596362 | 0.285305 | 0.338994 | -0.244140 | 0.417497 |
| Bigonial breadth | 0.169751 | -0.326281 | 0.648278 | -0.303653 | -0.314399 |
| Total mandibular length | -0.319540 | -0.196249 | 0.522157 | 0.552213 | -0.006397 |
| Gonial length | 0.575348 | 0.070121 | 0.043158 | 0.353135 | -0.511805 |
| Dental arcade length | 0.072017 | -0.647359 | 0.190920 | 0.227240 | -0.027364 |
| Dental arcade breadth | 0.734119 | -0.111142 | 0.198358 | -0.368347 | 0.018366 |
| Corpus thickness at symphysis | -0.171708 | -0.631541 | -0.151786 | -0.481166 | -0.211215 |
| Corpus thickness at mental foramen | 0.237860 | -0.011955 | -0.784391 | -0.072631 | 0.305462 |
| Corpus thickness at M2 | 0.004234 | -0.668769 | -0.405892 | 0.347318 | 0.307092 |
| Corpus height at symphysis | -0.616384 | 0.130427 | 0.486143 | 0.007877 | 0.385628 |
| Corpus height at mental foramen | -0.878707 | 0.186040 | 0.145736 | 0.070960 | 0.100864 |
| Corpus height at M2 | -0.496124 | 0.723506 | -0.123656 | 0.090936 | -0.145555 |

Note: Factor loadings >0.5 in bold.

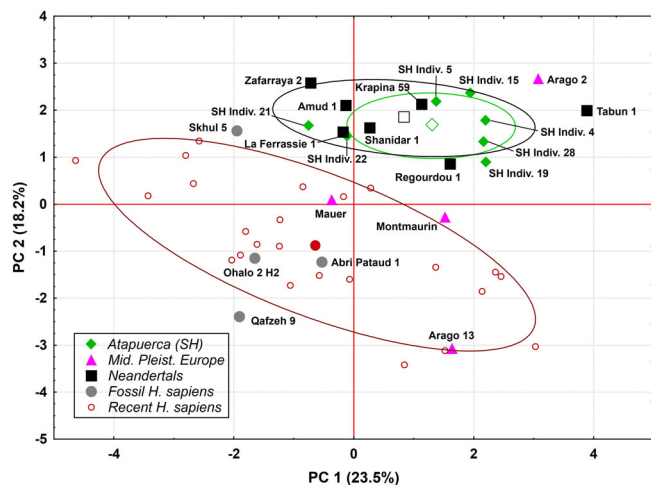


FIGURE 14 Scatterplot of the first two principal components based on the size-adjusted variables. The 95% equiprobability ellipse of the Atapuerca SH hominins essentially falls within that of the Neandertals. The position of the individual fossil specimens and the group centroids for the SH hominins (open diamond), Neandertals (open square) and recent *H. sapiens* (filled circle) are indicated.

hominins seems to be greater than that generally found in Neandertals. The relatively strong development of the superior transverse torus results in a sublingual fossa

being largely absent in the SH specimens, and Individual 27 shows the only example of a sublingual fossa within the collection.

The internal symphyseal tori are absent in *H. sapiens*, but most archaic *Homo* taxa show some development of the superior and inferior transverse tori (Rightmire, 1990; Wood, 1991), suggesting this is the primitive condition for the genus *Homo*. However, the early Pleistocene ATE9-1 mandible lacks any development of internal tori (Bermúdez de Castro et al., 2011; Carbonell et al., 2008). Although the symphysis in the adult *H. antecessor* mandible ATD6-96 is not preserved, there is no sign of the internal symphyseal tori at the level of the canine (Carbonell et al., 2005). Similarly, the internal symphyseal tori are absent or only weakly expressed in the *H. erectus* mandibles from the site of Zhoukoudian (Weidenreich, 1936) and are occasionally lacking in Neandertals, such as Amud 1 or Guattari 3. Despite some degree of variation within the genus *Homo*, the internal symphysis in the SH mandibles shows mainly primitive features.

In basal view, the SH specimens generally show a fairly square contour of the anterior basal corpus, and this feature is also commonly found in Neandertals (Quam & Smith, 1998). This square contour seems to be related to the

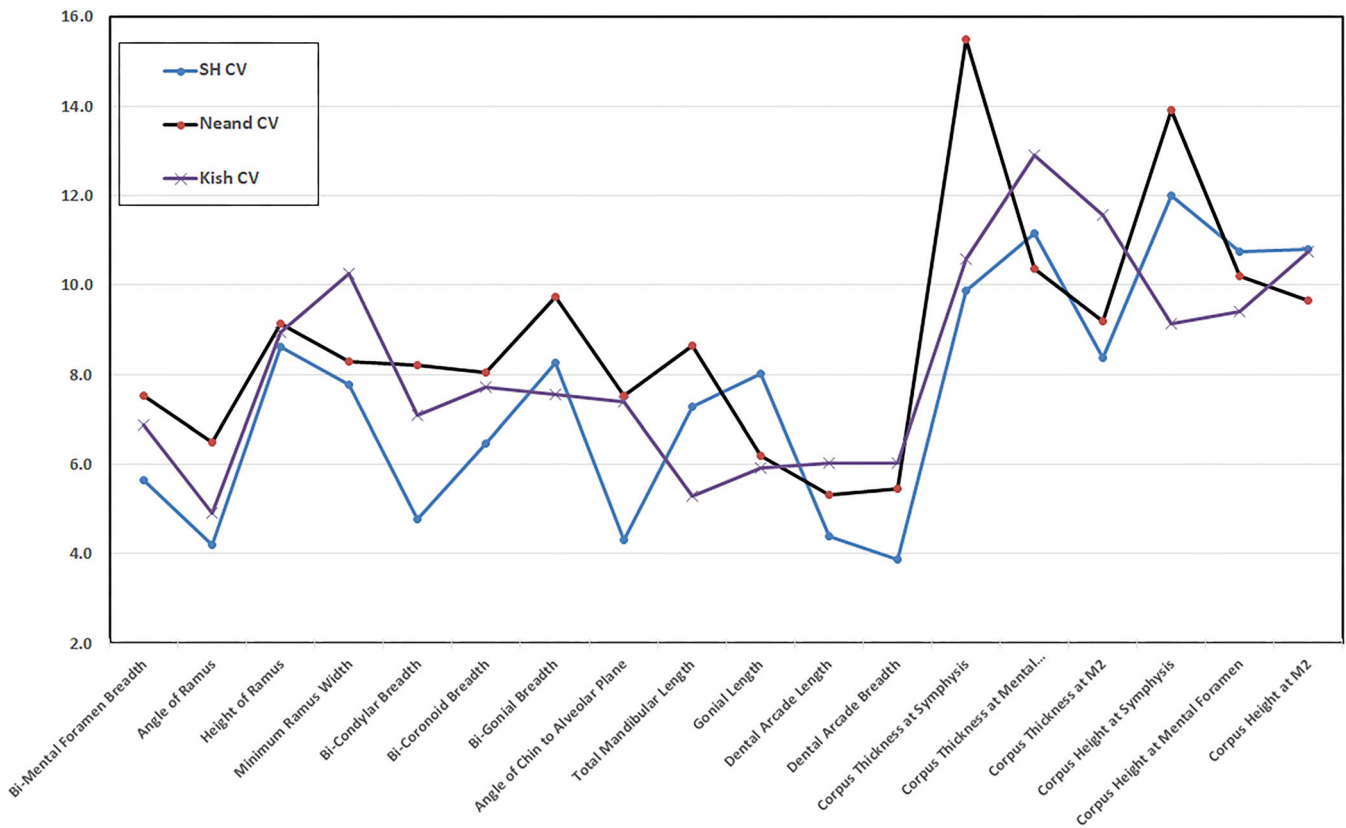


FIGURE 15 Comparison of the coefficient of variation (CV) for the metric variables in the SH hominins, Neandertals and the Kish sample of recent *H. sapiens*.

general lack of chin structures, the frontal alignment of the anterior teeth and the development of the anterior marginal tubercles. Within the SH sample, a square contour can clearly be seen in Individual 1 and the exaggerated square outline in Individual 12 represents an extreme expression of this feature within the Atapuerca (SH) sample. Nevertheless, it is similar to one of the Neandertal mandibles from the site of Sidrón in northern Spain (Rosas & Aguirre, 1999; Rosas, Martínez-Maza, et al., 2006). The degree of relief of the digastric fossae is quite variable within the sample and this feature does seem to be size related, with a more pronounced expression in larger individuals (e.g., Individuals 4 and 27) and a weaker development in smaller individuals (e.g., Individuals 15 and 28).

The anterior teeth in the SH sample generally show a frontal alignment and a more square contour to the anterior dental arcade (Table S3; Figure 17). This is expressed as a fairly straight contour of the alveolar margin between the right and left canines. In those specimens where it could be clearly observed, 9 of 11 (81.8%) of the SH fossils show a squared frontal alignment of the anterior teeth, best seen in SH Individuals 4 and 12, while the remaining specimens (Individuals 19 and 22) showed a more curved anterior dental arcade.

Among the European MP specimens, only Payre 15 shows a frontal alignment of the anterior dentition, with the remaining specimens showing a regular curvature of the dental arcade (Table 12). These observations agree with those reported by Stelzer et al. (2019) who also found that SH Individual 21 (Cranium 5), along with Petralona (in the maxilla), showed a squared anterior dental arcade and grouped with Neandertals. Among the Neandertals, some variation is present, but a squared frontal alignment of the teeth is common and is well expressed in the Regourdou and La Quina H9 mandibles. This square frontal alignment is also seen in Skhul 5 but is generally absent in fossil and recent *H. sapiens*.

6.2 | Corpus

In general, the SH mandibles show a retromolar space between the distal surface of the M_3 and the anterior margin of the ramus, as well as a relatively posterior placement of the mental foramen under the M_1 (Table S4; Figure 18). Similarly, the lateral corpus structures (anterior marginal tubercle and lateral prominence) are also located relatively posteriorly in the SH mandibles. This suite of features also generally characterizes

TABLE 10 Percentage of samples generated randomly that fall above the SH coefficient of variation (CV)^a.

| Variables | n | SH versus Kish |
|------------------------------------|----|----------------|
| Bimental foramen breadth | 10 | 72.0 |
| Angle of ramus | 7 | 62.8 |
| Height of ramus | 7 | 44.7 |
| Minimum ramus width | 8 | 74.7 |
| Bicondylar breadth | 8 | 83.5 |
| Bicoronoid breadth | 9 | 55.5 |
| Bigonial breadth | 7 | 29.4 |
| Angle of chin to alveolar plane | 11 | 98.1 |
| Total mandibular length | 8 | 3.5 |
| Gonial length | 7 | 3.1 |
| Dental arcade length | 11 | 91.1 |
| Dental arcade breadth | 11 | 88.9 |
| Corpus thickness at symphysis | 11 | 54.9 |
| Corpus thickness at mental foramen | 12 | 66.0 |
| Corpus thickness at M2 | 13 | 93.9 |
| Corpus height at symphysis | 10 | 6.5 |
| Corpus height at mental foramen | 12 | 14.7 |
| Corpus height at M2 | 12 | 41.9 |

^a5,000 randomly generated samples of recent *H. sapiens* with a similar sample size as the SH hominins.

Neandertal mandibles (Franciscus & Trinkaus, 1995; Heim, 1976; Trinkaus, 1983, 1993), and this combination is often considered to represent a derived condition in Neandertals. Variation in the expression of these features is dependent on attainment of adult size of the mandible and eruption of the M₃, complicating the assessment of these spatial relationships in juvenile specimens.

Among those individuals with the M₃ fully erupted and that preserve portions of the anterior margin of the ramus, a retromolar space is present in 9 of 11 (81%) of the SH mandibles and is lacking only in Individuals 12 and 19. The mental foramen is positioned under the M₁ or further posteriorly in 9 of 12 (75%) of the adult SH individuals, with the remaining three individuals showing a slightly more anterior placement under the P₄/M₁ alveolar septum. Individual 27 shows the largest retromolar space and a mental foramen positioned distal to the M₁. Large retromolar spaces and posteriorly located structures of the lateral corpus are also found in Individuals 4, 5, 7, 21 and 22. In contrast, a relatively forward placement of the anatomical structures of the corpus is present in Individuals 12, 15 and 19 (Figure 18).

The little evidence available from early Pleistocene European specimens shows they lack a retromolar space and have an anteriorly placed mental foramen (Table 12).

The non-SH European MP specimens also generally lack a retromolar space, except for l'Aubesier. The mental foramen position is somewhat more variable, with some individuals showing a more anterior placement under the P₃/P₄ (Visogliano 2), P₄ (Mala Balanica, Montmaurin) or P₄/M₁ (Mauer, Arago 13) and others showing a more posterior placement under the M₁ (Arago 2, Ehringsdorf 8, Payre 15, l'Aubesier 11).

The reasons behind this posterior placement of the lateral corpus structures and retromolar space emergence are complex (Franciscus & Trinkaus, 1995; Rak, 1986; Trinkaus, 1993), but it may be related to the emergence of the derived midfacial prognathism that characterizes the Neandertal evolutionary lineage (Rosas, 2001). Importantly, midfacial prognathism also characterizes the SH sample (Arsuaga, Martínez, Gracia, & Lorenzo, 1997) and the derived Neandertal craniofacial architecture seems to be essentially present in the SH hominins (Arsuaga et al., 2014). In particular, the presence of a retromolar space seems to be a result of the combination of a shortened dental arcade, an AP narrower ramus and an overall longer mandible (Franciscus & Trinkaus, 1995).

The placement of the lateral corpus structures (mental foramen, anterior marginal tubercle, and lateral prominence) and presence of a retromolar space do appear to be related to overall mandibular size in the SH sample, with more posterior placements and larger retromolar spaces found in larger individuals. Additionally, the fact that older individuals show generally large retromolar spaces suggests that interstitial tooth wear, resulting in mesial drift of the dentition through life, also plays a role in the size of the retromolar space. This may be particularly relevant in the cases of Individuals 5 and 21, which both represent old adult individuals with large retromolar spaces, heavily worn teeth and clear evidence of mesial drift in both the mandibular and maxillary dentition.

The mental foramina are nearly always single and invariably located within the lower half of the mandibular corpus in the SH specimens (Figure 18). The presence of a single mental foramen appears to be the primitive condition for the genus *Homo*, with the higher frequency of multiple foramina in Neandertals perhaps representing a derived condition (Table 12). Among the early Pleistocene European specimens, ATE 9-1 shows a single mental foramen, while ATD6-96 shows multiple foramina. All the Atapuerca (SH) specimens where this could be scored ($n = 12$) showed the presence of only a single mental foramen, as did all the other European MP specimens with the exceptions of Mauer and Montmaurin. However, this feature is somewhat variable across taxa (Trinkaus, 1993), obscuring its significance for phylogenetic reconstruction. In contrast, a low placement of the mental foramen, within the lower half of the mandibular corpus, has been argued

TABLE 11 Size-related metric variation in the SH mandibular sample.

| Variable | Correlation (<i>r</i>) with the geometric mean | | |
|------------------------------------|--|------------------|-----------------|
| | Fossil + Recent | Neandertal clade | SH sample |
| | (<i>n</i> = 43) | (<i>n</i> = 18) | (<i>n</i> = 7) |
| Total mandibular length | 0.820 | 0.876 | 0.943 |
| Gonial length | 0.885 | 0.742 | 0.955 |
| Bicondylar breadth | 0.857 | 0.238 | 0.453 |
| Bicoronoid breadth | 0.875 | 0.675 | 0.654 |
| Bi-gonial breadth | 0.641 | 0.775 | 0.851 |
| Dental arcade length | 0.557 | 0.291 | 0.254 |
| Dental arcade breadth | 0.742 | 0.430 | 0.566 |
| Angle of chin to alveolar plane | -0.640 | 0.292 | 0.266 |
| Corpus thickness at symphysis | 0.503 | 0.807 | 0.946 |
| Corpus height at symphysis | 0.688 | 0.824 | 0.884 |
| Bimental foramen breadth | 0.808 | 0.592 | 0.812 |
| Corpus thickness at mental foramen | 0.873 | 0.777 | 0.935 |
| Corpus thickness at M2 | 0.563 | 0.609 | 0.755 |
| Corpus height at mental foramen | 0.732 | 0.860 | 0.806 |
| Corpus height at M2 | 0.878 | 0.817 | 0.789 |
| Angle of ramus | -0.703 | -0.306 | -0.751 |
| Height of ramus | 0.761 | 0.654 | 0.916 |
| Minimum ramus width | 0.857 | 0.738 | 0.919 |

Note: Significant ($p < 0.05$) correlations in bold.

to be a derived condition within the genus *Homo* (Daura et al., 2005), one that aligns the Atapuerca (SH) specimens with the Neandertals. The mental foramen is placed at mid-corpus in the early Pleistocene European specimens ATE9-1 and ATD6-96, but most European MP specimens (except Mala Balanica and Montmaurin) show a low-placed mental foramen. Such a low placement has been argued to reflect the combination of a short corpus height and long tooth roots (Trinkaus, 2006).

On the internal face of the mandibular corpus, the mylohyoid line generally follows an oblique course, descending anteriorly. However, at the position of the M₃, the mylohyoid line in the SH specimens is somewhat lower (i.e., further from the alveolar margin) than is the case in Neandertals where it is placed very close to the alveolar margin (Rosas, 2001). Among European early and middle Pleistocene fossils, only Arago 2 shows a mylohyoid line placed close to the alveolar margin at the M₃ (Tables 12 and S4).

6.3 | Ramus

The ascending ramus in Neandertal mandibles generally shows a suite of derived features, including a coronoid

process that is taller than the condyle, an asymmetrical shape of the sigmoid notch with the deepest point being located posteriorly (closest to the condyle), a more medial placement of the insertion of the sigmoid notch at the condyle and a well-developed subcondylar tubercle laterally (Boule, 1911–1913; Rak et al., 2002; Suzuki & Takai, 1970). On the internal aspect, a well-developed medial pterygoid tubercle and the horizontal-oval (H-O) form of the mandibular foramen occur at high frequencies (Bermúdez de Castro et al., 2015; Smith, 1978), while the gonial margin is often very thin and truncated (Rosas, 2001). This suite of features also generally characterizes the SH sample (Table S5).

In contrast, *H. sapiens* shows a generally plesiomorphic mandibular ramus with the coronoid process and condyle being similar in height, a symmetrical sigmoid notch, with the deepest point located in the middle, a lateral insertion of the sigmoid notch at the condyle and no subcondylar tubercle. Internally, a well-developed medial pterygoid tubercle and H-O form of the mandibular foramen are only found at very low frequencies. This same suite of features also generally characterizes (non-Neandertal) archaic members of the genus *Homo* (Walker & Leakey, 1993; Weidenreich, 1936; Wood, 1991), suggesting that the anatomy of the ascending ramus in *H. sapiens*

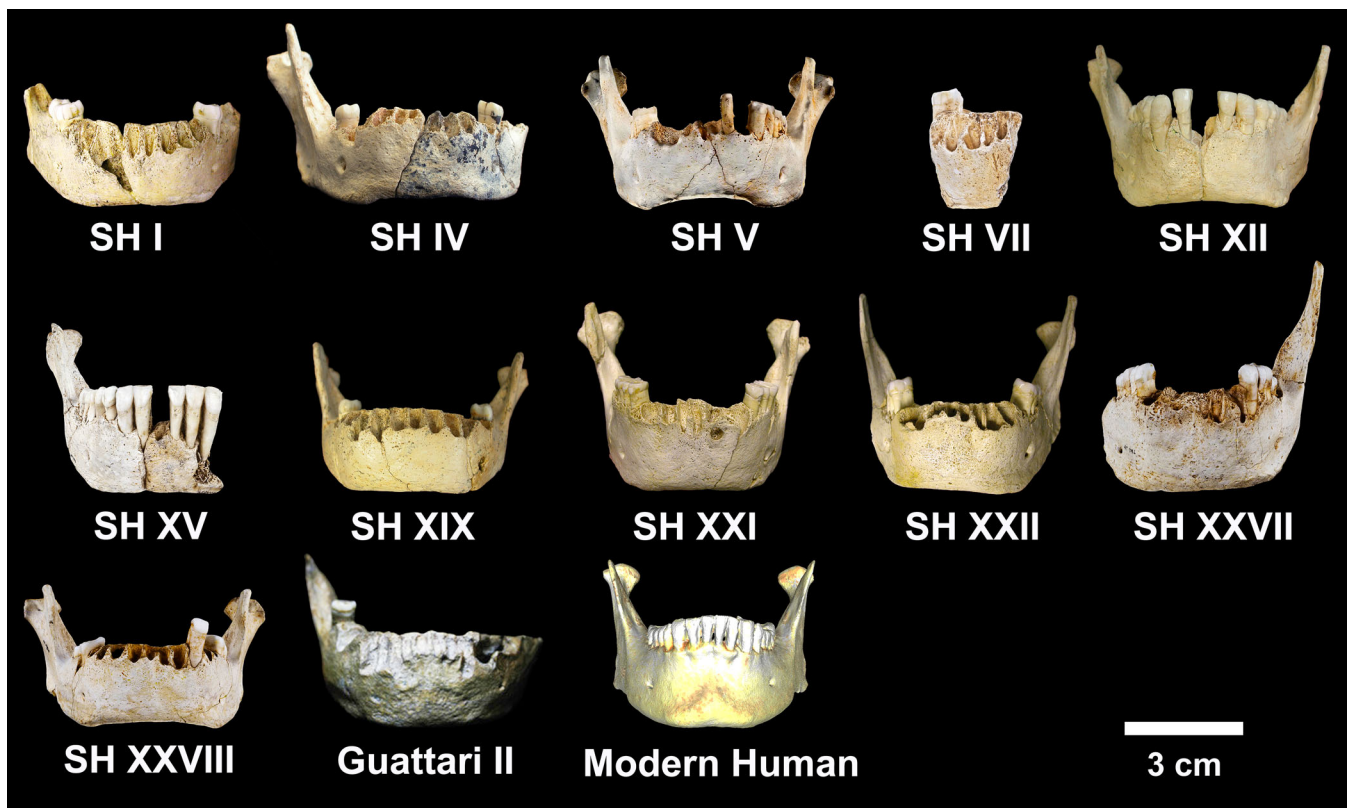


FIGURE 16 Symphyseal morphology in the adult SH mandibles compared with the Neandertal mandible Guattari II and a recent *H. sapiens* individual. *Source:* Image Credit: Javier Trueba, Madrid Scientific Films.

largely conforms to the primitive pattern, while the ramus in the Neandertal clade is derived (Rak et al., 2002).

Six of nine adult SH Individuals (67%) clearly show a coronoid process that is taller than the condyle, while in three individuals (Individuals 5, 21, and 28) the heights of the coronoid process and condyle are approximately even (Table S5; Figure 18). Similarly, the taller coronoid process is normally associated with an asymmetrical sigmoid notch, with the lowest point closer to the condyle. The one exception within the SH sample is Individual 28, which shows a similar height for the coronoid process and condyle, yet the sigmoid notch is clearly asymmetrical.

The precise insertion point of the sigmoid crest at the condyle is difficult to ascertain with certainty in some of the SH specimens due to abrasion of the condylar articular surface and/or damage to the subcondylar tubercle. Nevertheless, in eight of nine adult SH individuals (88%) where it can be seen clearly, the sigmoid notch inserts medially of the lateral margin of the condyle, and the incisure is lateral of the condylar articular surface only in Individual 15. The region of the subcondylar tubercle is frequently damaged in the SH individuals, but a clear subcondylar tubercle can be seen in Individuals 5 and 21. In addition, Individuals 4 and 28 also show a projection of bone in this region strongly suggesting a subcondylar

tubercle was present. While the remaining individuals show more damage at the site of the subcondylar tubercle, the presence of a tubercle would seem to be a constant feature (i.e., 100%) in the adult SH mandibles (Table S5).

The ascending ramus in the early Pleistocene ATD6-96 mandible conforms to the primitive condition for the genus *Homo*, with a symmetrical configuration of the coronoid process and condyle and an insertion of the sigmoid notch lateral of the condylar articular surface (Carbonell et al., 2005). Among European middle Pleistocene mandibles, some variation in the morphology of the upper border of the ramus is present (Table 12). Mauer shows a coronoid process that is approximately the same height as the condyle and a very shallow and asymmetrical sigmoid notch, whose deepest point is located posteriorly, closer to the condyle. In these features, Mauer most closely resembles SH Individual 28. The insertion of the sigmoid notch is lateral of the condylar articular surface in Mauer and a subcondylar tubercle is absent, while a shallow lateral pterygoid fossa is present. The configuration of the sigmoid notch insertion and condylar articular surface most closely resembles SH Individual 15. The ascending ramus in other European middle Pleistocene specimens also shows an even height between the

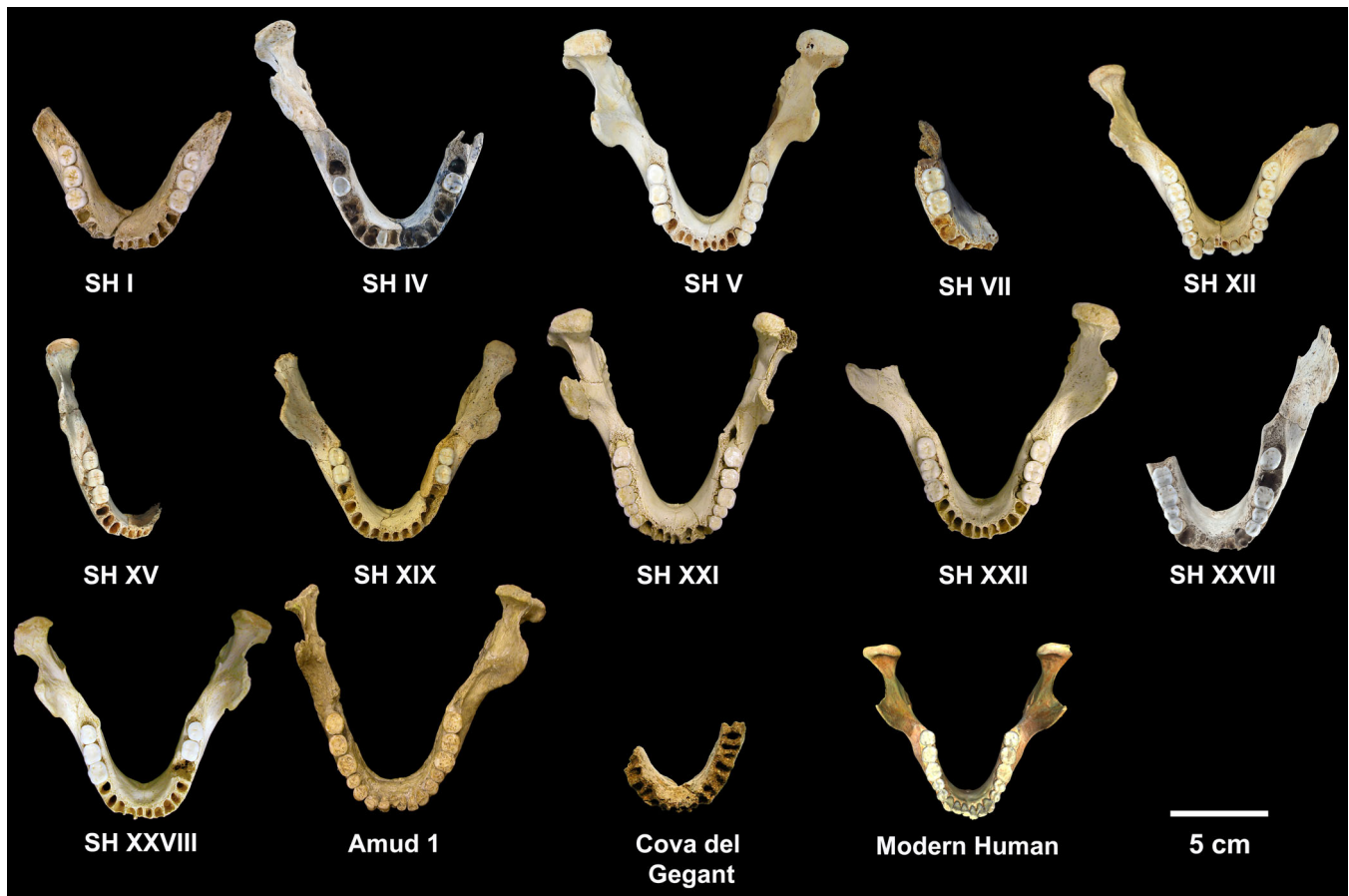


FIGURE 17 Superior view of the adult SH mandibles compared with the Amud 1 and Cova del Gegant Neandertals and a *H. sapiens* mandible. *Source:* Image Credit: Javier Trueba, Madrid Scientific Films.

coronoid process and condyle (Arago 2, 13 and Montmaurin) and a symmetrical sigmoid notch shape (Arago 13, Montmaurin) (Table 12). The sigmoid notch inserts laterally in Arago 2, but medially in Arago 13, Montmaurin and l'Aubesier and all specimens show a subcondylar tubercle.

On the internal aspect of the ramus, the presence of a horizontal/oval (H/O) mandibular foramen in Individual 4, in the form of a bony bridge covering the mandibular foramen and separating it from the exposed mylohyoid groove, represents the clearest example of this feature within the Atapuerca (SH) sample (Table S5; Figure 19). Although the lingula is damaged in Individual 15, the mylohyoid groove does not reach the mandibular foramen, and this specimen also shows what may be considered the H/O morphology. The remaining eight specimens (80%) show the normal condition of an exposed mylohyoid groove reaching the mandibular foramen and a lingula. The H/O mandibular foramen is variably present in modern humans, but reaches higher frequencies in the Neandertals (Quam & Smith, 1998; Smith, 1978). The mandibular foramen shows the normal

morphology in the early Pleistocene ATD6-96 mandible from the Gran Dolina, while a second mandible (ATD6-113) shows partial bony bridging of the mandibular foramen (Bermúdez de Castro et al., 2008). Aside from the SH sample, the H/O mandibular foramen morphology is not seen in any other European MP specimens (Table 12). Thus, this particular morphology seems to become common only with the emergence of the Neandertals and is seen in several individuals in the Krapina sample (Radovic et al., 1988).

The degree of expression of the medial pterygoid insertions along the internal aspect of the posterior border of the ramus in the SH specimens is variable (Bermúdez de Castro et al., 2015). Larger individuals (e.g., Individuals 22) generally show more marked muscle insertions and a medial pterygoid tubercle superiorly, while in some small specimens (e.g., Individual 19), the muscle insertions are barely discernible (Figure 19). Nevertheless, six of seven adult specimens (86%) show a medial pterygoid tubercle (Table S5). The presence of a medial pterygoid tubercle has been suggested to represent a derived Neandertal feature (Rak et al., 1994). While this structure is generally

TABLE 12 Expression of Neandertal features in the Atapuerca (SH) mandibles and some comparative samples and specimens.

| Feature | European middle Pleistocene | | | | Mala | | | | | | | | | |
|------------------------------------|-----------------------------------|-------------|-------------|-------------|-------------|------------|-------------|-----------|-----------------------------|-----------------------------|--------------------------|--------------------------------|--------------------------------|-------------|
| | European Pleistocene ^a | Mauer | Arago 2 | Arago 13 | Balanica | Visogliano | Montmaurin | Payre 15 | Ehringsdorf F 1/Aubesier 11 | Atapuerca (SH) ^a | Neandertals ^a | <i>H. sapiens</i> ^a | <i>H. sapiens</i> ^a | Recent |
| <i>Symphysis</i> | | | | | | | | | | | | | | |
| Frontal alignment of incisors | Curved | Curved | Curved | Curved | ? | Curved | Curved | Straight | Curved | ? | Straight | Straight | Curved | Curved |
| <i>Corpus</i> | | | | | | | | | | | | | | |
| Horizontal mental foramen position | Anterior | Anterior | Posterior | Anterior | Anterior | Anterior | Anterior | Posterior | Posterior | Posterior | Posterior | Posterior | Anterior | Anterior |
| Vertical mental foramen position | Midcorpus | Low | Low | Low | Midcorpus ? | Anterior | Midcorpus | Low | Low | ? | Low | Low | Midcorpus | Midcorpus |
| Number of mental foramina | Single | Multiple | Single | Single | Single | Single | Multiple | Single | Single | Single | Single | Multiple | Single | Single |
| Retromolar space | Absent | Absent | Absent | Absent | ? | ? | Absent | ? | ? | Present | Present | Present | Absent | Absent |
| Position of mylohyoid line at M3 | Low | Low | High | Low | ? | ? | Low | Low | Low | ? | Low | High | Low | Low |
| <i>Ramus</i> | | | | | | | | | | | | | | |
| H/O mandibular foramen | Absent | Absent | Absent | Absent | ? | ? | Absent | ? | ? | Absent | Absent | Present | Absent | Absent |
| Coronoid process and condyle | Symmetrical | Symmetrical | Symmetrical | Symmetrical | ? | ? | Symmetrical | ? | ? | ? | Asymmetrical | Asymmetrical | Symmetrical | Symmetrical |
| Mandibular incisure insertion | Lateral | Lateral | Lateral | Medial | ? | ? | Medial | ? | ? | Medial | Medial | Medial | Lateral | Lateral |
| Lateral pterygoid fossa | Absent | Absent | Absent | Absent | ? | ? | Present | ? | ? | ? | Present | Present | Absent | Absent |
| Medial pterygoid tubercle | Present | Absent | Absent | Absent | ? | ? | Present | ? | ? | Present | Present | Present | Absent | Absent |
| Gonial orientation | Straight | Straight | Straight | Everted | ? | ? | Inverted | ? | ? | ? | Everted | Inverted | Straight | Straight |
| Gonial truncation | Absent | Present | Absent | Incipient | ? | ? | Absent | ? | ? | Absent | Incipient | Present | Absent | Absent |

Note: ? = Damaged or missing information.

^aRepresents the dominant (modal) expression for the feature in each group.

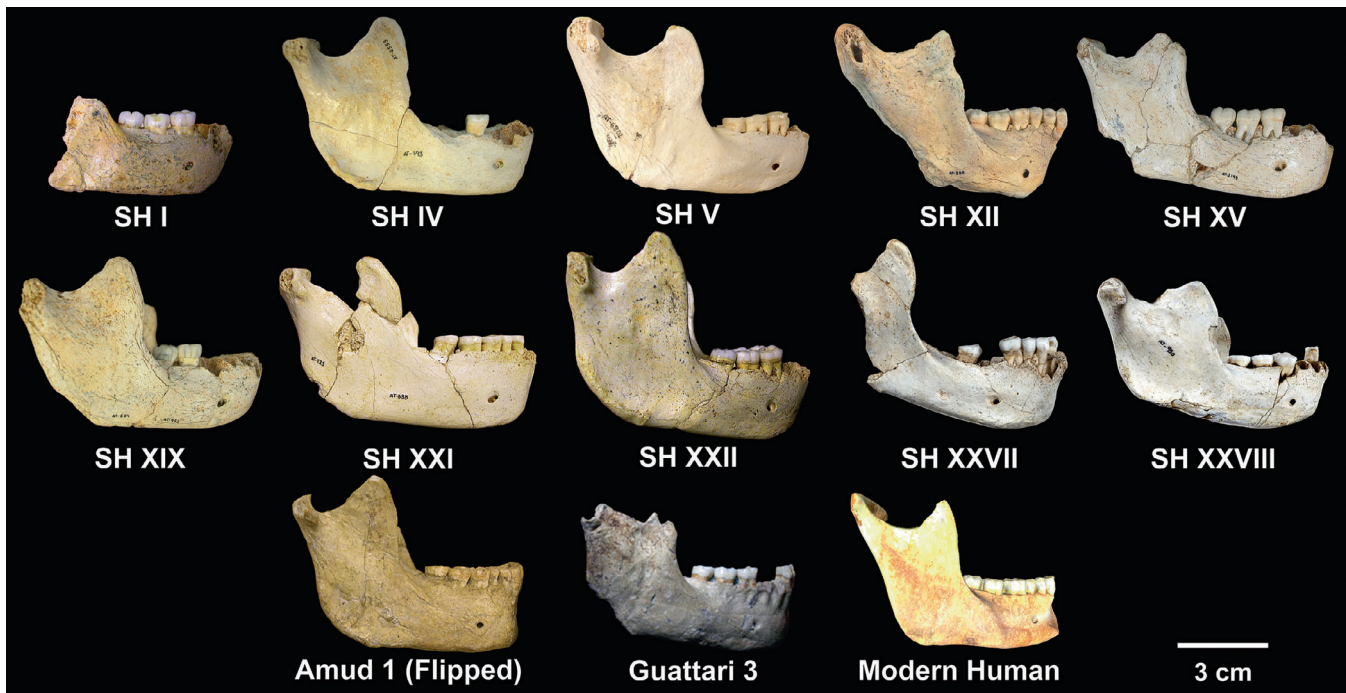


FIGURE 18 Morphology of the ramus and retromolar space in the adult SH individuals compared with the Amud 1 and Guattari 3 Neandertals and a *H. sapiens* individual. *Source:* Image Credit: Javier Trueba, Madrid Scientific Films.

absent in earlier members of the genus *Homo*, it is clearly present in the ATD6-96 mandible from the site of Gran Dolina, also in the Sierra de Atapuerca, attributed to *H. antecessor* (Carbonell et al., 2005). It is variably present in *H. sapiens* (20%–25%) but nearly ubiquitous (94%) in Neandertals (Bermúdez de Castro et al., 2015). Among European MP specimens, a medial pterygoid tubercle is absent in Mauer and three mandibles from Arago, but is present in Montmaurin and l'Aubesier (Bermúdez de Castro et al., 2015) (Table 12).

Superiorly, on the medial aspect of the condylar neck, just below the articular surface and medial to the mandibular incisure insertion, several of the mandibles in the SH sample show what appears to be a fossa and/or scars marking the insertions of the lateral pterygoid muscle (Figure 20). Some variation in the expression of this feature is found the SH sample, and it reaches its maximum expression in Individual 4 which shows a well-defined fossa and muscular insertion scars. In Individual 28, the fossa is less defined, but muscular insertion scars are clearly visible, while no trace of either a fossa or muscular insertions are visible in the smaller mandibles (e.g., Individuals 15 and 19). This feature has not been reported systematically in the literature, but it has been described as characteristic of Neandertal mandibles, including specimens from La Ferrassie, Regourdou and La Chapelle (Heim, 1976) as well as Amud 1 from southwest Asia. A lateral pterygoid fossa seems to be present in the

early Pleistocene ATD6-69 mandible, as well as the European MP specimens Mauer and Montmaurin. In contrast, this feature is not expressed in either Arago 2 or 13.

The presence of a masseteric fossa on the lateral face of the ramus is a nearly constant feature of the SH sample (Table S5; Figure 18). A clear fossa is present on the anterior portion of the ramus, below the level of the coronoid process even in the smallest individuals (e.g., Individual 19). In larger specimens (e.g., Individuals 4 and 22), the masseteric fossa extends further posteriorly reaching the gonial margin, particularly if some gonial eversion is present. The most pronounced expression of the masseteric fossa is in Individuals 4, 22, and 28.

A masseteric fossa is absent in the early Pleistocene ATD6-96 individual, but it is generally present in European middle Pleistocene specimens (except Montmaurin) (Table 12). In contrast, Neandertals frequently lack a masseteric fossa, and often show both an inversion and truncation of the gonial region (Rosas, 2001; Wolpoff et al., 1981). The truncated gonial profile in Neandertals shows a fairly straight but obliquely oriented margin running from the straight basal margin to the posterior ramus border. The gonial margin separates from the basal margin at a point just posterior to the tip of the coronoid process and reaches the posterior ramal margin at approximately half of the ramus height. In addition, the gonial margin of the ramus is often very thin in Neandertal mandibles (e.g., La Chapelle-aux-Saints).

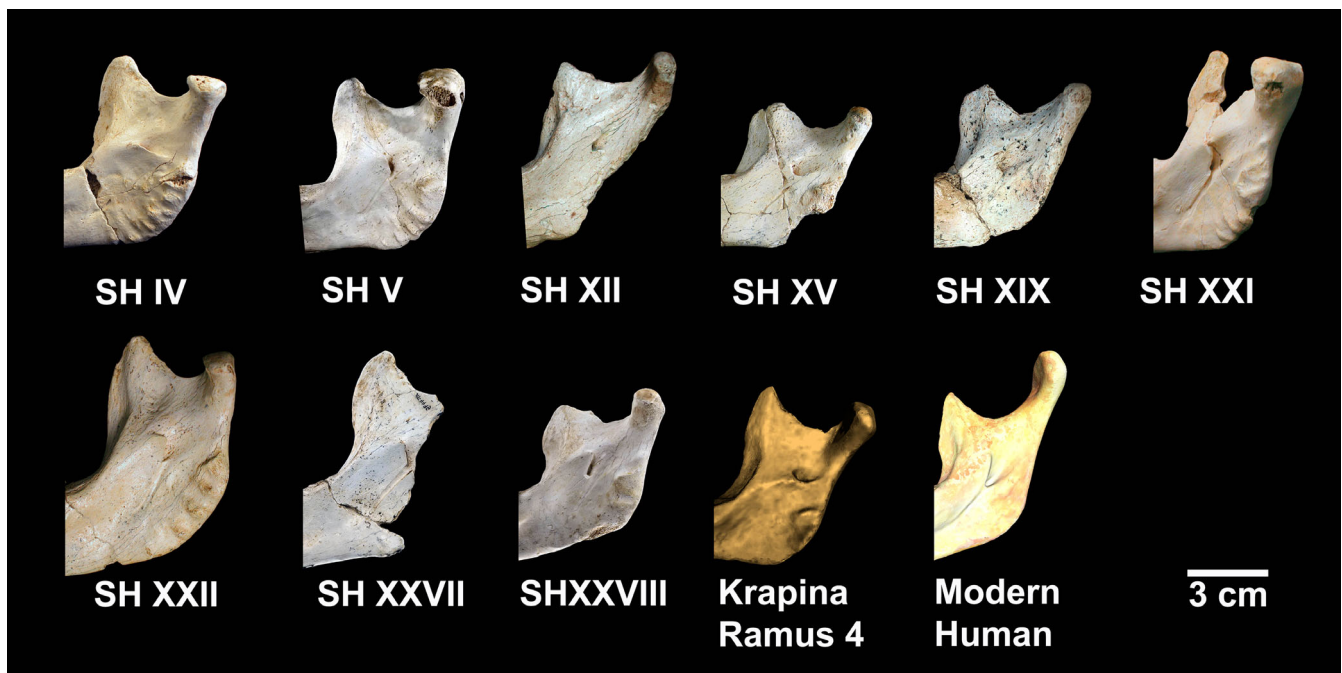


FIGURE 19 Internal aspect of the ascending ramus in the adult SH mandibles compared with Krapina ramus 4 and a *H. sapiens* individual showing details of the mandibular foramen and medial pterygoid insertions. Source: Image Credit: Javier Trueba, Madrid Scientific Films.

The SH mandibles show an incipient form of gonial truncation (Table S5). All five specimens where this could be clearly scored show an obliquely oriented gonial margin, which is not as straight as in Neandertals and separates from the basal margin at a point more posterior than in Neandertals. Clear examples of this morphology can be seen in SH Individuals 4, 5, and 22 (Figure 18). Thus, the gonial region foreshadows the gonial truncation seen in the Neandertals. However, the gonial margin in the SH mandibles is not thinned, as in some Neandertals.

The early Pleistocene mandible ATD6-96 shows a fairly regular (i.e., gently rounded) gonial profile. Among the European MP specimens, the gonial profile is regular in Arago 2, Montmaurin and l'Aubesier 11, but Mauer and Arago 13 show a truncation of the gonial region (Table 12). The gonial margin is thinnest in Arago 2, approaching the condition seen in some Neandertal specimens, while the remaining European MP specimens show a thicker gonial margin.

7 | SIZE-RELATED MORPHOLOGICAL VARIATION WITHIN THE SH SAMPLE

Variation in the expression of some morphological features in the SH mandibles has been argued to be related

to the overall size of the mandible, and the sample has been argued to follow a morphological gradient whereby smaller individuals show more primitive features, while larger individuals display more derived, Neandertal-like features (Rosas, 1997; Rosas et al., 2019; Rosas & Bastir, 2004). In particular, larger SH individuals are argued to show symphyses, which are more vertical and show a more pronounced degree of curvature on the anterior aspect, along with larger retromolar spaces and more posterior placement of the lateral corpus structures.

The symphysis has been argued to be more curved in SH Individuals 12 and 22 (Rosas, 1997; Rosas et al., 2019). The recovery of the left hemimandible for Individual 12 now allows for the assessment of the entire symphyseal region. The misalignment of the right I_2 , gives the right side of the symphysis the impression of being slightly more depressed. However, the intact left side shows little relief or curvature on the anterior surface, and this specimen falls comfortably within the limited range of variation documented in the entire SH sample. Individual 22 does show the maximum expression of curvature on the anterior surface of the symphysis, but even here, the depth of the curvature is minimal. Nor is there any indication that larger individuals show more vertical symphyses (Table 13). Comparison of the symphyseal angle with the corpus height at the symphysis and the geometric mean revealed nonsignificant correlations (Figure 21).



FIGURE 20 Details of the sigmoid notch insertion at the condyle in the adult SH mandibles compared with the Amud 1 Neandertal and a *H. sapiens* individual. *Source:* Image Credit: Javier Trueba, Madrid Scientific Films.

In contrast, larger individuals within the SH sample do indeed seem to show a more posterior placement of the lateral corpus structures and larger retromolar spaces (Table 13; Figure 22). The three SH individuals with a slightly more advanced placement of the mental foramen under the P_4/M_1 septum (Individuals 12, 15, and 19) represent smaller individuals within the sample and a retromolar space is absent in two of them (Individuals 12 and 19). The largest retromolar spaces are found in larger individuals within the SH sample (Individuals 4, 21, 22, and 27). In addition, the advanced tooth wear seen in the older SH Individuals 5 and 21 also contributes to a clear mesial drift of the entire dental arcade and results in a more posterior placement relative to the tooth row.

The development of the medial pterygoid muscular insertions, the presence of a defined fossa for the lateral pterygoid muscle, the relief of the masseteric fossa and digastric impressions all show a degree of variation in the SH sample, being more pronounced in larger specimens (Table 13). These larger muscular attachment areas suggest that larger individuals are characterized by a greater development of the muscles of mastication.

Despite this morphological variation in the SH sample, the phylogenetically informative features of the ramus and symphysis do not seem to vary with overall mandibular size (Table 13). The very small SH Individual 19 and very large SH Individual 22 both show similar expression for most of the discrete features scored on the ramus (Table S5). The few differences present include a deeper masseteric fossa, an everted gonial margin and a medial pterygoid tubercle in Individual 22 clearly reflect muscle attachment sites. Rather, the suite of features in the ascending ramus seems fairly stable within the SH sample and indicates a clear link with the later Neandertals. Similarly, the minor degree of variation in the inclination, anterior curvature or morphological features of the symphysis in the SH hominins does not seem to be clearly related to the overall size of the mandible, nor is it possible to characterize some of the SH specimens as more derived than others in these aspects. Rather, the morphology of the external symphysis in the adult SH individuals seems to conform to the condition generally found among archaic members of the genus *Homo* (Rightmire, 1990; Wood, 1991), including Neandertals (Quam et al., 2001; Trinkaus, 1983). Thus, it does not

TABLE 13 Stability and variability in morphological features in the adult SH mandibles.

| Feature | Constant | Variable | Size related |
|--|----------|----------|--------------|
| Expression of external symphysis features | X | | |
| Development of superior and inferior transverse tori | X | | X |
| Expression of digastric fossae | | X | X |
| Expression of incisura submentalis | | X | |
| Frontal alignment of anterior dentition | X | | |
| Posterior position of structures of lateral corpus | X | | X |
| Retromolar space presence | X | | X |
| Asymmetrical configuration of coronoid process and condyle | X | | |
| Medial insertion of sigmoid notch at condyle | X | | |
| Presence of lateral pterygoid fossa | | X | |
| Presence of medial pterygoid tubercle | | X | X |
| Morphology of mandibular foramen | | X | |
| Incipient gonial truncation | X | | |
| Presence of masseteric fossa | X | | X |
| Single mental foramen | X | | |

seem possible to define smaller specimens within the SH sample as evolutionarily more primitive and larger specimens as more derived, contrary to previous assertions (Rosas, 1995, 1997, 2001; Rosas et al., 2019).

8 | COMPARISON WITH EUROPEAN EARLY AND MIDDLE PLEISTOCENE MANDIBLES

8.1 | Comparison with European early Pleistocene mandibles

The evidence from the early Pleistocene is limited to a few fragmentary specimens from Atapuerca (Gran Dolina and Sima del Elefante). These fossils lack derived Neandertal features (Bermúdez de Castro et al., 2008; Bermúdez de Castro et al., 2011; Rosas & Bermúdez de Castro, 1999), but the ATD6-96 mandible does have a clear medial pterygoid tubercle (Carbonell et al., 2005). The teeth from this same site do show some Neandertal features, including a relative expansion of the anterior dentition, the crown outline and cusp proportions of the M¹ and the presence of a midtrigonid crest in the M₁ (Bermúdez de Castro et al., 1999; Gómez-Robles et al., 2007, 2011; Martínón-Torres et al., 2019). Some of these features can also be found in fossils outside Europe, making their phylogenetic polarity less clear, but they may indicate some degree of phylogenetic continuity between the Atapuerca (TD) and (SH) samples, as suggested in previous studies

(Arsuaga, Martínez, et al., 1999; Bermúdez de Castro et al., 1997; Martínón-Torres et al., 2007).

8.2 | Comparison with the Mauer mandible

The anterior dentition in the Mauer mandible does show a relative expansion of the buccolingual (BL) dimensions relative to the postcanine teeth (Rosas & Bermúdez de Castro, 1998). This feature generally characterizes Neandertal dentitions but can also be found in *H. antecessor* as well as in some non-European middle and early Pleistocene fossils (Martínón-Torres et al., 2019). Perhaps more significantly, a continuous midtrigonid crest is absent in the lower molars of Mauer (Bailey, 2002). This feature is nearly ubiquitous in Neandertal teeth and is also present at a high frequency in the Atapuerca (SH) fossils (Martínón-Torres et al., 2012). While it has also been reported in one *H. antecessor* individual as well as in some non-European Pleistocene fossils (Martínón-Torres et al., 2019), its high frequency and stability in expression is generally regarded as a characteristic feature of the Neandertal dentition. Its absence in Mauer, then, is notable and represents a clear point of departure from the SH hominins. Similarly, a recent 3D GM study of the dental arcade separates Mauer, which shows longer and more diverging tooth rows, from SH Cranium 5 (Individual 21), which shows a shorter arcade and more rounded postcanine dentition, resembling Neandertals more closely (Stelzer et al., 2019). Results in

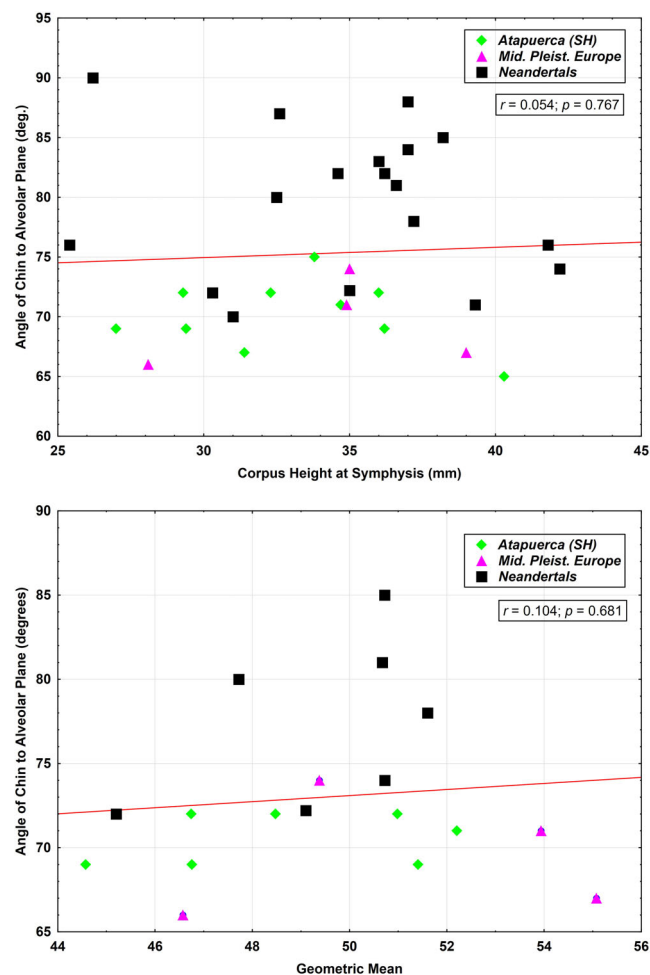


FIGURE 21 Comparison of the symphyseal angle with the corpus height at the symphysis (above) and the geometric mean (below) in the Atapuerca (SH) sample, European MP specimens and Neandertals. The pooled sample regression line is also provided.

the present study support this contention, with the dental arcade index in Mauer falling just outside the range of variation in the SH and Neandertal samples (Table 4).

The bony anatomy of the Mauer mandible has been the object of numerous previous studies. The most conspicuous feature is undoubtedly the great anteroposterior width of the ascending ramus and the extremely shallow sigmoid notch superiorly. Together, these aspects give the ramus an almost square appearance, and Mauer does indeed show the widest ramus of any fossil specimen in the present study (Table 8). This distinctive ramus anatomy has been argued to be the result of an unusual, but not necessarily pathological, insertion of the temporalis muscle at the coronoid process (Czarnetzki et al., 2003), and has been argued to be distinct from that observed in the SH hominins (Rak et al., 2011).

Details of the anatomical features in the Mauer mandible can be directly compared with the expanded sample

of SH mandibles (Table 12). In particular, similarities in the symphysis are largely primitive aspects, with a strongly retreating symphysis, little development of the chin structures and well-developed internal symphyseal tori. Similarities in the corpus can be seen in the low position of the mylohyoid line at the M_3 . The placement of the mental foramen under the P_4/M_1 septum in Mauer is also similar to some SH mandibles, although most show a more posterior placement, and the lateral prominence located under the M_3 in Mauer is similar to most of the SH mandibles. On the ascending ramus, Mauer resembles the SH hominins in showing a posterior placement of the deepest point of the sigmoid notch and lack of the H-O form of the mandibular foramen.

In contrast, the absence of a retromolar space in Mauer represents a clear point of departure with the SH mandibles. Based on the dental arcade length, ramus width and total mandibular length, Mauer was correctly predicted to lack a retromolar space (Franciscus & Trinkaus, 1995). However, Rosas and Bermudez de Castro (1998) argue that a retromolar space is essentially “covered up” by the very wide ramus. Aspects of the ramus anatomy, including similar height of the coronoid process and condyle, lateral insertion of the sigmoid notch at the condyle, lack of a medial pterygoid tubercle and more pronounced degree of gonial truncation also generally differentiate Mauer from the SH hominins.

Metrically, a few dimensions in Mauer fall outside the range of variation found in the SH sample, including the minimum ramus width, the dental arcade length and the corpus thickness at the symphysis and M_2 . In other dimensions, Mauer falls toward the upper end of the SH range of variation, and the geometric mean in Mauer is larger than in any of the SH fossils. The size-adjusted PCA results also showed Mauer falling outside the SH confidence ellipse in shape space.

In addition, Mauer can be said to differ from the SH hominins in the absence of a retromolar space, the shape of the dental arcade and details of the ramus anatomy. In all three of these anatomical regions, the SH hominins are clearly more derived towards Neandertals. Indeed, the single feature in Mauer that may seem more Neandertal-like than the SH hominins is the more pronounced degree of gonial truncation.

A recent study focused on the Mauer mandible and the definition of *H. heidelbergensis* contemplated a large number of morphological features and included an extensive comparative sample of fossil specimens (Mounier et al., 2009). A hierarchical cluster analysis based on the expression of these morphological features consistently grouped Mauer with the middle Pleistocene northern African specimen Tighenif 3. The European middle Pleistocene specimens from Arago and Montmaurin also

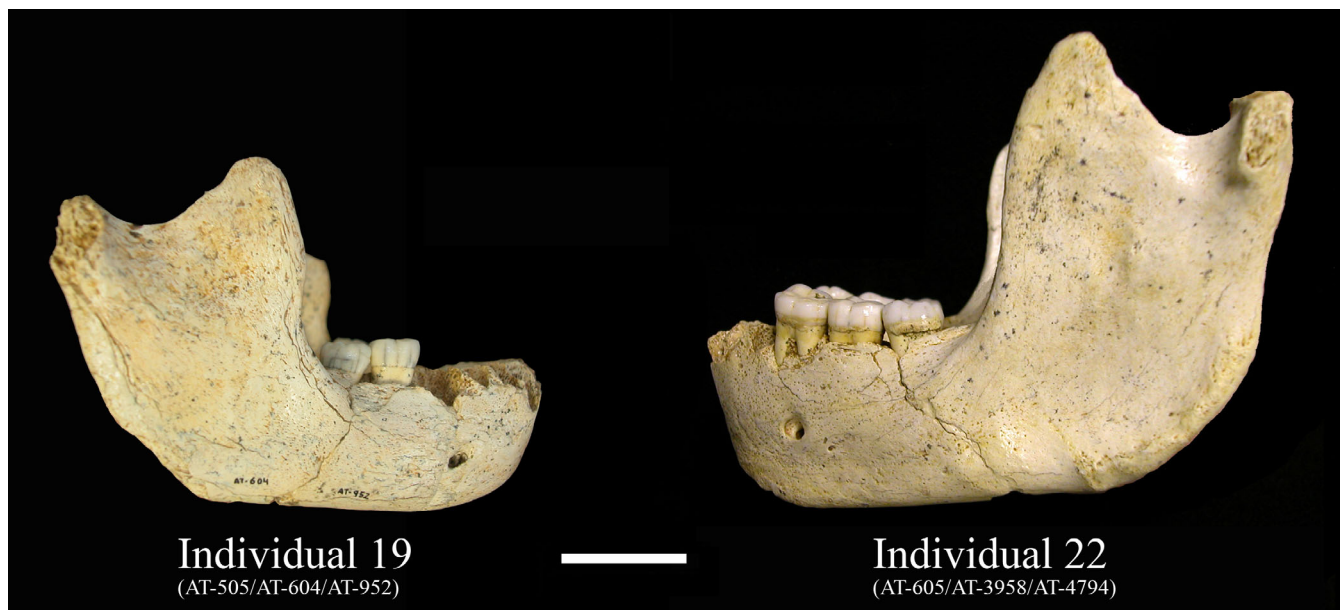


FIGURE 22 Comparison of the smallest (Individual 19) and largest (Individual 22) SH adult mandibles. The retromolar space is large in SH Individual 22, but the anatomical details of the ramus are similar between the two, suggesting a degree of morphological stability within the SH sample. Scale bar = 3 cm. *Source:* Image Credit: Javier Trueba, Madrid Scientific Films.

clustered fairly closely to Mauer in the different analyses. Among the SH fossils included in the study, Individual 28 (AT-950), and to a lesser extent Individual 21 (AT-888) were the specimens that grouped most closely with Mauer, albeit further than Tighenif 3, the Arago mandibles and Montmaurin.

Similarly, a recent 3D GM study of European Pleistocene mandibles (Rosas et al., 2019) included many of the same specimens considered here. PCA of Procrustes coordinates showed Mauer to group closely to Montmaurin, while SH Individuals 15, 19, and 21 were the closest within the SH sample. However, a neighbor-joining tree based on the Procrustes distances did not group Mauer with any of the SH individuals. Nevertheless, morphological similarities were suggested with SH Individual 28, including (1) the shape of the posterior border of the ramus; (2) a truncated gonion; (3) a thick coronoid process; (4) a well-defined intertoral sulcus; (5) a deep submental notch; (6) a well-developed fossa geni; (7) an ample retromolar area but covered by the ramus in lateral view; (8) a wide extramolar sulcus; and (9) a low position of the mylohyoid line at the level of the M3 (Rosas et al., 2019). Based on these similarities, as well as a relatively wide ramus, this SH individual has been argued to represent a morphological link between Mauer and the SH sample (Rosas et al., 2019; Tattersall, 2011).

Some of the features considered by Rosas et al. (2019) likely reflect the overall robusticity of the Mauer mandible, while others appear to be largely primitive features. The present study did not find a particular resemblance

between Mauer and SH Individual 28 (Figure 23). In particular, the minimum ramus width in SH Individual 28 is smaller than other individuals within the SH sample, even when compared with the overall mandibular length (Table 8). Indeed, SH Individual 28 seems unremarkable within the SH sample in these two measures, while Mauer falls far above the pooled sample regression line (Figure 13). Nor was SH Individual 28 the closest SH individual to Mauer in the size-adjusted PCA. Rather, SH Individuals 21 and 22 fall closer to Mauer, although the three nearest neighbors to Mauer in shape space are recent *H. sapiens* individuals, and Mauer clearly falls closer to the *H. sapiens* centroid than to the centroids of either Neandertals or the SH sample. SH Individual 28 also differs from Mauer in showing a retromolar space, a medial insertion of the sigmoid notch at the condyle, a less pronounced degree of gonial truncation and a clear medial pterygoid tubercle. Dentally, this individual also shows a midtrigonid crest in the lower molars (Martín-Torres et al., 2012). Thus, this individual is clearly more Neandertal-derived than is Mauer, and there is no morphological counterpart for the Mauer mandible within the SH sample.

While Mauer has been argued to represent an early member of the Neandertal lineage (Hublin, 1998), these distinctions suggest that derived Neandertal features are difficult to identify in the Mauer mandible, in contrast to the SH hominins. Rather, the most that can be said about the Neandertal nature of the Mauer mandible is that it shows "...a set of characteristics which are the structural basis on

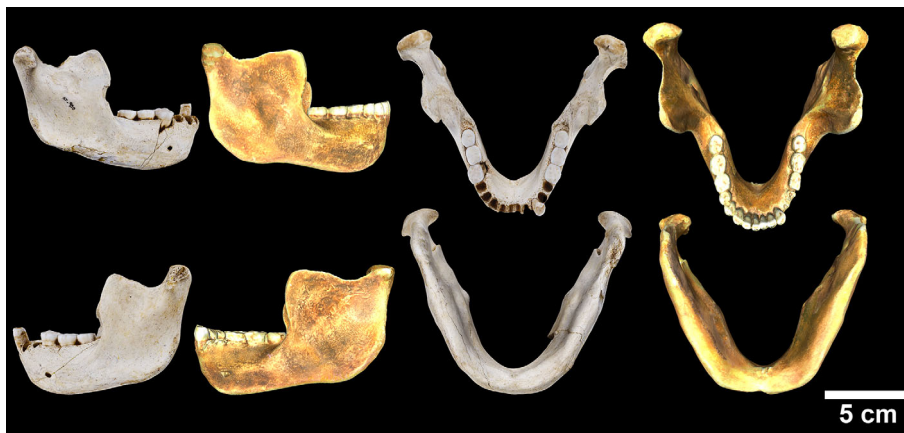


FIGURE 23 Comparison of Mauer (brown) and SH Individual 28 (light tan). While some superficial similarities are evident, clear differences can be seen in the presence of a retromolar space, medial insertion of the sigmoid notch at the condyle, pronounced medial pterygoid insertions and less pronounced gonial truncation in SH Individual 28. *Source:* Image Credit: Javier Trueba, Madrid Scientific Films.

which neandertal apomorphies will eventually be fully developed” (Rosas & Bermudez de Castro, 1998, p. 694).

8.3 | Comparison with the Arago mandibles

The SH mandibles are also generally more Neandertal-like than the approximately contemporaneous specimens from Arago. Dentally, the Arago hominins show some Neandertal features, including the presence of a midtrigonid crest in the lower molars of Arago 13 (Bermúdez de Castro et al., 2019), resembling the SH hominins. However, the two published mandibles from Arago (Arago 2 and 13) show a remarkable degree of size and morphological variation. Arago 2 is more gracile, and a number of mandibles in the Atapuerca (SH) sample show similar metric dimensions. Arago 13 is a large (presumably male) mandible whose corpus thickness is matched only by the largest, most robust specimen (Individual 7) within the Atapuerca (SH) sample. The superior transverse torus on the internal symphysis in Arago 13 surpasses the degree of expression in the Atapuerca (SH) sample, but in Arago 2, the torus is modest. Symphyseal tubercle development is difficult to establish reliably in the Arago specimens due to preservation issues, but neither of them appears to have a symphyseal tubercle, nor any other chin structures. The shape of the dental arcade in Arago 2 is similar to that in the SH hominins, showing an AP shortened and ML widened arcade. In contrast, that of Arago 13 is AP elongated, falling outside the range of variation in the SH hominins.

Neither of these specimens shows a retromolar space in lateral view, although the structures of the lateral corpus are relatively posteriorly placed in both the Arago specimens. The ramus morphology differs considerably between the two specimens. Arago 2 shows a wide ramus, with an angular notch. The coronoid process and condyle are even in height, but the sigmoid notch is

asymmetrical, with the deepest point located posteriorly, near the condyle where it inserts laterally. Internally, this specimen shows a normal morphology of the mandibular foramen, a nontruncated gonion and lacks a medial pterygoid tubercle. In contrast, the ramus in Arago 13 is narrow and tall with no angular notch anteriorly. The coronoid process and condyle are approximately equal in height. The sigmoid notch is very short and fairly symmetrical but shows a clear medial insertion at the condyle and (probably) a subcondylar tubercle. Externally, Arago 13 shows a deep masseteric fossa and a truncated gonial profile. Internally, the mandibular foramen shows the normal morphology and, while the medial pterygoid muscular insertions are marked, there is no clear medial pterygoid tubercle.

While Arago 13 shows a few derived Neandertal features, it does not have a clear counterpart in the SH sample. Comparison with SH Individual 7, the most robust specimen in the SH sample, reveals that both have extremely thick and robust mandibular corpora and show a medial insertion of the sigmoid notch at the condyle. However, the corpus is considerably shorter in height and the ramus is considerably narrower in Arago 13. Rosas et al. (2019) have compared the ramus morphology in Arago 13 with that in SH Individual 22. Both show tall rami and a medial insertion of the sigmoid notch at the condyle, but other details of the ramus differ considerably between these two individuals.

Based on these specific comparisons and the size-adjusted PCA results, the differences between Arago 2 and 13 exceed those seen in the Atapuerca SH hominins or Neandertals, making it difficult to accommodate the level of morphological variation between the two Arago specimens within either sample. Arago 2 shows closer affinities with the SH hominins. The metric dimensions are more similar to those in the SH sample, and this specimen grouped closest to the SH hominins and Neandertals in the PCA. In contrast, similarities between Arago 13 and the SH hominins are more difficult to

identify, and this individual fell far from the SH hominins in the PCA.

8.4 | Comparison with other middle Pleistocene and Neandertal mandibles

Additional fossils approximately contemporaneous with the SH hominins include the fragmentary mandibles from Visogliano and Mala Balanica, neither of which show any derived Neandertal features in the preserved corpus or dentition (Cattani et al., 1991; Roksandic et al., 2011; Skinner et al., 2016). In contrast, the SH fossils show nearly the full complement of derived Neandertal features in the mandibles, teeth, and facial morphology (Arsuaga et al., 2014; Arsuaga, Martínez, Gracia, & Lorenzo, 1997; Martínón-Torres et al., 2012; Rosas, 2001). The SH mandibles show a suite of derived features in the corpus and ramus, and differ from the later Neandertals mainly in the presence of an incipient form of gonial truncation, the lack of an H-O mandibular foramen, a low placement of the mylohyoid line at the M₃, a more retreating symphysis and somewhat less pronounced chin structures, and these would seem to represent primitive retentions in the SH fossils. Middle Pleistocene mandibles that postdate the SH sample include remains from Payre, Ehringsdorf, Montmaurin and l'Aubesier, and these fossils differ from Neandertals in these same features. Within this group, Payre, Ehringsdorf and l'Aubesier seem more similar to one another and to the SH fossils than they are to Montmaurin. This last specimen shows clear Neandertal features in the molar teeth but differs from the SH sample in the more anterior position of the lateral corpus structures, longer and narrower shape of the dental arcade, lack of a retro-molar space and symmetrical configuration of the coronoid process and condyle (Martínez de Pinillos et al., 2020; Stelzer et al., 2019; Vialet et al., 2018).

Despite some variation in the middle Pleistocene fossil record, the mandible in *H. neanderthalensis* differs from its middle Pleistocene precursors mainly in the expression of several late-appearing features, including truncated, thinned and inverted gonial margins, an H-O mandibular foramen, a high placement of the mylohyoid line at the M₃, more vertical symphyses and somewhat more pronounced chin structures. The *H. neanderthalensis* remains from Krapina already show the prevalence of the H-O mandibular foramen form, a truncated and inverted gonial profile and a higher placement of the mylohyoid line at the M₃ (Rosas, 2001; Smith, 1978). However, the symphyseal angles are low in the three Krapina individuals (70°, 71°, and 74°), along with Tabun 1 (72°) and Regourdou 1 (72°). The Krapina Neandertals likely date to the

beginning of the late Pleistocene (Rink et al., 1995). The dating for Tabun 1 (Grün et al., 1991; Grün & Stringer, 2000; Mercier et al., 1995; Mercier & Valladas, 2003) and Regourdou 1 (Maureille & Vandermeersch, 2007) are less certain, but these may also date to the earlier portion of the late Pleistocene. This suggests that changes in the symphyseal angle and chin structures only characterized later members of *H. neanderthalensis* (Dobson & Trinkaus, 2002).

9 | FUNCTIONAL IMPLICATIONS OF THE SH MANDIBLES

The mandibular ramus in Neandertals shows a suite of derived features, including a coronoid process which is taller than the condyle, an asymmetrical configuration of the sigmoid notch, with the deepest point located close to the condyle, a more medial insertion of the sigmoid notch relative to the condylar articular surface, the presence of a subcondylar tubercle, lateral pterygoid fossa, medial pterygoid tubercle, H/O mandibular foramen and a truncated, thinned and inverted gonial margin.

This suite of derived features of the Neandertal ramus has been interpreted as reflecting an increased gape potential in Neandertals, and is mainly related to a lowering of the mandibular condyle (Rak et al., 2002). It also appears to be associated with a derived anatomy in the glenoid fossa in Neandertals, which shows a flattened articular eminence anteriorly (Martínez et al., 2008). Importantly, Neandertal crania have long been characterized as showing a zygomatic process root that is aligned with the external auditory canal (Trinkaus, 1983). This distinctive configuration likely reflects a lower placement of the glenoid fossa to maintain articulation with the lowered mandibular condyle.

Although some variation is present, the SH mandibles largely conform to this same configuration, and the glenoid fossa also shows a flattened articular eminence (Martínez & Arsuaga, 1997). The presence of this full suite of features in the majority of the SH hominins suggests that the beginnings of the Neandertal clade can be tied to the emergence of this derived suite of features. Perhaps related to this is the finding that the dental arcade length and breadth, bicondylar breadth and angles of the symphysis and ramus do not vary with overall mandible size in the SH hominins and Neandertals (Table 11). Stelzer et al. (2019) similarly reported that the shape differences in the maxillary dental arcade are not size related. These may all be components of a single functional module to maintain dental occlusion with the maxillary dental arcade. The most consistent anatomical differences between the ramus in the Atapuerca SH hominins and Neandertals include a general absence of

the H/O mandibular foramen and an incipient form of gonial truncation, and these may represent the final derived mandibular ramus features to emerge in the Neandertals. The presence of a derived suite of features in the teeth, mandible and glenoid fossa provides a useful anatomical basis to include both mandibles and crania within the Neandertal clade. Notably, a lowered condyle is absent in Mauer (Rak et al., 2011), and this individual does not show the suite of derived traits seen in the Atapuerca SH hominins or Neandertals.

10 | TAXONOMIC CONSIDERATIONS

10.1 | Are the SH hominins *H. heidelbergensis*?

The Atapuerca (SH) hominins have previously been included in this taxon, mainly as a “chronospecies” with *H. neanderthalensis*. However, the type specimen of *H. heidelbergensis*, the Mauer mandible, lacks associated cranial remains, and this makes assigning crania to this taxon problematic. Thus, the only direct comparison that can be made between the Atapuerca SH hominins and Mauer is that based on the mandibular anatomy. The clear anatomical differences from Mauer suggest that the SH hominins should not be lumped in with this specimen in the same taxonomic category. Perhaps most importantly, the Mauer mandible does not show the lowered condyle considered characteristic of Neandertals and the SH hominins (Rak et al., 2011). Most of the remaining derived Neandertal features of the ramus are also not seen in Mauer, except for the gonial truncation.

The chronologically older age of Mauer may partially explain the lack of derived features. While Mauer does seem more Neandertal derived than the early Pleistocene *H. antecessor* remains, Hublin (2009, p. 10626) has argued “it is (and may always be) difficult to establish whether this specimen predated or postdated the beginning of the accretion of Neandertal features.” If *H. heidelbergensis* is characterized mainly by the lack of derived Neandertal features, then the mandibles from Mala Balanica, Montmaurin and (probably) Visogliano could also be included in this taxon (Roksandic et al., 2018). The mandibles from Arago differ more from one another than do any two SH specimens. Arago 13 could perhaps be included in this taxon as well, but Arago 2 shows stronger affinities to the SH fossils. The middle Pleistocene cranium from Ceprano is not associated with a mandible, but may also belong in this group, given its lack of Neandertal-derived features (Manzi, 2016).

10.2 | Are the SH hominins *H. neanderthalensis*?

The type specimen of this taxon does not preserve a mandible. Nevertheless, the mandibular evidence presented here has revealed a very close similarity between the Atapuerca SH sample and Neandertals. The main differences seem to be the lack of a few derived Neandertal features in the SH hominins, including a high prevalence of the H/O mandibular foramen, a thinned, truncated and inverted gonial margin, a high placement of the mylohyoid line at the level of the M₃, multiple mental foramina, a more vertical symphysis and somewhat more pronounced development of chin structures. Thus, the Atapuerca SH mandibles exhibit most but not all the derived Neandertal features.

Neandertal-derived craniodental features are also present in the face (Arsuaga et al., 2014), dentition (Martín-Torres et al., 2012) and glenoid fossa (Martínez & Arsuaga, 1997) in the SH hominins, and they can be considered fully Neandertal in these anatomical regions. Other aspects of the cranial remains, however, are clearly not Neandertal-like or show at most an incipient development of Neandertal features. The SH cranial remains differ from Neandertals in the reduced size of the postcanine dentition, the high and rounded cranial profile, large and projecting mastoid processes, the digastric groove morphology, incipient suprainiac fossa and lack of a bilaterally projecting occipital torus (Arsuaga et al., 2014; Bermúdez de Castro & Nicolás, 1995; Martínez & Arsuaga, 1997). In the inner ear, the bony labyrinth shows a Neandertal-derived pattern of semicircular canal proportions but lacks the low placement of the posterior canal (Quam et al., 2016), while the cochlea in the SH hominins differs from Neandertals in its smaller volume and in the proportional lengths of the cochlear turns (Conde-Valverde et al., 2019).

The postcranial morphology of the SH hominins includes features that are mainly primitive for the genus *Homo*, including a very wide pelvis (Arsuaga, Lorenzo, et al., 1999) and thick cortical bone in the long bones (Carretero et al., 2018; Rodríguez et al., 2018). Other features seem to represent potential Neandertal-derived traits, including a low degree of lumbar lordosis (Bonmatí et al., 2010). However, other Neandertal features are not present in the SH hominins, including a lateral orientation of the lumbar transverse processes and the very thin superior pubic ramus (Arsuaga et al., 2015) as well as relatively shortened distal limb proportions (Carretero et al., 2012). The SH postcranial skeleton, then, shows some differences from the Neandertals. mtDNA evidence showed the Atapuerca SH hominins were most closely aligned with the Denisovans (Meyer et al., 2014), while nuclear DNA evidence suggested a

sister group relationship with the Neandertals (Meyer et al., 2016). Thus, the combined anatomical and genetic evidence suggests the Atapuerca SH hominins share a close evolutionary relationship with, but remain distinct from, the Neandertals.

10.3 | Human evolution in middle Pleistocene Europe

Several authors have proposed an accretion model for the emergence of Neandertals (Dean et al., 1998; Hublin, 2009). Under this model, Neandertal features gradually accumulated during the course of the middle Pleistocene, with later specimens showing a higher concentration of Neandertal features than earlier specimens. The current evidence from the fossil record indicates that during the European Pleistocene, potentially derived Neandertal features appeared first in the dentition, followed by the more or less simultaneous appearance of features in the face, mandible and glenoid fossa. The Atapuerca SH fossils are the first to show all these features, while still retaining some primitive (non-Neandertal) aspects of the cranial vault. Hublin (2009) has argued the recognition of *H. neanderthalensis* could perhaps be tied to the emergence of the cranial vault features lacking in the SH hominins. Under this proposal, the more derived occipital bone morphology in the slightly younger Swanscombe specimen (c.400 kya) would make this the earliest specimen of *H. neanderthalensis* and implies that this taxon has relatively deep roots in the middle Pleistocene.

Alternatively, a two phase model has been proposed that sees the emergence of Neandertal features occurring in two distinct phases (Rosas et al., 2019; Rosas, Bastir, et al., 2006). The first phase includes changes related with midfacial prognathism and is reflected mainly in the dental arcade and external features of the mandibular corpus. The second phase occurs during the late middle Pleistocene and includes changes related to encephalization and is reflected mainly on the internal aspect of the mandibular body. This latter phase would represent a speciation event marking the appearance of *H. neanderthalensis*.

The European MP mandibles can be broadly divided into two chronological groupings. An early group includes specimens that range in age between approximately 600–350 kya and includes Mauer, Arago 2 and 13, Mala Balanica, Visogliano 2 and the Atapuerca (SH) specimens. A later group dates to approximately 250–150 kya and includes Payre 15, Ehringsdorf 8, l'Aubesier 11 and probably Montmaurin. This chronological division also reflects a morphological division between earlier specimens that lack Neandertal-derived features in the mandible and later ones that clearly show them. Nevertheless, within the

earlier group the Atapuerca SH and Arago 2 specimens seem more closely aligned morphologically with the later group, while the absence of most Neandertal features in the Montmaurin mandible aligns it with the early group.

If the earlier specimens are grouped into *H. heidelbergensis*, while the later specimens are considered to represent *H. neanderthalensis*, then a broad chronospecies concept might still seem to hold. However, the fact that the Atapuerca (SH) mandibles show a greater number of derived Neandertal features than other more or less contemporaneous European middle Pleistocene specimens suggests more than one evolutionary lineage coexisted in the middle Pleistocene. In addition, while the dating of Montmaurin is uncertain, it may represent a late survivor of the more primitive (less Neandertal-derived) group. Thus, while the accretion hypothesis is technically compatible with either an anagenetic or cladogenetic pattern of evolution, the chronological overlap of these distinct lineages is compatible only with the latter.

A cladogenetic pattern is also consistent with the relatively low degree of metric variation and general anatomical stability seen in the SH mandible sample (Figure 15). The SH mandibles were less variable than the Neandertal sample in most metric dimensions and are less variable anatomically than the two specimens from Arago. This low degree of intrapopulation variability implies that evolutionary change is a product of competition between groups and can be taken to reflect a cladogenetic pattern of evolution (Arsuaga et al., 2014).

The data from the Atapuerca SH mandibles suggest an early appearance of most Neandertal features, followed by little directional change during the later middle Pleistocene and culminating in the emergence of several late-appearing features at the very end of the middle Pleistocene, perhaps reflecting a speciation event and the emergence of *H. neanderthalensis*. This cladogenetic pattern would seem to reconcile the different predictions from the accretion model and the two phases model. The main difference remaining would be the underlying mechanism (evolutionary competition between groups vs. growth dynamics and encephalization in organismal evolution) that leads to the emergence of Neandertal features.

The present data continue to support the emergence of the Neandertal clade in Europe, with the Atapuerca SH hominins being the oldest fossils to clearly show many derived Neandertal craniodental features. The few taxonomically relevant similarities with *H. antecessor* would also imply some degree of phylogenetic continuity between early and middle Pleistocene populations in Europe. Nevertheless, the differences between *H. antecessor* and middle Pleistocene fossils could be due to an influx of genes or migration(s) of a population(s) from outside Europe that

showed variable frequencies of Neandertal traits (Bermúdez de Castro et al., 2016) and/or some local development due to genetic drift of small isolated populations.

Regardless, given the strong similarity of the SH mandibular remains with the later Neandertals, it is reasonable to hypothesize that the beginnings of the Neandertal clade can be tied to a speciation event reflected in the appearance of a suite of derived features in the mandible, face and dentition. If *H. heidelbergensis* is considered to represent a taxon that generally lacks Neandertal-derived features, as argued here, the absence of these mandibular features, particularly the lowered condyle, would appear to be the primary distinction from the SH hominins. The presence of derived features related to this lowered condyle in the glenoid fossa also offers a means to align other European middle Pleistocene crania that lack mandibles with the SH fossils and the Neandertals or to include them in *H. heidelbergensis* based on this same criteria. The specific identity of the SH fossils must contemplate additional sources of information from the cranium, teeth, and postcranial skeleton, all of which are preserved at the SH site.

11 | CONCLUSION

The recovery of additional mandibular remains from the Atapuerca (SH) site has extended the known range of variation in some metric dimensions and morphological details and has made it possible to confirm previous observations based on more limited evidence. Specific comparison with Mauer has revealed important anatomical differences and suggests that the SH hominins should no longer be classified as *H. heidelbergensis*. The mandibular evidence is consistent with at least two different evolutionary lineages being present in the European middle Pleistocene. One group lacks clear Neandertal-derived features and includes the specimens from Mauer, Mala Balanica, Montmaurin, Visogliano and one of the Arago mandibles. The other group shows the presence of Neandertal-derived features and includes the Atapuerca (SH) fossils, Arago 2 and specimens from Payre, Ehringsdorf and l'Aubesier.

The principal differences of the SH mandibles from Neandertals include a high prevalence of the H/O mandibular foramen, a truncated, thinned and inverted gonial margin, a high placement of the mylohyoid line at the level of the M3, a more vertical symphysis and somewhat more pronounced expression of the chin structures in Neandertals. Size-related morphological variation in the SH hominins included larger retromolar spaces, more posterior placement of the lateral corpus structures and stronger markings associated with the muscles of

mastication in larger specimens. However, phylogenetically relevant features in the SH sample are fairly stable and do not vary with the overall size of the mandible.

The dating of the site to c.430 kya indicates that mid-facial prognathism, a suite of derived Neandertal features in the ascending ramus and corpus of the mandible, the expansion of the anterior dentition, the bulging, rhomboidal crown outline of the M¹ and a flat articular eminence in the glenoid fossa were already present at a very early stage of the Neandertal evolutionary lineage. This is consistent with the idea that the derived Neandertal features appeared first in the splanchnocranium and only later in the neurocranium. These features seem to be largely absent in the earlier material from the Sima del Elefante (TE) and Gran Dolina (TD) sites, also in the Sierra de Atapuerca. The appearance of a suite of derived Neandertal features in the face, dentition and mandible, all of which are present in the Atapuerca (SH) hominins, reflects a speciation event at the origin of the Neandertal clade.

AUTHOR CONTRIBUTIONS

Rolf Quam: Conceptualization; formal analysis; investigation; methodology; supervision; writing – original draft. **María Cruz Ortega Martínez:** Methodology; resources. **Brian Keeling:** Investigation; visualization; writing – review and editing. **Bill Hylander:** Writing – review and editing. **Yoel Rak:** Investigation; writing – review and editing. **Ignacio Martínez:** Conceptualization; funding acquisition; investigation; project administration; writing – review and editing. **Mercedes Conde-Valverde:** Investigation; writing – review and editing. **Carlos Lorenzo:** Formal analysis; methodology; software; writing – review and editing. **Ana Pantoja Perez:** Investigation; methodology; software.

ACKNOWLEDGMENTS

The following individuals provided access to original specimens or high-quality casts of fossil mandibles housed under their care: J.M. Bermúdez de Castro (Cenieh), Y. Rak (Tel Aviv University), P. Menecier, A. Balzeau (Musée de l'Homme), H. de Lumley (IPH), D. Lieberman (Peabody Museum, Harvard University), I. Tattersall and G. Garcia (AMNH). R. Franciscus and E. Trinkaus provided some unpublished measurements on the Dolni Vestonice mandibles. B. Keeling and H. Brandt collected some data on the recent *H. sapiens* sample housed at Binghamton University. Portions of this research were supported by Binghamton University and a grant from the Ministerio de Ciencia e Innovación y Universidades of the Government of Spain (Project No. PGC 2018-093925-B-C33) and the Junta de Castilla y León (Project Nos. BU032A06 and BU005A09).

ORCID

Rolf Quam  <https://orcid.org/0000-0002-1140-5615>

REFERENCES

- Aguirre, E., & de Lumley, M. (1977). Fossil men from Atapuerca, Spain: Their bearing on human evolution in the middle Pleistocene. *Journal of Human Evolution*, *6*, 681–688.
- Arsuaga, J. L., Carretero, J.-M., Lorenzo, C., Gómez-Olivencia, A., Pablos, A., Rodríguez, L., García-González, R., Bonmatí, A., Quam, R. M., Pantoja-Pérez, A., Martínez, I., Aranburu, A., Gracia-Téllez, A., Poza-Rey, E., Sala, N., García, N., Alcázar de Velasco, A., Cuenca-Bescós, G., Bermúdez de Castro, J. M., & Carbonell, E. (2015). Postcranial morphology of the middle Pleistocene humans from Sima de los Huesos, Spain. *Proceedings of the National Academy of Sciences*, *112*, 11524–11529.
- Arsuaga, J. L., Carretero, J. M., Lorenzo, C., Gracia, A., Martínez, I., Bermúdez de Castro, J., & Carbonell, E. (1997). Size variation in middle Pleistocene humans. *Science*, *277*, 1086–1088.
- Arsuaga, J. L., Lorenzo, C., Carretero, J. M., Gracia, A., Martínez, I., García, N., Bermúdez de Castro, J., & Carbonell, E. (1999). A complete human pelvis from the middle Pleistocene of Spain. *Nature*, *399*, 255–258.
- Arsuaga, J. L., Martínez, I., Arnold, L., Aranburu, A., Gracia-Téllez, A., Sharp, W., Quam, R., Falguères, C., Pantoja-Pérez, A., Bischoff, J., Poza-Rey, E., Parés, J., Carretero, J., Demuro, M., Lorenzo, C., Sala, N., Martínón-Torres, M., García, N., Alcázar de Velasco, A., ... Carbonell, E. (2014). Neandertal roots: Cranial and chronological evidence from Sima de los Huesos. *Science*, *344*, 1358–1363.
- Arsuaga, J. L., Martínez, I., Gracia, A., Carretero, J. M., & Carbonell, E. (1993). Three new human skulls from the Sima de los Huesos site in Sierra de Atapuerca, Spain. *Nature*, *362*, 534–537.
- Arsuaga, J. L., Martínez, I., Gracia, A., Carretero, J. M., Lorenzo, C., García, N., & Ortega, A. (1997). Sima de los Huesos (Sierra de Atapuerca, Spain). The Site. *Journal of Human Evolution*, *33*, 109–128.
- Arsuaga, J. L., Martínez, I., Gracia, A., & Lorenzo, C. (1997). The Sima de los Huesos crania (Sierra de Atapuerca, Spain). A comparative study. *Journal of Human Evolution*, *33*, 219–282.
- Arsuaga, J. L., Martínez, I., Lorenzo, C., Gracia, A., Muñoz, A., Alonso, O., & Gallego, A. (1999). The human cranial remains from Gran Dolina Lower Pleistocene site (Sierra de Atapuerca, Spain). *Journal of Human Evolution*, *37*, 431–457.
- Bailey, S. (2002). A closer look at Neanderthal postcanine dental morphology: The mandibular dentition. *The Anatomical Record*, *269*, 148–156.
- Barroso Ruiz, C., De Lumley, M. A., Caparros, M., & Verdu Bermejo, L. (2006). Les resteshumains néandertaliens et *Homo sapiens* de la grotte du Boquete deZafarraya. In C. Barroso Ruiz & H. de Lumley (Eds.), *La Grotte du Boquete deZafarraya (Malaga, Andalousie)* (pp. 1167–1396). Junta de Andalucía. Consejería de Cultura.
- Benazzi, S., Gruppioni, G., Strait, D. S., & Hublin, J. J. (2014). Virtual reconstruction of KNM-ER 1813 *Homo habilis* cranium. *American Journal of Physical Anthropology*, *153*, 154–160.
- Berger, G., Pérez-González, A., Carbonell, E., Arsuaga, J., Bermúdez de Castro, J., & Ku, T. (2008). Luminescence chronology of cave sediments at the Atapuerca paleoanthropological site, Spain. *Journal of Human Evolution*, *55*, 300–311.
- Bermúdez de Castro, J., Martínón-Torres, M., Gómez-Robles, A., Prado-Simón, L., Martín-Francés, L., Lapresa, M., Olejniczak, A., & Carbonell, E. (2011). Early Pleistocene human mandible from Sima del Elefante (TE) cave site in Sierra de Atapuerca (Spain): A comparative morphological study. *Journal of Human Evolution*, *61*, 12–25.
- Bermúdez de Castro, J., Martínón-Torres, M., Lozano, M., Sarmiento, S., & Muela, A. (2004). Paleodemography of the Atapuerca-Sima de los Huesos hominin sample: A revision and new approaches to the paleodemography of the European middle Pleistocene population. *Journal of Anthropological Research*, *60*, 5–26.
- Bermúdez de Castro, J. M., Arsuaga, J. L., Carbonell, E., Rosas, A., Martínez, I., & Mosquera, M. (1997). A hominid from the lower Pleistocene of Atapuerca, Spain: Possible ancestor to Neanderthals and modern humans. *Science*, *276*, 1392–1395.
- Bermúdez de Castro, J. M., Martínez, I., Gracia-Téllez, A., Martínón-Torres, M., & Arsuaga, J. L. (2020). The Sima de los Huesos middle Pleistocene hominin site (Burgos, Spain). Estimation of the number of individuals. *The Anatomical Record*, *304*, 1463–1477.
- Bermúdez de Castro, J. M., Martínón-Torres, M., Rosell, J., Blasco, R., Arsuaga, J. L., & Carbonell, E. (2016). Continuity versus discontinuity of the human settlement of Europe between the late early Pleistocene and the early middle Pleistocene. The mandibular evidence. *Quaternary Science Reviews*, *153*, 51–62.
- Bermúdez de Castro, J. M., Martínón-Torres, M., de Pinillos, M. M., García-Campos, C., Modesto-Mata, M., Martín-Francés, L., & Arsuaga, J. L. (2019). Metric and morphological comparison between the Arago (France) and Atapuerca-Sima de los Huesos (Spain) dental samples, and the origin of Neanderthals. *Quaternary Science Reviews*, *217*, 45–61.
- Bermúdez de Castro, J. M., Pérez-González, A., Martínón-Torres, M., Gómez-Robles, A., Rosell, J., Prado, L., Sarmiento, S., & Carbonell, E. (2008). A new early Pleistocene hominin mandible from Atapuerca-TD6, Spain. *Journal of Human Evolution*, *55*, 729–735.
- Bermúdez de Castro, J. M., Quam, R., Martínón-Torres, M., Martínez, I., Gracia-Téllez, A., Arsuaga, J. L., & Carbonell, E. (2015). The medial pterygoid tubercle in the Atapuerca early and middle Pleistocene mandibles: Evolutionary implications. *American Journal of Physical Anthropology*, *156*, 102–109.
- Bermúdez de Castro, J. M., Rosas, A., & Nicolás, M. E. (1999). Dental remains from Atapuerca-TD6 (Gran Dolina site, Spain). *Journal of Human Evolution*, *37*, 523–566.
- Bermúdez de Castro, J. M., Sarmiento, S., Cunha, E., Rosas, A., & Bastir, M. (2001). Dental size variation in the Atapuerca-SH middle Pleistocene hominids. *Journal of Human Evolution*, *41*, 195–209.
- Bermúdez de Castro, J. M., & Nicolás, M. E. (1995). Posterior dental size reduction in hominids: The Atapuerca evidence. *American Journal of Physical Anthropology*, *96*, 335–356.
- Blackwell, B., & Schwarcz, H. P. (1986). U-series analyses of the lower travertine at Ehringsdorf, DDR. *Quaternary Research*, *25*, 215–222.
- Bonmatí, A., Gómez-Olivencia, A., Arsuaga, J.-L., Carretero, J. M., Gracia, A., Martínez, I., Lorenzo, C., Bermúdez de Castro, J. M., & Carbonell, E. (2010). Middle Pleistocene lower back and pelvis from an aged human individual from the Sima

- de los Huesos site, Spain. *Proceedings of the National Academy of Sciences*, 107, 18386–18391.
- Boule, M. (1911–1913). *L'homme fossile de la Chapelle-aux-Saints*. Masson, Paris.
- Carbonell, E., Bermúdez de Castro, J., Arsuaga, J. L., Allue, E., Bastir, M., Benito, A., Cáceres, I., Canals, T., Díez, J., van der Made, J., Mosquera, M., Ollé, A., Pérez-González, A., Rodríguez, J., Rodríguez, X., Rosas, A., Rosell, J., Sala, R., Vallverdú, J., & Vergés, J. (2005). An early Pleistocene hominin mandible from Atapuerca-TD6, Spain. *Proceedings of the National Academy of Sciences of the United States of America*, 102, 5674–5678.
- Carbonell, E., Bermúdez de Castro, J., Parés, J., Pérez-González, A., Cuenca-Bescós, G., Ollé, A., Mosquera, M., Huguet, R., van der Made, J., Rosas, A., Sala, R., Vallverdú, J., García, N., Granger, D., Martín-Torres, M., Rodríguez, X., Stock, G., Vergés, J., Allué, E., ... Arsuaga, J. (2008). The first hominin of Europe. *Nature*, 452, 465–469.
- Carretero, J.-M., Rodríguez, L., García-González, R., Arsuaga, J.-L., Gómez-Olivencia, A., Lorenzo, C., Bonmatí, A., Gracia, A., Martínez, I., & Quam, R. (2012). Stature estimation from complete long bones in the middle Pleistocene humans from the Sima de los Huesos, Sierra de Atapuerca (Spain). *Journal of Human Evolution*, 62, 242–255.
- Carretero, J. M., Rodríguez, L., García-González, R., Quam, R. M., & Arsuaga, J. L. (2018). Exploring bone volume and skeletal weight in the middle Pleistocene humans from the Sima de los Huesos site (Sierra de Atapuerca, Spain). *Journal of Anatomy*, 233, 740–754.
- Cattani, L., Cremaschi, M., Ferraris, M., Mallegni, F., Masini, F., Scola, V., & Tozzi, C. (1991). Le gisement du Pléistocène Moyen de Visogliano (Trieste): restes humains, industries, environnement. *L'Anthropologie (Paris)*, 95, 9–36.
- Chen, F., Welker, F., Shen, C.-C., Bailey, S. E., Bergmann, I., Davis, S., Xia, H., Wang, H., Fischer, R., Freidline, S. E., Yu, T.-L., Skinner, M. M., Stelzer, S., Dong, G., Fu, Q., Dong, G., Wang, J., Zhang, D., & Hublin, J.-J. (2019). A late middle pleistocene denisovan mandible from the tibetan plateau. *Nature*, 569, 409–412.
- Conde-Valverde, M., Martínez, I., Quam, R. M., Bonmatí, A., Lorenzo, C., Velez, A. D., Martínez-Calvo, C., & Arsuaga, J. L. (2019). The cochlea of the Sima de los Huesos hominins (Sierra de Atapuerca, Spain): New insights into cochlear evolution in the genus *Homo*. *Journal of Human Evolution*, 136, 102641.
- Condemi, S. (2001). *Les Néandertaliens de La Chaise*. CTHS.
- Crégut-Bonnoure, É., Boulbes, N., Guérin, C., Pernaud, J., Tavoso, A., & Cammas, R. (2010). Le contexte géomorphologique et faunique de l'homme de Montmaurin (Haute-Garonne). *Préhistoires Méditerranéennes*, 1, 3–85.
- Czarnetzki, A., Jakob, T., & Pusch, C. (2003). Paleopathological and variant conditions of the *Homo heidelbergensis* type specimen (Mauer, Germany). *Journal of Human Evolution*, 44, 479–495.
- Daura, J., Sanz, M., Subirá, M., Quam, R., Fullola, J., & Arsuaga, J. L. (2005). A Neandertal mandible from the Cova del Gegant (Sitges, Barcelona, Spain). *Journal of Human Evolution*, 49, 56–70.
- Dean, D., Hublin, J., Holloway, R., & Ziegler, R. (1998). On the phylogenetic position of the pre-Neandertal specimen from Reilingen, Germany. *Journal of Human Evolution*, 34, 485–508.
- DeLumley, M., De Lumley, H., & Fournier, A. (1982). *Les mandibules de l'Arago et leur comparaison avec des autres mandibules anténéandertaliennes* (pp. 147–164). *Congrès Internationale de Paleontologie Humaine*. Centre National de la Recherche Scientifique.
- Demuro, M., Arnold, L. J., Aranburu, A., Sala, N., & Arsuaga, J.-L. (2019). New bracketing luminescence ages constrain the Sima de los Huesos hominin fossils (Atapuerca, Spain) to MIS 12. *Journal of Human Evolution*, 131, 76–95.
- Doboş, A., Soficaru, A., & Trinkaus, E. (2010). *The prehistory and paleontology of the Peştera Muierii (Romania)*. Université de Liège.
- Dobson, S., & Trinkaus, E. (2002). Cross-sectional geometry and morphology of the mandibular symphysis in middle and Late Pleistocene *Homo*. *Journal of Human Evolution*, 43, 67–87.
- Falguères, C., Bahain, J.-J., Tozzi, C., Boschian, G., Dolo, J.-M., Mercier, N., Valladas, H., & Yokoyama, Y. (2008). ESR/U-series chronology of the lower Palaeolithic palaeoanthropological site of Visogliano, Trieste, Italy. *Quaternary Geochronology*, 3, 390–398.
- Falguères, C., Shao, Q., Han, F., Bahain, J. J., Richard, M., Perrenoud, C., Moigne, A. M., & Lumley de, H. (2015). New ESR and U-series dating at Caune de l'Arago, France: A key-site for European middle Pleistocene. *Quaternary Geochronology*, 30, 547–553.
- Franciscus, R., Vlcek, E., & Trinkaus, E. (2006). The mandibular remains. In E. Trinkaus & J. Svoboda (Eds.), *Early modern human evolution in central Europe. The people of Dolni Vestonice and Pavlov* (pp. 156–178). Oxford University Press, Oxford.
- Franciscus, R., & Trinkaus, E. (1995). Determinant of retromolar space presence in Pleistocene *Homo* mandibles. *Journal of Human Evolution*, 28, 577–595.
- Gómez-Olivencia, A., Carretero, J. M., Arsuaga, J. L., Rodríguez-García, L., García-González, R., & Martínez, I. (2007). Metric and morphological study of the upper cervical spine from the Sima de los Huesos site (Sierra de Atapuerca, Burgos, Spain). *Journal of Human Evolution*, 53, 6–25.
- Gómez-Robles, A., Bermúdez de Castro, J., Martín-Torres, M., & Prado-Simón, L. (2011). Crown size and cusp proportions in *Homo antecessor* upper first molars. A comment on Quam et al. 2009. *Journal of Anatomy*, 218, 258–262.
- Gómez-Robles, A., Martín-Torres, M., Bermúdez de Castro, J., Margvelashvili, A., Bastir, M., Arsuaga, J. L., Pérez-Pérez, A., Estebanaraz, F., & Martínez, L. (2007). A geometric morphometric analysis of hominin upper first molar shape. *Journal of Human Evolution*, 53, 272–285.
- García-Campos, C., Modesto-Mata, M., Martín-Torres, M., de Pinillos, M. M., Martín-Francés, L., Arsuaga, J. L., & Bermúdez de Castro, J. M. (2020). Sexual dimorphism of the enamel and dentine dimensions of the permanent canines of the middle Pleistocene hominins from Sima de los Huesos (Burgos, Spain). *Journal of Human Evolution*, 144, 102793.
- Grün, R., Stringer, C. B., & Schwarcz, H. P. (1991). ESR dating of teeth from Garrod's Tabun cave collection. *Journal of Human Evolution*, 20, 231–248.
- Grün, R., & Stringer, C. (2000). Tabun revisited: Revised ESR chronology and new ESR and U-series analyses of dental material from Tabun C1. *Journal of Human Evolution*, 39, 601–612.
- Harvati, K., Hublin, J.-J., & Gunz, P. (2010). Evolution of middle-late Pleistocene human cranio-facial form: A 3-D approach. *Journal of Human Evolution*, 59, 445–464.
- Heim, J. L. (1976). *Les Hommes Fossiles de La Ferrassie. Tome I*. Masson.

- Howell, F. (1960). European and Northwest African middle Pleistocene hominids. *Current Anthropology*, 1, 423–447.
- Hublin, J. (2009). The origin of Neandertals. *Proceedings of the National Academy of Sciences*, 106, 16022–16027.
- Hublin, J. J. (1998). Climatic changes, paleogeography, and the evolution of the Neandertals. In T. Akazawa, K. Aoki, & O. Bar-Yosef (Eds.), *Neandertals and modern humans in Western Asia* (pp. 295–310). Plenum Press.
- Kachigan, S. (1991). *Multivariate statistical analysis. A conceptual introduction* (2nd ed.). Radius Press.
- Lebel, S., & Trinkaus, E. (2002). Middle Pleistocene human remains from the Bau de l'Aubesier. *Journal of Human Evolution*, 43, 659–685.
- Lebel, S., Trinkaus, E., Faure, M., Fernandez, P., Guerin, C., Richter, D., Mercier, N., Valladas, H., & Wagner, G. (2001). Comparative morphology and paleobiology of middle Pleistocene human remains from the Bau de l'Aubesier, Vaucluse, France. *Proceedings of the National Academy of Sciences*, 98, 11097–11102.
- Levin, J., Fox, J., & Forde, D. (2014). *Elementary statistics in social research* (12th ed.). Pearson.
- Lorenzo, C., Carretero, J. M., Arsuaga, J. L., Gracia, A., & Martínez, I. (1998). Intrapopulation body size variation and cranial capacity variation in middle Pleistocene humans: The Sima de los Huesos sample (Sierra de Atapuerca, Spain). *American Journal of Physical Anthropology*, 106, 19–33.
- Manzi, G. (2016). Humans of the middle Pleistocene: The controversial calvarium from Ceprano (Italy) and its significance for the origin and variability of *Homo heidelbergensis*. *Quaternary International*, 411, 254–261.
- Manzi, G., Gracia, A., & Arsuaga, J. L. (2000). Cranial discrete traits in the middle Pleistocene humans from Sima de los Huesos (Sierra de Atapuerca, Spain). Does hypostosis represent any increase in "ontogenetic stress" along the Neanderthal lineage? *Journal of Human Evolution*, 38, 425–446.
- Martínez de Pinillos, M., Martín-Francés, L., Bermúdez de Castro, J. M., García-Campos, C., Modesto-Mata, M., Martín-Torres, M., & Viallet, A. (2020). Inner morphological and metric characterization of the molar remains from the Montmaurin-La Niche mandible: The Neanderthal signal. *Journal of Human Evolution*, 145, 102739.
- Martínez, I., Quam, R., & Arsuaga, J. (2008). Evolutionary trends in the temporal bone in the Neanderthal lineage: A comparative study between the Sima de los Huesos (Sierra de Atapuerca) and Krapina samples. In J. Monge, A. Mann, D. Frayer, & J. Radović (Eds.), *New insights on the Krapina Neandertals: 100 years after Gorjanović-Kramberger* (pp. 75–80). Zagreb.
- Martínez, I., & Arsuaga, J. L. (1997). The temporal bones from Sima de los Huesos middle Pleistocene site (Sierra de Atapuerca, Spain). A phylogenetic approach. *Journal of Human Evolution*, 33, 283–318.
- Martín-Torres, M., Bermúdez de Castro, J., Gómez-Robles, A., Prado-Simón, L., & Arsuaga, J. (2012). Morphological description and comparison of the dental remains from Atapuerca-Sima de los Huesos site (Spain). *Journal of Human Evolution*, 62, 7–58.
- Martín-Torres, M., Bermúdez de Castro, J. M., Gómez-Robles, A., Bastir, M., Sarmiento, S., Muela, A., & Arsuaga, J. L. (2007). Gran Dolina-TD6 and Sima de los Huesos dental samples: Preliminary approach to some dental characters of interest for phylogenetic studies. In S. Bailey & J. J. Hublin (Eds.), *Dental perspectives on human evolution. State-of-the-art research in dental paleoanthropology* (pp. 65–80). Springer.
- Martín-Torres, M., Bermúdez de Castro, J. M., de Pinillos, M. M., Modesto-Mata, M., Xing, S., Martín-Francés, L., García-Campos, C., Wu, X., & Liu, W. (2019). New permanent teeth from Gran Dolina-TD6 (Sierra de Atapuerca). The bearing of *Homo* antecedent on the evolutionary scenario of early and middle Pleistocene Europe. *Journal of Human Evolution*, 127, 93–117.
- Martin, H. (1926). Machoire humaine Moustérienne trouvée dans la station de. *La Quina.L'Homme Préhistorique*, 13, 3–21.
- Martin, R., & Saller, K. (1956). *Lehrbuch der Anthropologie*. Gustav Fisher Verlag.
- Maureille, B., & Vandermeersch, B. (2007). Les sépultures néandertaliennes. In B. Vandermeersch & B. Maureille (Eds.), *Les Néandertaliens. Biologie et Cultures* (pp. 311–322). C.T.H.S.
- McCown, T., & Keith, A. (1939). The Stone Age of Mount Carmel. In *The fossil human remains from the Levallois-Mousterian* (Vol. II). Clarendon Press, Oxford.
- Mercier, N., Valladas, H., Valladas, G., Reyss, J.-L., Jelinek, A., Meignen, L., & Joron, J.-L. (1995). TL dates of burnt flints from Jelinek's excavations at Tabun and their implications. *Journal of Archaeological Science*, 22, 495–509.
- Mercier, N., & Valladas, H. (2003). Reassessment of TL age estimates of burnt flints from the Paleolithic site of Tabun cave, Israel. *Journal of Human Evolution*, 45, 401–409.
- Meyer, M., Arsuaga, J.-L., de Filippo, C., Nagel, S., Aximu-Petri, A., Nickel, B., Martínez, I., Gracia, A., Bermúdez de Castro, J. M., & Carbonell, E. (2016). Nuclear DNA sequences from the middle Pleistocene Sima de los Huesos hominins. *Nature*, 531, 504–507.
- Meyer, M., Fu, Q., Aximu-Petri, A., Glocke, I., Nickel, B., Arsuaga, J.-L., Martínez, I., Gracia, A., Bermúdez de Castro, J. M., & Carbonell, E. (2014). A mitochondrial genome sequence of a hominin from Sima de los Huesos. *Nature*, 505, 403–406.
- Mounier, A., Marchal, F., & Condemi, S. (2009). Is *Homo heidelbergensis* a distinct species? New insight on the Mauer mandible. *Journal of Human Evolution*, 56, 219–246.
- Muttoni, G., Scardia, G., Kent, D., Swisher, C., & Manzi, G. (2009). Pleistocene magnetostratigraphy of early hominin sites at Ceprano and Fontana Ranuccio, Italy. *Earth and Planetary Science Letters*, 286, 255–268.
- Piveteau, J. (1963–1966). La Grotte de Regourdou (Dordogne). Paléontologie humaine. *Annales de Paléontologie (Vertébrés)*, 48, 155–194, 49, 50, 52, 285–304, 163–194.
- Quam, R. (1996). Tabun too? A morphometric comparison of upper Pleistocene mandibles. In *Anthropology*. Northern Illinois University.
- Quam, R., Arsuaga, J. L., Bermúdez de Castro, J. M., Díez, J. C., Lorenzo, C., Carretero, J. M., García, N., & Ortega, A. (2001). Human remains from Valdegoba cave (Huérmedes, Burgos, Spain). *Journal of Human Evolution*, 41, 385–435.
- Quam, R., Lorenzo, C., Martínez, I., Gracia-Téllez, A., & Arsuaga, J. L. (2016). The bony labyrinth of the middle Pleistocene Sima de los Huesos hominins (Sierra de Atapuerca, Spain). *Journal of Human Evolution*, 90, 1–15.
- Quam, R., & Smith, F. H. (1998). Reassessment of the Tabun C2 mandible. In T. Akazawa, K. Aoki, & O. Bar-Yosef (Eds.), *Neandertals and modern humans in Western Asia* (pp. 405–421). Plenum Press.

- Radovic, J., Smith, F., Trinkaus, E., & Wolpoff, M. (1988). *The Krapina hominids: An illustrated catalog of the skeletal collection*. Mladost Press & Croatian Natural History Museum.
- Rak, Y. (1986). The Neanderthal: A new look at an old face. *Journal of Human Evolution*, *15*, 151–164.
- Rak, Y., Ginzburg, A., & Geffen, E. (2002). Does *Homo neanderthalensis* play a role in modern human ancestry? The mandibular evidence. *American Journal of Physical Anthropology*, *119*, 199–204.
- Rak, Y., Hylander, W., Quam, R., Martinez, I., Gracia, A., & Luis, A. J. (2011). The problematic hypodigm of *Homo heidelbergensis* (abstract). *American Journal of Physical Anthropology*, *144*, 247.
- Rak, Y., Kimbel, W., & Hovers, E. (1994). A Neandertal infant from Amud cave, Israel. *Journal of Human Evolution*, *26*, 313–324.
- Rightmire, G. P. (1990). *The evolution of Homo erectus*. Cambridge University Press.
- Rightmire, G. P. (2008). *Homo* in the middle pleistocene: Hypodigms, variation, and species recognition. *Evolutionary Anthropology*, *17*, 8–21.
- Rink, W., Schwarcz, H., Smith, F. H., & Radovic, J. (1995). ESR ages for Krapina hominids. *Nature*, *378*, 24.
- Rink, W. J., Mercier, N., Mihailović, D., Morley, M. W., Thompson, J. W., & Roksandic, M. (2013). New radiometric ages for the BH-1 Hominin from Balanica (Serbia): Implications for understanding the role of the Balkans in middle Pleistocene human evolution. *PLoS One*, *8*, e54608.
- Rodríguez, L., Carretero, J. M., García-González, R., & Arsuaga, J. L. (2018). Cross-sectional properties of the lower limb long bones in the middle Pleistocene Sima de los Huesos sample (Sierra de Atapuerca, Spain). *Journal of Human Evolution*, *117*, 1–12.
- Roksandic, M., Mihailović, D., Mercier, N., Dimitrijević, V., Morley, M., Rakočević, Z., Mihailović, B., Guibert, P., & Babb, J. (2011). A human mandible (BH-1) from the Pleistocene deposits of Mala Balanica cave (Sićevo Gorge, Niš, Serbia). *Journal of Human Evolution*, *61*, 186–196.
- Roksandic, M., Radović, P., & Lindal, J. (2018). Revising the hypodigm of *Homo heidelbergensis*: A view from the eastern Mediterranean. *Quaternary International*, *466*, 66–81.
- Rosas, A. (1987). Two new mandibular fragments from Atapuerca/Ibeas (SH site). A reassessment of the affinities of the Ibeas mandibles sample. *Journal of Human Evolution*, *16*, 417–427.
- Rosas, A. (1992). Ontogenia y filogenia de la mandíbula en la evolución de los homínidos. Aplicación de un modelo de morfogenia a las mandíbulas fosiles de Atapuerca. In *In*. Universidad Complutense.
- Rosas, A. (1995). Seventeen new mandibular specimens from the Atapuerca/Ibeas middle Pleistocene Hominids sample. *Journal of Human Evolution*, *28*, 533–559.
- Rosas, A. (1997). A gradient of size and shape for the Atapuerca sample and middle Pleistocene hominid variability. *Journal of Human Evolution*, *33*, 319–331.
- Rosas, A. (2000). Ontogenetic approach to variation in middle Pleistocene hominids. Evidence from the Atapuerca-SH mandibles. *Human Evolution*, *15*, 83–98.
- Rosas, A. (2001). Occurrence of Neandertal features in mandibles from the Atapuerca-SH site. *American Journal of Physical Anthropology*, *114*, 74–91.
- Rosas, A., Bastir, M., Martínez-maza, C., García-Taberner, A., & Lalueza-Fox, C. (2006). Inquiries into Neandertal craniofacial development and evolution: “accretion” versus “organismic” models. In K. Harvati & T. Harrison (Eds.), *Neandertals revisited: New approaches and perspectives* (pp. 37–69). Springer.
- Rosas, A., Bastir, M., Martínez-Maza, C., & Bermúdez de Castro, J. (2002). Sexual dimorphism in the Atapuerca-SH hominids: The evidence from the mandibles. *Journal of Human Evolution*, *42*, 451–474.
- Rosas, A., Bastir, M., & Alarcón, J. A. (2019). Tempo and mode in the Neandertal evolutionary lineage: A structuralist approach to mandible variation. *Quaternary Science Reviews*, *217*, 62–75.
- Rosas, A., Martínez-Maza, C., Bastir, M., García-Taberner, A., Lalueza-Fox, C., Huguet, R., Ortíz, J. E., Julia, R., Soler, V., de Torres, T., Martínez, E., Canaveras, J. C., Sánchez-Moral, S., Cuezva, S., Lario, J., Santamaría, D., de la Rasilla, M., & Fortea, J. (2006). Paleobiology and comparative morphology of a late Neandertal sample from El Sidron, Asturias, Spain. *PNAS*, *103*, 19266–19271.
- Rosas, A., Perez, P., & Bone, J. (1999). Senescence in European middle Pleistocene hominids: The Atapuerca evidence. *Human Evolution*, *14*, 83–98.
- Rosas, A., & Aguirre, E. (1999). Restos humanos neandertales de la Cueva del Sidrón, Piloña, Asturias Nota preliminar. *Estudios Geológicos*, *55*, 181–190.
- Rosas, A., & Bastir, M. (2004). Geometric morphometric analysis of allometric variation in the mandibular morphology of the hominids of Atapuerca, Sima de los Huesos site. *Anatomical Record Part A*, *278A*, 551–560.
- Rosas, A., & Bermúdez de Castro, J. (1999). The ATD6-5 mandibular specimen from Gran Dolina (Atapuerca, Spain). Morphological study and phylogenetic implications. *Journal of Human Evolution*, *37*, 567–590.
- Rosas, A., & Bermudez de Castro, J. (1998). The Mauer mandible and the significance of *Homo heidelbergensis*. *Geobios*, *31*, 126–137.
- Rosas, A., & Martínez-Maza, C. (2010). Bone remodeling of the *Homo heidelbergensis* mandible; the Atapuerca-SH sample. *Journal of Human Evolution*, *58*, 127–137.
- Schoetensack, O. (1908). Der Unterkiefer des Homo Heidelbergensis aus den Sanden von Mauer bei Heidelberg. Ein Beitrag zur Paläontologie des Menschen. *Zeitschrift für induktive Abstammungs- und Vererbungslehre*, *1*, 408–410.
- Sergi, S. (1954). La mandibola Neandertaliana Circeo II. *Rivista di Antropologia*, *41*, 305–344.
- Sergi, S., & Ascenzi, A. (1955). La mandibola Neandertaliana Circeo III. *Rivista di Antropologia*, *42*, 337–403.
- Skinner, M. M., de Vries, D., Gunz, P., Kupczik, K., Klassen, R. P., Hublin, J.-J., & Roksandic, M. (2016). A dental perspective on the taxonomic affinity of the Balanica mandible (BH-1). *Journal of Human Evolution*, *93*, 63–81.
- Sládek, V., Trinkaus, E., Hillson, S., & Holliday, T. (2000). *The People of the Pavlovian. Skeletal Catalogue and Osteometrics of the Gravettian Fossil Hominids from DolníVestonice*. Academy of Sciences of the Czech Republic.
- Smith, F. (1978). Evolutionary significance of the mandibular foramen area in Neandertals. *American Journal of Physical Anthropology*, *48*, 523–531.
- Stefan, V., & Trinkaus, E. (1998). La Quina 9 and Neandertal mandibular variability. *Bulletins et Memoires de la Societe d'Anthropologie de Paris*, *10*, 293–324.

- Stelzer, S., Neubauer, S., Hublin, J. J., Spoor, F., & Gunz, P. (2019). Morphological trends in arcade shape and size in middle Pleistocene *Homo*. *American Journal of Physical Anthropology*, *168*, 70–91.
- Stringer, C. (2012). The status of *Homo heidelbergensis* (Schoetensack 1908). *Evolutionary Anthropology*, *21*, 101–107.
- Suzuki, H., & Takai, F. (1970). *The Amud man and his cave site*. Academic Press of Japan.
- Tattersall, I. (2011). Before the Neanderthals: Hominid evolution in middle Pleistocene Europe. In S. Condemi & G. Weniger (Eds.), *Continuity and discontinuity in the peopling of Europe* (pp. 47–53). Springer.
- Trinkaus, E., & Walker, M. (2017). *The People of Palomas: Neanderthals from the Sima de las Palomas del Cabezo Gordo*. Southeastern Spain. Texas A&M University Press.
- Trinkaus, E., Constantin, S., & Zilhão, J. (2013). *Life and death at the Peştera cu Oase: A setting for modern human emergence in Europe*. Oxford University Press.
- Trinkaus, E. (1983). Age and sex of the Shanidar Neandertals. In *The Shanidar Neandertals*. Academic Press.
- Trinkaus, E. (1993). Variability in the position of the mandibular mental foramen and the identification of Neandertal apomorphies. *Rivista de Anthropologia*, *71*, 259–274.
- Trinkaus, E. (2006). Modern human versus Neandertal evolutionary distinctiveness. *Current Anthropology*, *47*, 597–620.
- Verna, C., Détroit, F., Kupczik, K., Arnaud, J., Balzeau, A., Grimaud-Hervé, D., Bertrand, S., Riou, B., & Moncel, M.-H. (2020). The middle Pleistocene hominin mandible from Payre (Ardèche, France). *Journal of Human Evolution*, *144*, 102775.
- Vialet, A., Modesto-Mata, M., Martínón-Torres, M., Martínez de Pinillos, M., & Bermúdez de Castro, J.-M. (2018). A reassessment of the Montmaurin-La Niche mandible (Haute Garonne, France) in the context of European Pleistocene human evolution. *PLoS One*, *13*, e0189714.
- Vlcek, E. (1993). *Fossile Menschenfunde von Weimar-Ehringsdorf*. Konrad Theiss Verlag, Stuttgart.
- Wagner, G., Krbetschek, M., Degering, D., Bahain, J., Shao, Q., Falguères, C., Voinchet, P., Dolo, J., Garcia, T., & Rightmire, G. (2010). Radiometric dating of the type-site for *Homo heidelbergensis* at Mauer, Germany. *Proceedings of the National Academy of Sciences*, *107*, 19726–19730.
- Walker, A., & Leakey, R. (1993). *The Nariokotome Homo erectus skeleton*. Springer-Verlag.
- Weidenreich, F. (1936). *The mandibles of Sinanthropus pekinensis: A comparative study*, Paleontologica Sinica, New Series D. No. 7. Geological Survey of China.
- Wolpoff, M., Smith, F., Males, M., Radovic, J., & Rukavina, D. (1981). Upper Pleistocene human remains from Vindija cave, Croatia, Yugoslavia. *American Journal of Physical Anthropology*, *54*, 499–545.
- Wood, B. (1991). Koobi Fora Research Project. In *Hominid Cranial Remains* (Vol. 4). Clarendon Press.

SUPPORTING INFORMATION

Additional supporting information can be found online in the Supporting Information section at the end of this article.

How to cite this article: Quam, R., Martínez, I., Rak, Y., Hylander, B., Pantoja, A., Lorenzo, C., Conde-Valverde, M., Keeling, B., Ortega Martínez, M. C., & Arsuaga, J. L. (2023). The Neandertal nature of the Atapuerca Sima de los Huesos mandibles. *The Anatomical Record*, 1–51. <https://doi.org/10.1002/ar.25190>